University of Cyprus

DEPARTMENT OF BIOLOGICAL SCIENCES

Phytoplankton in the coastal waters of Cyprus (eastern Levantine): phenology, spatiotemporal variations, and microphytoplankton community structure

Monica Demetriou

A Dissertation Submitted to the University of Cyprus in Partial Fulfilment of the Requirements for the Degree of Doctor of Philosophy

December 2021

VALIDATION PAGE

Doctoral Candidate: Monica Demetriou

Doctoral Dissertation Title: Phytoplankton in the coastal waters of Cyprus (eastern Levantine): phenology, spatiotemporal variations, and microphytoplankton community structure

The present Doctoral Dissertation was submitted in partial fulfilment of the requirements for the Degree of Doctor of Philosophy at the ***Department of*** *Biological Sciences and was approved on the ……. by the members of the* ***Examination Committee****.*

Examination Committee:

Research Supervisor:

Dr Spyros Sfenthourakis, Professor …….

Committee Member:

Dr Anna Papadopoulou, Assistant Professor …….

Committee Member:

Dr Vasilis Promponas, Associate Professor …….

Committee Member:

Dr Maria Moustaka-Gouni, Professor …….

Committee Member:

Dr Eyal Rahav …….

DECLARATION OF DOCTORAL CANDIDATE

The present doctoral dissertation was submitted in partial fulfilment of the requirements for the degree of Doctor of Philosophy of the University of Cyprus. It is a product of original work of my own, unless otherwise mentioned through references, notes, or any other statements.

Monica Demetriou ……..

ΠΕΡΙΛΗΨΗ

Το θαλάσσιο φυτοπλαγκτόν βρίσκεται στη βάση των τροφικών πλεγμάτων και είναι υπεύθυνο για περίπου το ήμισυ της παγκόσμιας πρωτογενούς παραγωγής. Η ποικιλότητα και η βιομάζα του φυτοπλαγκτού ποικίλλουν στο χώρο και στο χρόνο, και ελέγχονται από διάφορους παράγοντες, όπως ο ανταγωνισμός και οι αλληλεπιδράσεις θηρευτή/θηράματος, καθώς και από τη θερμοκρασία, το φως, τη στήλη του νερού και την κυκλοφορία. Το φυτοπλαγκτόν ρυθμίζει το κλίμα μεταφέροντας διοξείδιο του άνθρακα από την ατμόσφαιρα στον ωκεανό, μέσω του κύκλου του άνθρακα. Είναι επίσης ευαίσθητο στις περιβαλλοντικές αλλαγές, καθώς λόγω του μικρού κύκλου ζωής ανταποκρίνεται πολύ γρήγορα στις όποιες αλλαγές στο φυσικό περιβάλλον. Οποιεσδήποτε αλλαγές στη σύνθεση των φυτοπλαγκτονικών κοινοτήτων θα έχουν κλιμακωτές επιπτώσεις στα θαλάσσια οικοσυστήματα και επομένως, η μελέτη των φυτοπλαγκτονικών κοινοτήτων και η ταξινομική με βάση λειτουργικά χαρακτηριστικά, σε σχέση πάντα με τις φυσικές διεργασίες και τις εισροές θρεπτικών ουσιών, είναι ζωτικής σημασίας για την παρακολούθηση της επίδρασης των περιβαλλοντικών αλλαγών στη δομή των φυτοπλαγκτονικών κοινοτήτων. Αυτή η εργασία παρέχει, για πρώτη φορά στα παράκτια ύδατα της Κύπρου, πληροφορίες σχετικά με τη δομή και τη δυναμική της φυτοπλαγκτονικών κοινοτήτων, χρησιμοποιώντας έναν συνδυασμό μεθόδων, όπως είναι η συλλογή δεδομένων στο πεδίο, για διάστημα 12 μηνών κατά το 2016, καθώς και η ανάλυση δεδομένων τηλεπισκόπησης.

Τα αποτελέσματα από τον πρώτο πλήρη εποχιακό κύκλο φαινολογίας του φυτοπλαγκτού στα παράκτια ύδατα της Κύπρου, καταδεικνύουν ότι η δορυφορική τηλεπισκόπηση μπορεί να χρησιμοποιηθεί για την αποτελεσματική παρακολούθηση του θαλάσσιου οικοσυστήματος της Κύπρου και της ανατολικής Λεβαντίνης, όπου τα *in situ* δεδομένα είναι σπάνια. Οι συγκεντρώσεις των χρωστικών του φυτοπλαγκτού συμφωνούν με τα δορυφορικά δεδομένα, όπου η περίοδος ανάπτυξης του φυτοπλαγκτού ξεκινά τον Νοέμβριο και τελειώνει τον Μάρτιο/Απρίλιο, και είναι σύμφωνη με τη «no bloom» κατηγοριοποίηση της ανατολικής Μεσογείου. Τα δεδομένα τηλεπισκόπησης για την περίοδο δειγματοληψίας του 2016 έδειξαν νωρίτερο τερματισμό της περιόδου ανάπτυξης του φυτοπλαγκτού, επομένως, μικρότερη διάρκεια, σε σύγκριση με την κλιματολογική 23ετία. Γενικά, τα παράκτια ύδατα της Κύπρου αντικατοπτρίζουν τις υπερολιγοτροφικές συνθήκες της ανατολικής Μεσογείου, καθώς οι τιμές ολικής χλωροφύλλης-α που καταγράφονται είναι εξαιρετικά χαμηλές. Οι υδρολογικές συνθήκες στην περιοχή μελέτης δείχνουν ότι η υδάτινη στήλη αναμειγνύεται καλά μεταξύ

Δεκεμβρίου και Απριλίου, ενώ το υπόλοιπο του έτους η στήλη νερού είναι στρωματοποιημένη. Η αλατότητα στην περιοχή είναι πολύ υψηλή (> 39), και οι θερμοκρασίες φτάνουν μέχρι και 29 °C το καλοκαίρι. Παρόλο που οι συγκεντρώσεις των θρεπτικών συστατικών ήταν γενικά χαμηλές, καταγράφηκαν ορισμένες ακραίες τιμές συγκεντρώσεων φωσφορικών αλάτων το χειμώνα και την άνοιξη, οι οποίες θα μπορούσαν να αποδοθούν σε τοπικές πηγές εισροών θρεπτικών συστατικών κατά μήκος της ακτής (π.χ. ηλεκτροπαραγωγικός σταθμός, μονάδα αφαλάτωσης, μη επεξεργασμένα λύματα). Λαμβάνοντας υπόψη τις κατηγορίες μεγέθους του φυτοπλαγκτού, το πικο- και το νανοφυτοπλαγκτόν είχαν την υψηλότερη συμβολή στις κοινότητες φυτοπλαγκτού, όπως αναμένεται για τα ολιγοτροφικά ύδατα της Λεβαντίνης. Συγκεκριμένα, η συμβολή του πικο- και του νανοφυτοπλαγκτόντος ήταν ίση στο μεγαλύτερο μέρος του έτους (~50%), ενώ το καλοκαίρι το νανοφυτοπλαγκτόν συνεισέφερε κοντά στο 60%. Ο συνδυασμός του αλγορίθμου CHEMTAX και της ανάλυσης χρωστικών μέσω HPLC επιβεβαίωσε προηγούμενες μελέτες στη Μεσόγειο, όπου τα Πρυμνησιόφυτα έχουν καταγραφεί ως η πιο άφθονη ομάδα καθ' όλη τη διάρκεια του έτους, τόσο στα ρηχά όσο και στα βαθύτερα στρώματα. Η ανάλυση της κοινότητας του μικροφυτοπλαγκτού αποκάλυψε συνολικά 50 taxa, με τον υψηλότερο αριθμό να καταγράφεται στο σταθμό PYR (45), ακολουθούμενο από το AKR (41), το VAS2 (38) και το VAS1 (35).

Τα αποτελέσματα αυτής της διατριβής παρέχουν μια πρώτη εικόνα της σύνθεσης και της εποχικής διαδοχής των κοινοτήτων φυτοπλαγκτού στα παράκτια ύδατα της Κύπρου και ανοίγουν το δρόμο για μελλοντική έρευνα που θα πρέπει να αξιολογήσει πώς η υπερθέρμανση των ωκεανών επηρεάζει τη φαινολογία του φυτοπλαγκτού και την εποχιακή διαδοχή των χρωστικών φυτοπλαγκτού στην περιοχή.

ABSTRACT

Marine phytoplankton is at the base of marine food webs and responsible for approximately half of the global primary production. The diversity and biomass of phytoplankton vary spatiotemporally and are controlled by various factors, such as competition and predator/prey interactions and by physical processes such as temperature, light availability, water-column structure and circulation. Phytoplankton regulate the Earth's climate over time, by transferring carbon dioxide from the atmosphere to the ocean, via the carbon cycle. Phytoplankton are also sensitive to environmental changes, responding very quickly to climate induced changes in their physical habitat, due to their short turnover times. Any changes in phytoplankton community composition can have cascading effects on marine ecosystems, affecting food web dynamics and ecosystem production. Therefore, understanding phytoplankton community dynamics, as well as the taxonomy of functional types, in relation to physical processes and nutrient inputs, is crucial in order to monitor the influence of environmental changes on phytoplankton community structure, with implications in biogeochemical cycles and the functioning of the entire marine ecosystem. This work provides, for the first time in the coastal waters of Cyprus, insights on the phytoplankton community structure and dynamics, using a combination of ocean colour remote sensing observations and a 12-month long timeseries of *in situ* data, collected from four coastal stations in Cyprus during 2016.

The results from the first complete seasonal cycle of phytoplankton phenology in the coastal waters of Cyprus, demonstrate that ocean colour remote sensing can be used to effectively monitor the marine ecosystem of Cyprus, and the eastern Levantine, where *in situ* data are scarce. The *in situ* data on phytoplankton pigments are consistent with the satellite-derived phytoplankton phenology, where the phytoplankton growth period initiates in November and terminates in March/April, consistent with the "no bloom" classification. The remote sensing data for the sampling period of 2016 showed an earlier termination and thus, a shorter duration, when compared to the 23-year climatology. In general, the coastal waters of Cyprus reflect the ultra-oligotrophic conditions of the eastern Mediterranean since the total chlorophyll-a values recorded are extremely low. The hydrological conditions in the study area show that the water column is well mixed between December to April, and the remainder of the year the water column is stratified. The salinity in the area is very high (> 39), and temperatures reaching a maximum of 29 °C in the summer. Even though the concentrations of nutrients were generally

low, some extreme values of phosphate concentrations were recorded in winter and spring, which could be attributed to localised sources of nutrient inputs along the coast (power station, desalination plant, untreated sewage). Considering phytoplankton size classes, pico- and nanophytoplankton had the highest contribution in the phytoplankton communities, consistent with the oligotrphic Levantine open waters. Specifically, the contribution of pico- and nanophytoplankton was equal throughout most of the year (~50%), whereas in the summer nanophytoplankton contributed closer to 60%. The combination of CHEMTAX algorithm and HPLC pigments analysis confirmed previous studies in the Mediterranean, where Prymnesiophytes have been recorded as the most abundant group throughout the year, in both the shallow and deeper layers. The analysis of the microphytoplankton community revealed a total of 50 taxa, with the highest number recorded in PYR station (45), followed by AKR (41), VAS2 (38) and VAS1 (35).

The results of this thesis provide a first picture of the composition and seasonal succession of phytoplankton communities in the coastal waters of Cyprus and pave the way for future research that should assess how oceanic warming is affecting phytoplankton phenology and the seasonal succession of phytoplankton pigments in the area.

To my mum…

Acknowledgments

First and foremost, I would like to thank my supervisor, Dr. Spyros Sfenthourakis, for believing in my potential, trusting me to carry out this work and giving pragmatic solutions whenever needed. A special thanks to my co-supervisor, Dr. Stella Psarra, for her expertise, guidance, and support throughout this thesis. This work would not have been possible without the input of Dr. Dionysios Raitsos and Anastasia Kournopoulou, who I thank for their assistance, thoughtful advice, and excellent collaborative work. Special thanks to Dr. Manolis Mandalakis who spend over a month with me at HCMR while analysing samples and who run the HPLC methodology, and to Andreas Oikonomou for his assistance with CHEMTAX. I am grateful to the late Dr. Daniel Danielides who assisted with the early stages of this thesis, as well as to Dr. Vasiliki Lamprinou for her invaluable expertise and guidance on taxonomy. I would also like to thank Dr. Konstantinos Antoniades at the Department of Fisheries and Marine Research, for carrying out the nutrient analysis. Special thanks to Dr. Bruce Monger for his valuable assistance with satellite remote sensing data scripts, and to Dr. Daniel Hayes for his advice on physical oceanography.

I would like to thank the three fishermen (Giorgos, Christakis, and Kostas) who, for twelve months, made sampling possible, as well as Georgios Fyttis who shared the logistics of organising and carrying out all sampling trips.

Thanks goes to all the members of the Ecology and Biodiversity Lab, past and present; Pantelis Savvides, Aggelos Agathangelou, Theodora Antoniou. Special thanks go to my friends and office mates, who shared both happy and difficult moments throughout these years. In particular I would like to thank Yianna Samuel for being a great friend and co-worker, Emmanouela Karameta for being there during some very difficult moments, and finally Andreas Dimitriou who kept my head above water for the past 8 years.

My deepest gratitude goes to my parents, for always supporting me and believing in me, and to my sister for always being there. Finally, I would like to thank my partner, for his love and support throughout these years, and my son who put up with many “we’ll play later, mummy has to work” until this thesis was completed. This work would not have been possible without the love and support of my family and friends.

Table of Contents

List of Figures

List of Tables

I. Introduction

1.1. Marine phytoplankton

1.1.1. The importance of phytoplankton

The first to introduce the term "plankton" to describe everything drifting in the water, was Victor Hensen in 1887. Hensen believed that life in the sea was supported by the "life blood of the sea", the planktonic primary producers (Mills 2012), and he can be regarded as the first quantitative plankton ecologist (Reynolds 2006). Marine phytoplankton are unicellular or colonial organisms that range in size from less than 1 μm to over 1 mm (Falkowski and Raven 2007). Despite comprising only ~1% of the autotrophic biomass, they are responsible for approximately half of the global primary production (Field *et al.* 1998, Falkowski *et al.* 2004, Falkowski and Raven 2007). The diversity and biomass of phytoplankton vary widely both spatially and temporally, and interactions within the planktonic communities are complex (Hoppenrath *et al.* 2009).

Marine phytoplankton, through photosynthesis, regulate the Earth's climate over time (Falkowski *et al.* 1998), being responsible for most of the transfer of carbon dioxide (CO_2) from the atmosphere to the ocean, via the global carbon cycle. A major component of the global carbon cycle, the biological carbon pump, transfers carbon as the net result of phytoplankton photosynthesis, calcification and respiration of phytoplankton to the deep ocean, where it is made available to other trophic levels (Falkowski *et al.* 1998, Field *et al.* 1998, Robinson 2017). Specifically, phytoplanktonic photosynthesis taking place in the surface layers of the ocean transforms CO_2 into particulate and dissolved organic carbon (POC, DOC). This is exported to the deep from where it is respired back to dissolved organic carbon by heterotrophic prokaryotes and zooplankton (Robinson 2017) (Figure I.***1***).

Phytoplankton not only affect the Earth's climate, they are also sensitive to environmental changes, responding very quickly to climate induced changes in their physical habitat, due to their short turnover times (Falkowski and Oliver 2007). Given their fundamental role in the oceans' biogeochemical cycles, the effects of any changes (temperature, nutrient concentration) on phytoplankton, ultimately impact the entire ecosystem (Beaugrand 2005). The simple life history traits of phytoplankton (Litchman *et al.* 2007, Litchman and Klausmeier 2008) and their short life cycles make them ideal organisms to study the response of populations to environmental changes.

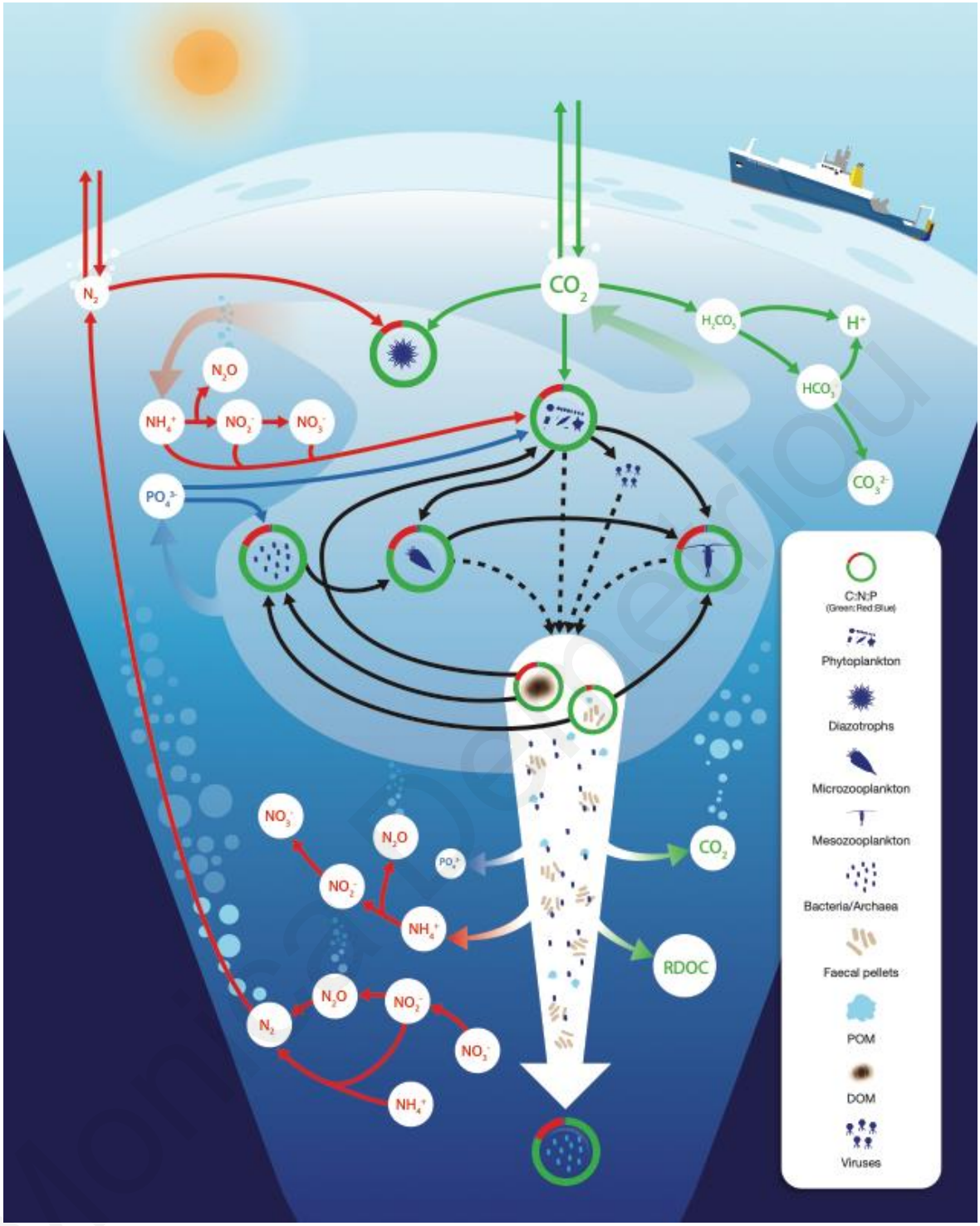

Figure I.1: Interactions between the biogeochemical cycles of carbon, nitrogen and phosphorus. Solid arrows denote "intake" (osmotrophic assimilation or grazing) and dashed arrows denote "exudation" of DOM processes. Figure by Robinson *et al.* (2015) shared under a Creative Commons license at https://doi.org/10.6084/m9.figshare.1585741.v1

1.1.2. Phytoplankton growth

In order to study potential climate induced changes to the ocean biogeochemical cycles, understanding what drives the growth of phytoplankton is essential. The investigation of the factors controlling variations in phytoplankton growth, biomass and diversity has been a central question in marine ecology (De Baar 1994). Competition for mineral nutrients

(bottom-up) and predator/prey interactions (top-down) control the diversity and biomass of phytoplankton, and these interactions are controlled by physical processes such as temperature, salinity, and circulation (Falkowski *et al.* 1998, Finkel *et al.* 2010).

An essential resource for photosynthesis is light, which in the marine environment is controlled by the vertical mixing of the water column, and depending on the water's clarity, irradiance is reduced to 1% of its surface value in the top 20-120 m (Holliday and Henson 2017). Since the light intensity and spectral signatures in the ocean are vastly different, phytoplankton had to adapt using different traits in order to efficiently utilise all available light. For example, diatoms, dinoflagellates, and cyanobacteria can utilise low light more efficiently than green algae, resulting in a dominance of diatoms and cyanobacteria under low-light conditions (Richardson *et al.* 1983, Reynolds 2006). Further, the various phytoplanktonic pigments apart from chlorophyll-a absorb in different wavelengths, thus increasing the range of light spectral that can be utilised by phytoplankton (Falkowski and Raven 2007, Kirk 2011).

Macro- (nitrate, phosphate, silicate) and micronutrients (iron, zinc) are essential for phytoplankton growth, taken up by phytoplankton in the surface layers of the ocean in inorganic forms (Raven 2017). As the supply of nutrients increases, phytoplankton growth rates increase to a theoretical maximum rate where the concentrations of nutrients are not limiting (Klausmeier *et al.* 2008). Then, they may be further released as dissolved organic matter (DOM) by grazing and sloppy feeding (Møller 2007), by viral lysis (Fuhrman 1999), as well as by phytoplankton exudation (Fogg 1983, Bjørrisen 1988). Bacterial uptake of DOM results in the recycling of nutrients, either in the surface layers or in the deep, following sinking of particulate matter and microbial degradation at depth (Raven 2017). The sedimentation particulate matter and the partial recycling of its nutrient content means that in relation to the deep ocean, the surface layers are depleted in the inorganic nutrient forms (Falkowski and Raven 2007, Raven 2017). The availability of nutrients in oligotrophic, temperate areas is the principal limiting factor for phytoplankton growth, where increased Chl-a concentrations are observed between November-December and last until spring, coinciding with the deepening of the mixed layer (Holliday and Henson 2017). Besides to their principal photosynthetic activity and subsequent metabolic pathways of assimilation of essential macronutrients into organic macromolecules, various phytoplankton taxa have developed different trophic traits related to the acquisition and utilisation of nutrients, such as nitrogen fixation (a unique ability of cyanobacteria, (Herrero and Flores 2008)), and mixotrophy (the ability to feed heterotrophically) (Raven *et al.* 2009).

Nutrients cycles in the ocean are linked, that is carbon (C) cycling is linked to that of nitrogen (N) and phosphorus (P), and a global average ratio for the three elements has been identified to be 106C:16N:1P, also known as Redfield ratio (Redfield 1958). This global ratio of 16N:1P can vary in different oceanic regions. For example, the deep-water N:P ratio of ~28:1 (Krom *et al.* 1991, Kress and Herut 2001) observed in the eastern Mediterranean is much higher than the Redfield ratio of 16 and thus productivity is phosphorus (P) limited (Krom *et al.* 1991) and/or nitrogen and phosphorus co-limited (Thingstad *et al.* 2005). The high N:P ratio is believed to be a result of the high values of N:P from external nutrient inputs, including atmospheric deposition, and the low denitrification rates because of the oligotrophic water column (Krom *et al.* 2010, 2014). Contrary to what was expected, the phosphate addition to surface layers of the ultra-oligotrophic eastern Mediterranean during the CYCLOPS project Lagrangian experiment in the Cyprus eddy (Krom *et al.* 2005) resulted in a decrease in chlorophyll-a concentration (Psarra *et al.* 2005) and an increase in bacterial production (Pitta *et al.* 2005) and copepod egg concentration, suggesting the existence of a microbial/phytoplankton food web (Pasternak *et al.* 2005). Further experiments (Zohary *et al.* 2005) revealed the N and P co-limitation of phytoplankton and P limitation of bacteria in the eastern Mediterranean. Because of their higher cellular surface-to-volume ratio, bacteria acquire nutrients more efficiently (Chisholm 1992), thus out-competing phytoplankton for P. According to Thingstad and Rassoulzadegan (1999), if competition alone is taken into consideration, then Hutchinson's paradox (Hutchinson 1961) can be modified as follows: "Why do bacteria not outcompete phytoplankton until primary production decreases to levels where bacteria become carbon-limited?". The microbial food web (competition and predator-prey relationship of phytoplankton and bacteria) can explain this paradox in P-starved systems (Tanaka *et al.* 2003).

Apart from the physicochemical conditions, the phytoplankton growth is also controlled by top down interactions by grazers, as well as an often overlooked factor, viral infections (Hoppenrath *et al.* 2009). Different phytoplankton taxa have developed different strategies against predation and infections, which have to do with morphological traits (size, colony formation etc.), or even physiological traits such as the production of toxins (Hoppenrath *et al.* 2009).

1.1.3. Phytoplankton communities and species diversity

Marine phytoplankton is an extremely diverse group, with over 4000 species described (Sournia *et al.* 1991, Reynolds and Padisák 2013). Phytoplankton cell size cover a large

range of sizes, from < 2 μm to over 200 μm (Finkel *et al.* 2010) (Figure I.***2***). Phytoplankton also differ in morphology and physiology, as well as their requirements in light and nutrients and have developed various strategies to avoid predation (Falkowski *et al.* 2004). At any one point, a phytoplanktonic community comprises of multiple species successfully coexisting on limited resources, something that has been knows as the "plankton paradox" (Hutchinson 1961).

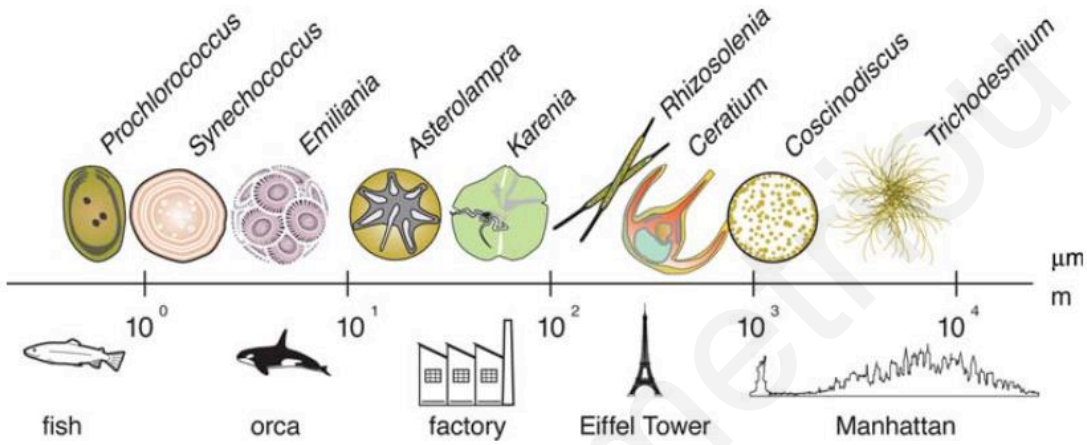

Figure I.2: A comparison between phytoplankton size and macroscopic objects. Image from Finkel *et al.* (2010).

Many theories have tried to explain Hutchinson's paradox of the plankton, with Hutchinson himself arguing that to assume that the aquatic habitats are homogenous is wrong (Reynolds and Padisák 2013). On the contrary, the marine environment exhibits great variation in physicochemical properties, and thus, the phytoplankton communities alter their structure as a response to changes in these properties, with species selected based on habitat constrains and suitability (Reynolds and Padisák 2013).

In order to understand phytoplankton diversity dynamics and species coexistence, the approach of a traits-based analysis has gained ground, where functional traits are defined as morphological, physiological, and phenological traits that impact fitness through growth, reproduction, and survival (Violle *et al.* 2007). Therefore, by following a trait-based approach, the response of phytoplanktonic communities to a changing environment can be predicted (Litchman *et al.* 2007, Litchman and Klausmeier 2008). Cell size is a key trait since many other traits such a nutrients utilization and grazer pressure are correlated with it (Litchman and Klausmeier 2008). For example, smaller cells have a higher surface to volume ratio, thus being more efficient in limiting nutrients acquisition, have lower sinking rates and higher growth rates, with the trade-off however that they are more susceptible to grazing (Thingstad *et al.* 2005, Litchman *et al.* 2007).

The impact of phytoplankton communities and diversity is great, both on the Earth's climate, as well on the biogeochemical cycles on geological time scales (Falkowski *et al.* 1998, Field *et al.* 1998). For example, coccolithophores contribute to the calcium carbonate pump, diatoms regulate silica biogeochemical cycles due to their silicate frustule, and some cyanobacteria fix nitrogen (Castellani and Edwards 2017).

The importance of phytoplankton communities for the functioning of marine ecosystems, and the distinct functional roles of various groups, makes the study of phytoplankton community dynamics, as well as the taxonomy of functional types crucial, in order to monitor the influence of environmental changes on phytoplankton community structure, with implications in biogeochemical cycles and the functioning of the entire marine ecosystem.

1.2. The Mediterranean Sea

The Mediterranean Sea is the largest semi-enclosed sea (Coll *et al.* 2010), with unique thermohaline circulation, intense meso- and sub-mesoscale activity, gyre formation, eddies and jets (POEM 1992, Siokou-Frangou *et al.* 2010 and references therein, Skliris 2014). It is because these complex physical dynamics also drive the global ocean that the Mediterranean is considered as a miniature ocean (Bethoux *et al.* 1999) and a laboratory basin for investigating global processes (Margalef 1985, Malanotte-Rizzoli and Eremeev 1999, Malanotte-Rizzoli *et al.* 2014).

As a semi-enclosed sea, the Mediterranean is a concentration basin, where evaporation exceeds precipitation, resulting in an anti-estuarine circulation. The strait of Sicily connects the western (WMED) and eastern (EMED) sub-basins of the Mediterranean. The thermohaline circulation of the Mediterranean comprises of an open vertical cell (whole basin) and two closed vertical cells (WMED and EMED respectively), analogous to the global ocean conveyor belt (Malanotte-Rizzoli *et al.* 2014). The open thermohaline cell (Wüst 1961) involves the inflow of low salinity Atlantic Water (AW) at the surface through the straits of Gibraltar, its progressive modification with gradual temperature and salinity increase as it moves towards the eastern basin (Modified Atlantic Water - MAW), its transformation to Levantine Intermediate Water (LIW) and its outflow in a bottom layer through the straits of Gibraltar (Malanotte-Rizzoli 1994, Robinson and Golnaraghi 1994). The warm (T=>25°C) and saline (S=39.30) Levantine Surface Water (LSW) dominates the surface layer of the Levantine during summer (Ovchinnikov *et al.* 1987), creates a mixed

layer with MAW during winter and re- appears in spring with T=19.5°C and S=39.10 (Özsoy *et al.* 1993).

Studies carried out until the 1980s showed that the Eastern Mediterranean Deep Water (EMDW) was mainly formed in the Southern Adriatic cyclonic gyre (Ovchinnikov *et al.* 1987), with the physical functioning of the eastern Mediterranean existing in a quasi-steady state (Velaoras *et al.* 2019). Following the results of the multi-national collaborative program POEM (Physical Oceanography of the Eastern Mediterranean) that took place between 1984 – 1987, the image of a simple, stationary thermohaline circulation shifted to a much more complex, time-varying picture (Robinson *et al.* 1991, Malanotte-Rizzoli *et al.* 1997, Velaoras *et al.* 2019). A transition that occurred in the eastern Mediterranean thermohaline closed cell between 1987 and 1995, named the Eastern Mediterranean Transient (EMT) shifted the main source of the EMDW from the Adriatic to the Aegean (Roether *et al.* 1996, Malanotte-Rizzoli *et al.* 1999, Tsimplis *et al.* 2006). During the EMT event, a massive outflow of deep Aegean Sea waters gradually replaced the deep Adriatic sea waters in the deep layers of the eastern Mediterranean (Velaoras *et al.* 2019) (Figure I.***3***).

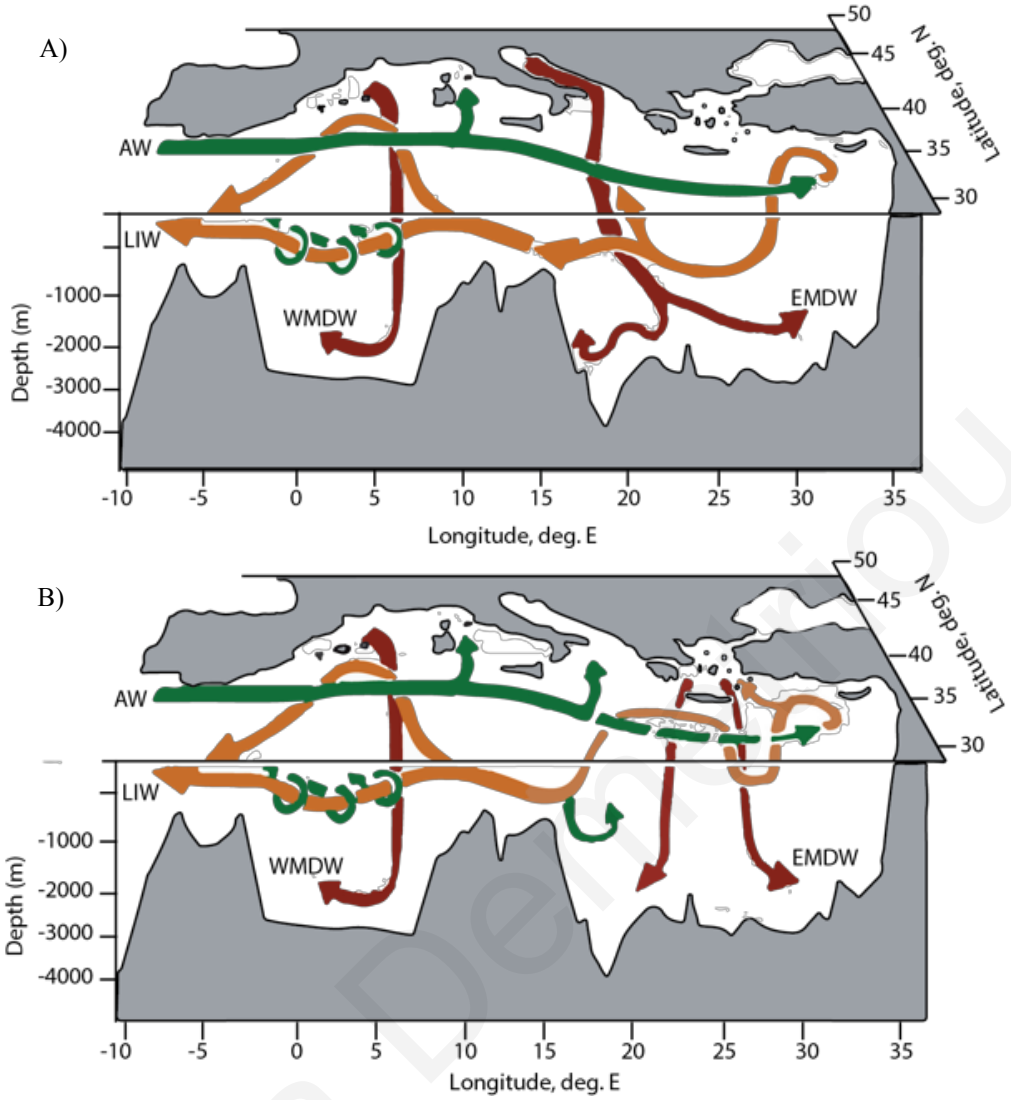

Figure I.3: Mediterranean Sea thermohaline circulation scheme before (A) and during (B) the Eastern Mediterranean Transient (EMT) (from Tsimplis *et al.* (2006)).

The complicated general circulation of the Levantine basin consists of strong currents and multiscale eddies (Özsoy *et al.* 1989, POEM 1992). The cyclonic Rhodes gyre dominates the eastern Levantine basin, extending towards Crete during winter and restricted to the east during summer, towards the western coast of Cyprus, where it creates a secondary eddy centre (Ovchinnikov, I.M. 1984). The Rhodes gyre is flanked to the north by the Asia Minor Current (AMC) and to the south by the Mid-Mediterranean Jet (MMJ) (Robinson *et al.* 1991). The MMJ separates the Rhodes gyre from the Mersa-Matruh anticyclone before bifurcating south of Cyprus. The branch flowing to the south of Cyprus comprises anticyclonic centres such as the Cyprus and Shikmona eddies, whereas the branch flowing towards the north and around Cyprus joins the Asia Minor Current (Figure I.***4***). The POEM scheme depicted in Figure I.***4***, and the circulation of the AW in the eastern Mediterranean in particular, has been questioned by Hamad *et al.* (2006) with the analysis of infrared satellite

data, showing the circulation of the AW in the eastern Mediterranean along the African coast. Studies carried out in the framework of the Cyprus Basin Oceanography (CYBO) (Zodiatis *et al.* 1998) showed that the Cyprus eddy controls the direction of the MMJ south of Cyprus and its bifurcation southwest, while it dominates the general circulation of the south-eastern Levantine. During the CYCLOPS experiment cruises (Krom *et al.* 2005), a shift of the Cyprus eddy towards the west was observed, along with the generation of a secondary anticyclonic eddy and the development of a third anticyclonic eddy close to the Egyptian coast, providing evidence for the re-establishment of the Shikmona gyre (Zodiatis *et al.* 2005). More recent observations revealed that the Cyprus eddy is a quasi-permanent feature with a radius of 45 km, consisting of an anticyclonic core of LIW to approximately 400 m depth (Hayes *et al.* 2011).

The eastern Mediterranean seems to be very sensitive to climate changes and it responds to them much faster when compared to the global ocean (Velaoras *et al.* 2019, and references within).

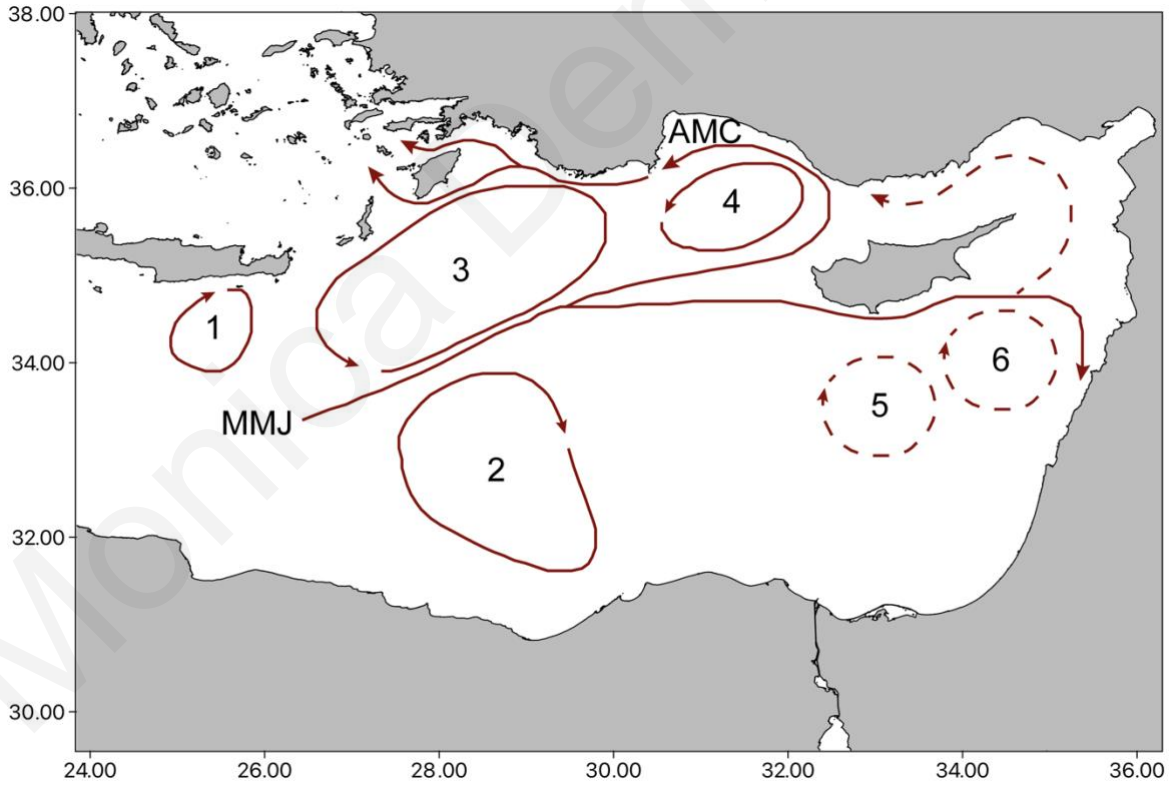

Figure I.4: Main traits of the eastern Mediterranean circulation. 1: Ierapetra gyre; 2: Mersa Matruh gyre; 3: Rhodos gyre; 4: West Cyprus eddy; 5: Cyprus eddy; 6: Shikmona gyre. MMJ: Mid-Mediterranean Jet, AMC: Asia Minor Current. Solid lines are permanent features, dashed lines are transient and recurrent features. (adapted from Malanotte-Rizzoli *et al.* (1997), Robinson and Gonaraghi (1994), Robinson *et al.* (2001) and Karageorgis *et al.* (2008)).

1.3. Chemotaxonomy

Apart from Chl-a which has been used routinely as a proxy for phytoplankton biomass (Jeffrey and Vesk 1997), additional pigments are restricted to certain phytoplankton taxa, allowing the quantitative chemotaxonomic phytoplankton analysis and the mapping of phytoplankton distribution and community composition (Higgins *et al.* 2011). A challenge for chemotaxonomic quantification is the fact that many pigments are not unique markers but rather are shared between taxonomic groups. However, groups of similar evolutionary lineages tend to share the same group of pigments (Falkowski *et al.* 2004), making it possible to relate biomarker pigments to size classes (Kramer and Siegel 2019).

1.4. Ocean colour remote sensing

When sunlight interacts with water and its constituents, part of the irradiance penetrating surface layers is attenuated (adsorption and backscattering) while part of it is reflected as water leaving reflectance. Spectral variations in the water leaving reflectance are detected by satellites and this signal in the ocean depends on phytoplankton (Chl-a) and coloured dissolved organic matter (CDOM) (IOCCG 2000, Groom *et al.* 2019).

The spatial and temporal changes of phytoplankton can be monitored over time via chlorophyll-a concentration, the most direct indicator of phytoplankton biomass (Jeffrey and Vesk 1997). Ocean colour remote sensing is the only method that allows global data retrieval of the pattern of Chl-a concentration trends over large spatial and temporal scales, that would not be otherwise achieved through *in situ* data collection alone. Ocean colour remote sensing has been applied, among others, to detecting phytoplankton phenology metrics (Racault *et al.* 2012, Gittings *et al.* 2019b, Salgado-Hernanz *et al.* 2019). Phytoplankton phenology metrics such as growth initiation, time of maximum amplitude, duration and termination, are categorised as ecological indicators (Platt and Sathyendranath 2008), and are a key factor in determining the structure of food webs and ecosystem function (Edwards and Richardson 2004, Racault *et al.* 2012). The monitoring of these indicators offers a way to observe the response of marine ecosystems to environmental change (Platt and Sathyendranath 2008, Racault *et al.* 2014, Gittings *et al.* 2018).

It has been shown that the use of the standard global empirical algorithms in the Mediterranean Sea (OC4v4 for SeaWiFS and OC3M for MODIS Aqua) lead to a significant overestimation of chlorophyll-a concentration, when compared to *in situ* measurements (Bricaud *et al.* 2002, Claustre *et al.* 2002, D'Ortenzio *et al.* 2002). Possible explanations for this bias between *in situ* and satellite retrieved concentrations have been proposed, attributed

to the specific bio-optical characteristics of the basin. These include an abundance in coccolithophores (D'Ortenzio *et al.* 2002) as well as the presence of desert dust in the water column (Claustre *et al.* 2002). In order to improve the retrieval of chlorophyll-a concentration in the Mediterranean, several regional algorithms have been proposed (Bricaud *et al.* 2002, Claustre *et al.* 2002, D'Ortenzio *et al.* 2002). Even though the regional algorithms perform better compared to the global algorithms, they are not accurate when dealing with the very low Chl-a concentrations observed in the eastern Mediterranean. This could be attributed partly to the fact that *in situ* observations in the area are sparse (Groom *et al.* 2005). The concentration of dissolved organic matter (CDOM), the position of chlorophyll-a maximum in relation to the optical depth and the optical properties of the phytoplankton communities, have been proposed by Volpe et al. (2007) as limiting factors in the performance of regional algorithms.

Volpe et al. (2007) have shown that the regional SeaWiFS algorithms BRIC and DORMA perform better at low chlorophyll-a values (<0.4 mg m^{-3}), compared to the global algorithms. However, BRIC overestimates concentrations between 0.1-0.4 mg m^{-3} and performs better at chlorophyll-a values <0.1 mg m^{-3}, whereas DORMA is less efficient for concentrations >1 mg m^{-3} and performs better at low chlorophyll-a values (Volpe *et al.* 2007). The regional MedOC4 algorithm proposed by Volpe et al. (2007) performs better at a wider range of chlorophyll-a values (0.02 – 7.0 mg m^{-3}). Hattab et al. (2013) have shown that the regional MedOC3 algorithm overestimates the concentration of chlorophyll-a in the eastern Mediterranean. Until recently (El Hourany *et al.* 2017, Bengil and Mavruk 2018), the bio-optical characteristics of the Levantine basin have rarely been studied.

The marine processing service of Copernicus (https://www.copernicus.eu/, a European programme for Earth Observations through satellite products), the Copernicus Marine Environment Monitoring Service (CMEMS), uses OLCI, VIIRS and MODIS-Aqua data to produce near-real time and reprocessed time series of global and regional products (Groom *et al.* 2019). The multi-sensor Chl-a (mg/m3) daily product at 1-km resolution is a merge of MODIS-Aqua, NOAA-20-VIIRS, NPP-VIIRS, Sentinel3A-OLCI data. Chl-a estimation are obtained by means of the Mediterranean-tuned regional algorithms: an updated version of the MedOC4 (Case 1 waters, Volpe *et al.* 2019) and AD4 (Case 2 waters, Berthon and Zibordi 2004).

Despite the obvious advantages of ocean colour remote sensing data processing, there is a limitation, that is, the information it provides is restricted to the first spectral optical depth, and thus no information is available on the vertical structure of the water column. Only ~

25% of ocean production takes place in the upper 10 m of the ocean and phytoplankton species distribution varies considerably with depth (Mouritsen and Richardson 2003, Richardson and Bendtsen 2019), therefore satellite observations provide only a fraction of the information in the water column by determining only total Chl-a at the surface and do not offer information of individual pigments contribution to total Chl-a. Knowing the individual pigment composition is important in assessing the phytoplanktonic community composition sine most pigments are biomarkes for specific groups and can reflect the contribution of phytoplankton size classes to the community (Vidussi *et al.* 2001, Wright and Jeffrey 2006). This limitation can be overcome when remote sensing data are analysed in combination with available *in situ* data. For instance, the synergistic use of *in situ* phytoplankton pigment data and satellite observations can lead to a deeper understanding of phytoplankton dynamics in data-poor regions, where lengthy *in situ* timeseries are not available.

1.5. Thesis objectives and structure

This thesis aims to study, for the first time in the coastal waters of Cyprus, the spatial and temporal variability of phytoplankton communities in relation to physicochemical parameters, by using ocean colour remote sensing data and a 12-month *in situ* timeseries collected from four coastal stations around Cyprus. The aim is to fulfil a gap in knowledge on phytoplankton dynamics in the coastal waters of Cyprus, for which *in situ* data are scarce.

Given the importance of phytoplankton for the functioning of marine ecosystems, they are suitable indicators for changes in the marine environment, including climate changes. Phytoplankton is among the key biological elements in the classification of the ecological status of coastal waters according to the Water Framework Directive (WFD, 2000/60/EC), since they respond fast to changes in water quality, hydrology or climate (Domingues *et al.* 2008).

In order to effectively monitor and predict any future impact of environmental change or anthropogenic pressures to phytoplankton in the coastal waters of Cyprus, the phytoplankton communities will first have to be described and their structure and distribution assessed in relation to factors such as temperature, salinity and nutrients.

The following specific objectives are addressed:

- Investigate phytoplankton phenology, the associated pigment composition, and their seasonal succession, using a combination of 23 years of remotely sensed ocean-colour

observations of chlorophyll-a and a unique *in situ* timeseries of monthly biophysical datasets collected in the coastal waters of Cyprus in 2016.

- Assess the phytoplankton size fractions and chemotaxonomic groups in the coastal zone of Cyprus, and the seasonal phytoplankton variability in relation to physicochemical parameters, using a 12-month timeseries of *in situ* collected data, in four coastal stations.
- Provide, for the first time, a record of microphytoplankton species composition from net samples, investigate any relations between the species present in the four stations and abiotic parameters, and use methods such as rarefaction and extrapolation curves to estimate the expected species diversity at the sampling sites.

The thesis is structured in six main chapters, as follows:

- Chapter I: General introduction to the subject and thesis aims and objectives.
- Chapter II: Phytoplankton phenology in the coastal zone of Cyprus, based on remote sensing and *in situ* observations.
- Chapter III: Seasonal phytoplankton variability in relation to environmental parameters in the coastal waters of Cyprus (eastern Mediterranean).
- Chapter IV: Microphytoplankton species assemblages in the coastal waters of Cyprus
- Chapter V: Conclusion and future work.

II. Phytoplankton phenology in the coastal zone of Cyprus, based on remote sensing and *in situ* observations*

Abstract

Alterations in phytoplankton biomass, community structure and timing of their growth (phenology), are directly implicated in carbon cycle and energy transfer to higher trophic levels of the marine food web. Due to the lack of long-term *in situ* datasets, there is very little information on phytoplankton seasonal succession in Cyprus (eastern Mediterranean Sea). On the other hand, satellite-derived measurements of ocean colour can only provide long-term timeseries of chlorophyll (an index of phytoplankton biomass) up to the 1st optical depth (surface waters). The coupling of both means of observations is essential for understanding phytoplankton dynamics and their response to environmental change. Here, we use 23-years of remotely sensed, regionally-tuned ocean colour observations, along with a unique timeseries of *in situ* phytoplankton pigment composition data, collected in coastal waters of Cyprus during 2016. The satellite observations show an initiation of phytoplankton growth period in November, peak in February and termination in April, with an overall mean duration of ~4 months. An in-depth exploration of *in situ* total Chl-a concentration and phytoplankton pigments revealed that pico- and nanoplankton cells dominated the phytoplankton community. The growth peak in February was dominated by nanophytoplankton and potentially larger diatoms (pigments of *19'* hexanoyloxyfucoxanthin and fucoxanthin, respectively), in the 0-20 m layer. The highest total Chl-a concentration was recorded at a station off Akrotiri peninsula in the south, where strong coastal upwelling has been reported. Another station in the southern part, located next to a fish farm, showed a higher contribution of picophytoplankton during the most oligotrophic period (summer). Our results highlight the importance of using available *in situ* data coupled to ocean colour remote sensing, for monitoring marine ecosystems in areas with limited *in situ* data availability.

* Published in *Remote Sensing* Journal: Demetriou, M., Raitsos, E. D., Kournopoulou, A., Mandalakis, M., Sfenthourakis, S., Psarra, S. 2022, Phytoplankton Phenology in the Coastal Zone of Cyprus, Based on Remote Sensing and *In Situ* Observations. *Remote Sensing*. 14(1), 12, https://doi.org/10.3390/rs14010012

2.1. Introduction

The eastern Mediterranean Sea is characterised as an ultra-oligotrophic region, comparable to the most oligotrophic parts of the global ocean, even considered as a marine desert (Azov 1991, Krom *et al.* 2003). This ultra- oligotrophic nature is reflected in the very low primary production, chlorophyll-a (Chl-a, a proxy of phytoplankton biomass (Jeffrey and Vesk 1997)) and nutrient concentrations, predominance of small-sized phytoplankton and its extremely clear waters (Berman *et al.* 1984b, 1984a, Azov 1986, Li *et al.* 1993, Yacobi *et al.* 1995, Psarra *et al.* 2000, Christaki *et al.* 2001, Vidussi *et al.* 2001). Cyprus, the third largest island in the Mediterranean, located in the Levantine Basin, has a highly exposed coastline and very narrow shelf area, implying that coastal conditions may not significantly differ and thus be representative of the physicochemical regime of the open waters (Petrou *et al.* 2012). The ultraoligotrophic character of the eastern Mediterranean is also documented in Cyprus' coastal waters, through coastal stations' monitoring by the Department of Fisheries and Marine Research (DFMR) as part of the implementation of the European Marine Strategy Framework Directive (MSFD, 2008/56/EC) (EEA 2021). Average mineral nutrient concentrations in the surface layers are at the low-end of the global coastal concentration ranges (Petrou *et al.* 2012). Further, Chl-a values showed some of the lowest concentrations ever recorded in coastal waters (0.01 – 0.09 μg/l) (Bianchi *et al.* 1996). Another characteristic of Cyprus' coastal waters is the extremely limited runoff. In addition, due to the increased drought incidences, 108 dams have been constructed in almost all the streams of the country (Sofroniou and Bishop 2014, WDD 2017), leading to an overexploitation (by 40%) of groundwater resources (Georgiou 2002), ultimately further limiting the natural supply of coastal waters with nutrients.

Phytoplankton is responsible for approximately half of the global primary production (Field *et al.* 1998, Falkowski and Raven 2007), directly implicated in carbon cycle and energy transfer to higher trophic levels, supporting the marine food webs by providing essential food source for many commercially important fish species' larvae and juveniles (Reynolds 2006). Phytoplankton phenology metrics such as growth initiation, time of maximum amplitude, duration and termination, are categorised as ecological indicators (Platt and Sathyendranath 2008). Phenology metrics are a key factor in determining the structure of food webs and ecosystem function (Edwards and Richardson 2004, Racault *et al.* 2012). Monitoring these indicators offers a way to observe the response of marine ecosystems to environmental change (Edwards and Richardson 2004, Platt and Sathyendranath 2008, Racault *et al.* 2014, Gittings

et al. 2018). Marine phytoplankton play a fundamental role in climate through carbon cycling. Alterations in phytoplankton abundance and composition driven by climate change may alter the marine biogeochemical cycles, with far reaching consequences for the marine environment (Robinson 2017). Further, oceanic warming may cause mismatches between marine organisms' reproductive cycles and their planktonic diet (Koeller *et al.* 2009). According to the match / mismatch hypothesis, fish stock recruitment depends on the synchronous production of food (Cushing 1990), and any interannual variations in phytoplankton phenology can have widespread ecosystem implications. Therefore, changes in the phytoplankton phenology can have detrimental cascade effects on the survival of commercially important species (Platt *et al.* 2003, Koeller *et al.* 2009, Gittings *et al.* 2021).

Despite the significance of phytoplankton in the functioning of marine ecosystems, the seasonal succession of phytoplankton in Cyprus' coastal waters has yet to be determined, primarily due to the lack of *in situ* measurements. The only study to determine Chl-a and carotenoids based on a High-Performance Liquid Chromatography (HPLC) method took place in June and July 1993, where the dominant phytoplankton classes were determined to be chlorophytes, cyanobacteria and prochlorophytes, based on chlorophyll-b and zeaxanthin concentrations (Bianchi *et al.* 1996).

Alternatively, ocean colour remote sensing provides long-term monitoring of Chl-a concentrations. Therefore, measuring Chl-a concentration using remote sensing can assess phytoplankton ecological indicators and characterise the status of marine ecosystems (Platt and Sathyendranath 2008, Racault *et al.* 2014). Since knowledge on long-term and large-scale data on phytoplankton phenology based on *in situ* data in Cyprus is not available, ocean colour remote sensing offers the only means to obtain such information in this area. However, satellite observations are limited in determining only total Chl-a at surface and do not offer information on the contribution of individual pigments to TChl-a. Knowledge of the pigment composition is important for assessing the composition of phytoplanktonic communities, since most of the pigments have chemotaxonomic associations (i.e. they are biomarkers for specific phytoplankton groups), and may reflect the contribution of phytoplankton size classes (pico-, nano- and microphytoplankton) (Vidussi *et al.* 2001, Wright and Jeffrey 2006). On the other hand, *in situ* measurements are limited in space and time. The synergy of both *in situ* and satellite observations may lead to a deeper understanding of phytoplankton dynamics in data-poor regions, such as the coastal waters of Cyprus.

Here, 23 years of remotely sensed ocean-colour observations are combined with a unique *in situ* timeseries of monthly biophysical datasets collected in the coastal waters of Cyprus in 2016, to investigate phytoplankton phenology, the associated pigment composition and their seasonal succession. Further, we investigate if coastal waters of Cyprus are indeed representative of the oligotrophic offshore waters of the eastern Mediterranean Sea.

2.2. Materials and Methods

2.2.1. Satellite Remote Sensing Data

The multi-sensor Chl-a (mg/m3) daily product at 1-km resolution was obtained from the EU Copernicus Marine Environment Monitoring Service (CMEMS) at https://marine.copernicus.eu/ that is a merge of MODIS-Aqua, NOAA-20-VIIRS, NPP-VIIRS, Sentinel3A-OLCI data, covering the time period from September 1997 to December 2020. The bio-optical algorithm used to estimate Chl-a concentration is a combination of MedOC4 for Case 1 (Volpe *et al.* 2019) and AD4 for Case 2 waters (Berthon and Zibordi 2004), regionally-tuned for the Mediterranean Sea. We note that remotely-sensed ocean colour algorithms have known limitations in shallow oligotrophic waters, generally resulting in an overestimation in chlorophyll concentrations (D'Ortenzio *et al.* 2000, Volpe *et al.* 2007, Brewin *et al.* 2013). We acknowledge that regardless of the usage of a regionally tuned algorithm (MEDOC4), there are still some slight discrepancies in comparison to our *in situ* datasets, especially during the most oligotrophic period (summer). Further validation of the current available algorithms with additional ground-truth datasets, could ultimately lead to an improved product.

The computation of the phenology metrics, as implemented in this study, follows the approach of Racault et al. (2015). First, we extracted the 7-day chlorophyll-a climatology (23 years of data) and the seasonal cycle of 2016 (during which the in situ data were collected), using the average of a 3×3 pixel window centred in the location of each sampling station. Chlorophyll-a climatology (Chl-aSat climatology) was generated by calculating the 7-day average Chl-a for the period 1997-2020, while the seasonal cycle of 2016 (Chl-aSat 2016) refers to the weekly Chl-a variations of this specific year. The in situ Chl-a data were matched up in time (temporal matchup) and space (latitude and longitude) with satellite derived datasets. In order to detect the main phytoplankton growth, the calendar year was delimited from August to July. Thus, the phenology indices computation for 2016 required time-series from August 2015 to July 2017. Resampling the data (i.e., calculating 7-day composites from daily observations)

provided a full, gap-free seasonal cycle that is essential for the calculation of the phenology indices (Gittings *et al.* 2019b).

Using the cumulative sum of anomalies approach, the timings of initiation, peak, termination, and duration were determined using a threshold criterion of median plus 15% (Gittings *et al.* 2018), that was recognized as the most representative for capturing the main phytoplankton growth in the study area. Various thresholds have been utilised in different phenology studies (Racault *et al.* 2012, Gittings *et al.* 2018, Salgado-Hernanz *et al.* 2019), depending on the type of the analysis (e.g. interannual or seasonal), but also on the chlorophyll variation within a region. Using this threshold, the anomalies were calculated by subtracting the threshold criterion and the cumulative sum of the anomalies was then produced. The gradient of the cumulative sums, smoothed with a Gaussian filter, was used to identify each one of the four metrics. Timing of initiation was recognised as the first time Chl-a concentration rose above the threshold criterion, while termination was found when the gradient went from positive to negative. Peaking time was set, as the time Chl-a reached the maximum value and duration expresses the number of 7-day periods between initiation and termination.

2.2.2. *In situ* data

Sampling was carried out monthly, between January and December 2016. Samples were collected from three coastal stations (Figure II.***1***). Station Pyrgos (PYR) is located off Pyrgos village on the northwest of Cyprus, whereas station Akrotiri (AKR) is located off Akrotiri peninsula in the south. Station Vasilikos Fish Farm (VAS) is in Vasilikos bay in the south, next to an aquaculture farm.

Conductivity – temperature – depth (CTD) measurements were collected with an SBE-19plus profiler. Seawater for biogeochemical analyses was collected with a 5 L Niskin bottle at different depths (2, 10, 20, 50, 75, 100 m), according to the bathymetry of each station (PYR 134 m, AKR 130 m, VAS 55 m).

For the HPLC pigment analysis, 4 L of seawater were filtered through Whatman GF/F filters under low vacuum pressure (<150 mmHg). The filters were immediately frozen in liquid nitrogen and stored at -80 °C until analysis, following the protocol described by van Heukelem and Thomas (Van Heukelem and Thomas 2001), as modified by Lagaria *et al.* (2017). Samples were further analysed for Chl-a utilizing a microplate-based assay, as per Mandalakis *et al.* (2017).

In total, 36 profiles were analysed. For each profile, Chl-a concentrations were calculated by integrating Chl-a between the surface and 20 m depth, according to the trapezoid rule (Laws 1997). The integrated values per surface area (m^{-2}) were further normalised over the respective depth to provide a mean weighted value (m^{-3}). The *in situ* Chl-a profiles were averaged over the first 20m depth, to be comparable with the satellite-derived observations. We calculated the first optical depth (Z90), which represents how deep the satellite-derived radiance penetrates in the water column. We firstly determined the diffuse attenuation coefficient Kd(490), utilizing the OC-CCI Kd product, as per Al-Naimi *et al.* (2017). The overall averaged first optical depth of the coastal zone of Cyprus over the studied period was estimated to be ~26 m depth ($Z90=1/Kd(490) \approx 25.9$ m). The Mixed Layer Depth (MLD) was calculated using a fixed threshold criterion on temperature values ($\Delta T = 0.2^{o}C$), for which the MLD is the depth at which temperature changes by the given threshold value relative to the near-surface depth of 10 m (de Boyer Montégut 2004).

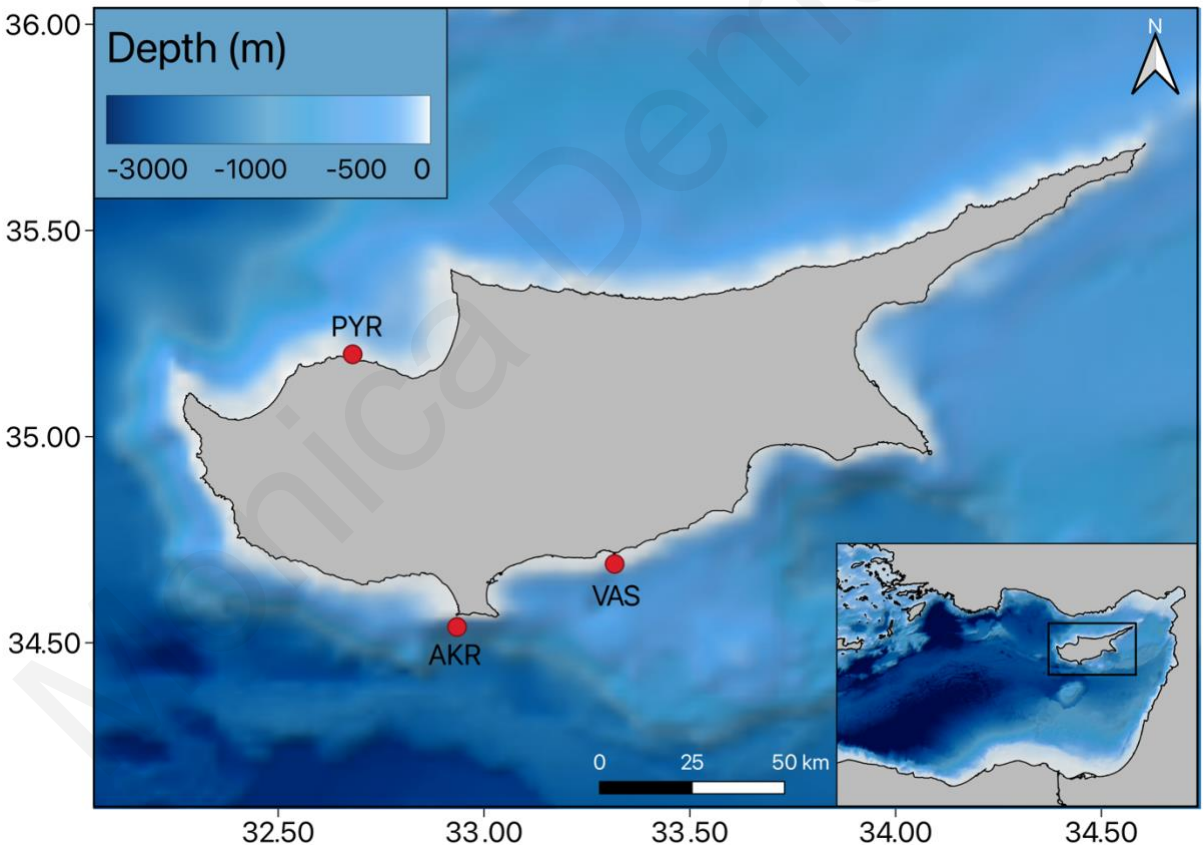

Figure II.1: The location of Cyprus at the eastern Mediterranean, indicating the bathymetry and the three sampling stations, Pyrgos (PYR), Akrotiri (AKR), and Vasilikos Fish Farm (VAS1). Bathymetric data obtained from the National Geophysical Data Centre (NGDC) database ETOPO1 (Amante and Eakins 2009), and coastline data obtained from naturalearthdata.com.

2.2.3. Phytoplankton pigment-based size classes

The composition of phytoplankton communities can be estimated using phytoplankton accessory pigments as biomarkers. Seven major diagnostic pigments (DP) that are associated with phytoplankton size classes have been used (Vidussi *et al.* 2001, Uitz *et al.* 2006), under the following assumptions: (1) microphytoplankton (>20 μm) is comprised of diatoms and dinoflagellates, which are characterized by fucoxanthin and peridinin, (2) nanophytoplankton (2 – 20 μm) is composed of cryptophytes, chromophytes and nanoflagellates (alloxanthin, 19' hex- and 19' butanoyloxyfucoxanthin), and (3) green flagellates, prochlorophytes and cyanobacteria (zeaxanthin and TChlb) make up picophytoplankton (<2 μm) (Table II.***1***) (Lagaria *et al.* 2017, Brewin *et al.* 2019, Gittings *et al.* 2019a).

Table II.1: Phytoplankton diagnostic pigments, abbreviations, taxonomic significance and size classes (from Jeffrey *et al.* (2011).

Pigments	Abbreviations	Taxonomic significance	Size μm
Zeaxanthin	Zea	Cyanobacteria and Prochlorophytes	< 2
Divinyl-chlorophyll a	DVChl-a	Prochlorophytes	< 2
19' hexanoyloxyfucoxanthin	Hex	Prymnesiophytes (major)	2-20
19' butanoyloxyfucoxanthin	But	Pelagophytes (major), Prymnesiophytes	2-20
Alloxanthin	Allo	Cryptophytes	2-20
Fucoxanthin	Fuc	Diatoms (major), Prymnesiophytes	> 20
Peridinin	Peri	Dinoflagellates	> 20

The equations described by Uitz *et al.* (2006) have been used to derive the relative proportions of the phytoplankton size classes (Eqs. 1-3), as well as the total Chl-a (TChl-a) concentration associated with each size class (Eqs. 5-7):

$$f_{micro} = (1.41[Fuc] + 1.41[Peri])/DP_w \quad (1)$$

$$f_{nano} = (1.27[Hex] + 0.35[But] + 0.60[Allo])/DP_w \quad (2)$$

$$f_{pico} = (1.01[TChlb] + 0.86[Zea])/DP_w \quad (3)$$

Where DP_w is the weighted sum of the seven diagnostic pigments:

$$DP_w = 1.41[Fuc] + 1.41[Peri] + 1.27[Hex] + 0.35[But] + 0.60[Allo] + 1.01[TChlb] + 0.86[Zea] \quad (4)$$

$$micro - [TChla] = f_{micro} * [TChla] \quad (5)$$

$$nano - [TChla] = f_{nano} * [TChla] \quad (6)$$

$$pico - [TChla] = f_{pico} * [TChla] \quad (7)$$

2.2.4. Data analysis

A one-way ANOVA was performed to test for differences between stations, among sampling periods (mixed and stratified), and between the surface (0-20 m) and the deeper layer. Data were log-transformed in order to meet normality and homogeneity of variance requirements. All analysis were carried out in R 4.1.0 , using package stats (R Core Team 2021).

Vertical profiles were created in R 4.1.0 (R Core Team 2021), using the Multilevel B-spline Approximation (MBA) algorithm for interpolation, with packages MBA *(*Finley *et al. 2017)* and ggplot2 (Wickham 2016).

2.3. Results

2.3.1. Phenology metrics from satellite and *in situ* data retrievals

Twenty-three years of satellite-derived Chl-a (Chl-a_{sat} climatology (1997-2020)) were used to compute the seasonal climatology of phytoplankton biomass and phenology. The phytoplankton growth period in the coastal waters of Cyprus initiates in early November in PYR and VAS and late November in AKR. The growth period terminates in mid-April in PYR and early April in AKR and VAS. The mean duration of the growth period lasts approximately 4 to 5 months. In 2016 (the period of *in situ* sampling), an earlier initiation of the growth period was observed in all stations, with PYR and VAS growth initiating in mid-November and AKR in early December. The growth period in all stations terminated in mid-March, and the growth duration was shorter by almost a month (Figure II.***2*** - Figure II.***4***).

The highest TChl-a concentration is detected in AKR, with the highest growth period occurring between January and March. The peak in PYR occurs towards the end of March. The growth period in VAS is more stable, without prominent peaks as seen in the other two stations. The results from the integrated, HPLC derived TChl-a ($Chla_{int}$, *in situ* data) were compared to the satellite derived values. A correlation between $Chla_{sat}$ 2016 and $Chla_{int}$ was observed ($n = 30$, $\rho = 0.5$, $p<0.005$). The satellite and *in situ* data match in regard to the initiation of the main growth period, which occurs in the autumn, as well as in the timing of termination, which occurs in spring. The timing of the growth period initiation in November matches the deepening of the Mixed Layer Depth and higher concentrations of Chl-a in the surface layers. The termination of the growth period in April coincides with a shallow MLD and low surface Chl-a concentrations.

A strong stratification was observed starting in spring and lasting until December, in all sampled stations (Figure II.***2*** - Figure II.***4***). A sharp thermocline was located at 20 – 50 m in PYR and AKR and at 10 – 40 m in VAS. Salinity was high throughout the year (>38.7), representative of the high salinity Levantine waters. The halocline followed the distribution of the thermocline in all sampled stations.

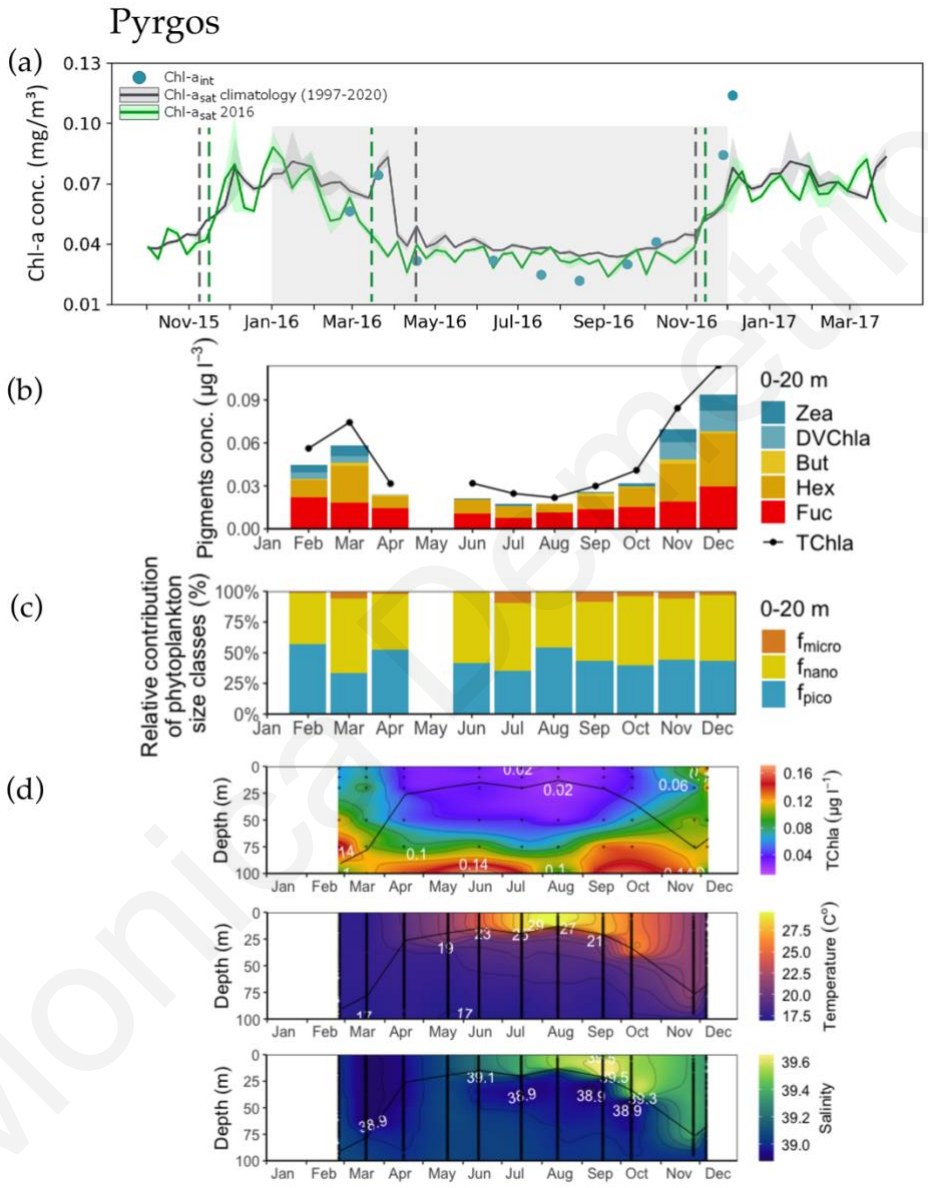

Figure II.2: Time series of satellite-derived Chl-a consecrations, diagnostic pigment concentrations and vertical profiles of total Chl-a, temperature and salinity in Pyrgos (PYR) station. **(a)** Climatology time-series (based on 23-year OC-CNR data of daily composites) (Chl-a_{sat} climatology (1997-2020) in comparison with satellite-derived Chl-a concentration from October 2015 to March 2017 (Chl-a_{sat} 2016). Blue dots represent the in situ measurements (Chl-a_{int}) taken between January and December 2016 (shaded area). The dashed lines represent the timing of initiation and termination of the main phytoplankton growth, **(b)** Diagnostic pigments concentrations for the 0-20 m layer, **(c)** Percentages associated to the pico- (fpico), nano- (fnano) and microphytoplankton (fmicro) size classes, for the 0-20 m layer, **(d)** Vertical profiles of CTD temperature, salinity, and HPLC total Chl-a concentration. The black line represents the Mixed Layer Depth (MLD). Note: The in situ data are a snapshot (one day in each month) compared to the weekly averages of the satellite retrieved data.

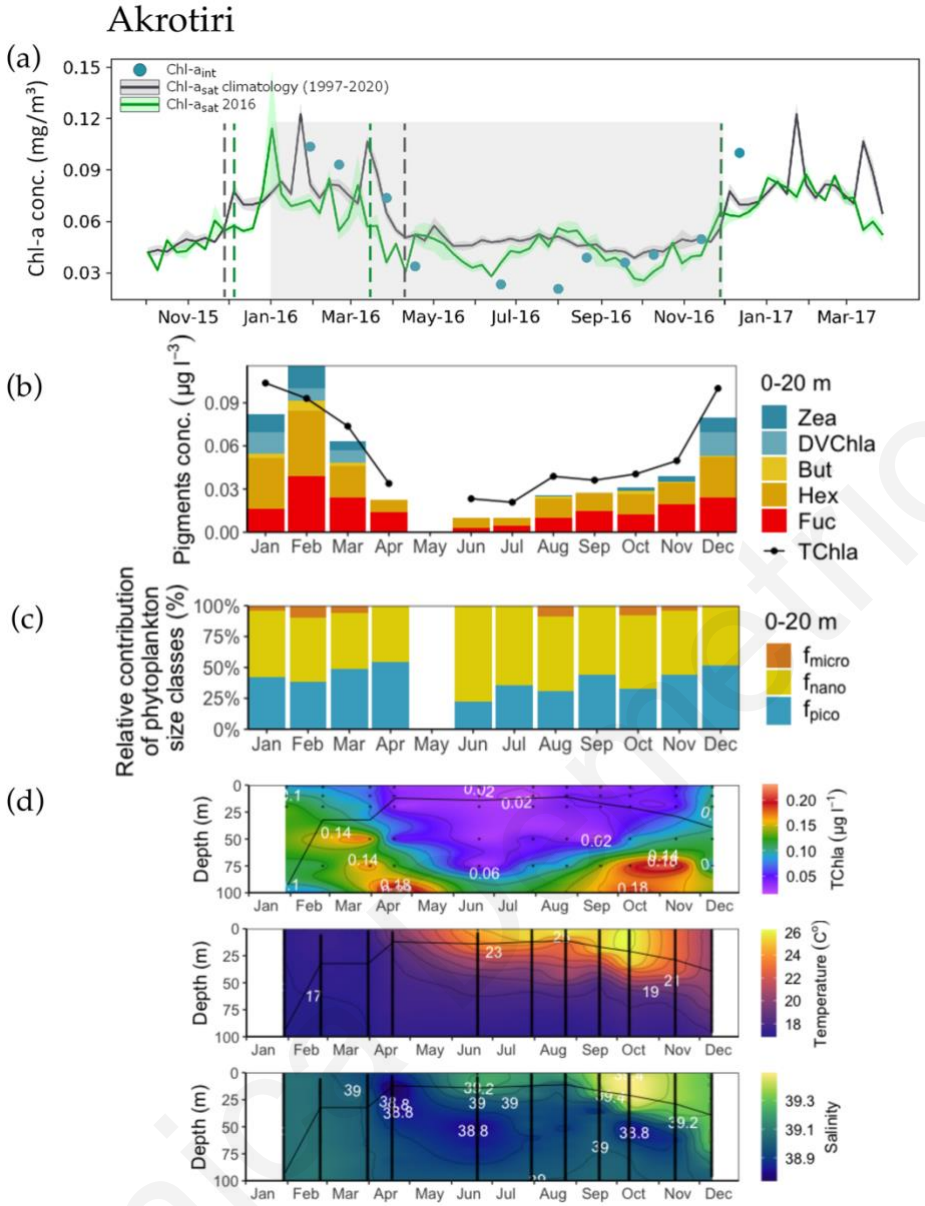

Figure II.3: Time series of satellite-derived Chl-a consecrations, diagnostic pigment concentrations and vertical profiles of total Chl-a, temperature, and salinity in Akrotiri (AKR) station. Panels as in figure 2.

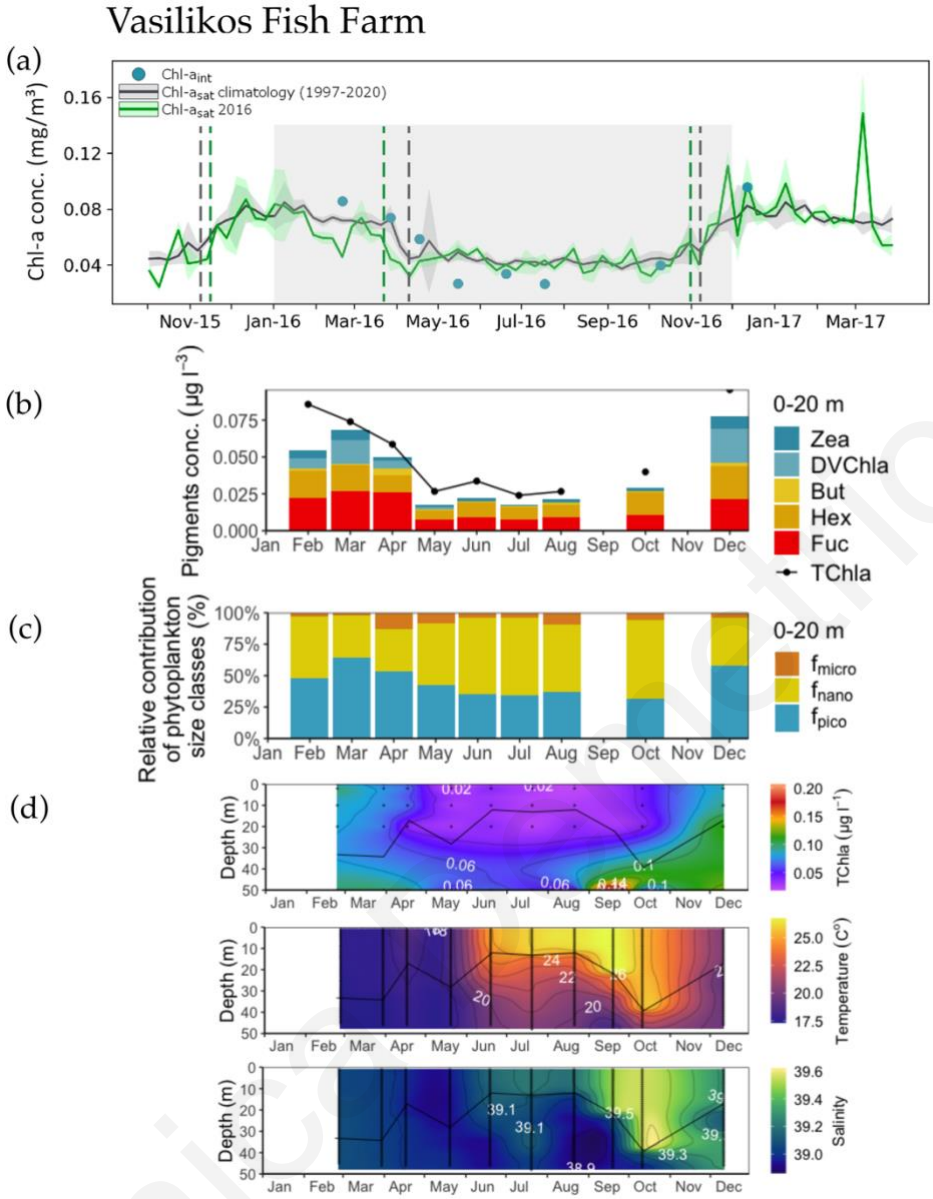

Figure II.4: Time series of satellite-derived Chl-a consecrations, diagnostic pigment concentrations and vertical profiles of total Chl-a, temperature, and salinity in Vasilikos Fish Farm (VAS) station. Panels as in figure 2.

2.3.2. Concentration and spatial distribution of phytoplankton pigments

During the stratified period (May to November), TChl-a had a homogenous distribution in all stations (Figure II.***2*** - Figure II.***4***). The lowest TChl-a values (0.01 µg L-1 in PYR and 0.02 µg L-1 in AKR and VAS) were recorded in the upper layer (0 – 20 m), whereas the maximum values were recorded at 100 m depth in PYR (0.17 µg L-1) and AKR (0.23 µg L-1) and at 50 m in VAS (0.21 µg L-1). Maximum concentrations of Chl-a were more prominent during spring and summer, indicating the presence of a subsurface chlorophyll maximum (SCM) layer (Figure S1).

Other diagnostic pigments typically detected in all stations were DVChl-a, Zea, But, Hex and Fuc (Table II.***1*** for abbreviations, Figure S2). Hex (prymnesiophytes) and But (pelagophytes and chrysophytes) showed a similar distribution pattern to Chl-a. Zea (cyanobacteria) showed a decreasing trend with depth during the mixed period (January – April) in VAS station, whereas highest values of Zea were recorded in the deepest layers in PYR during the stratified period (May – December) (Figure S3). Zea and DVChl-a had minimal concentrations during the stratified period in all stations (Figure II.***2*** - Figure II.***4***).

The dynamics of HPLC diagnostic pigments data revealed the seasonal changes in the phytoplankton community structure. TChl-a, Zea, DVChl-a, But and Fuc did not show a significantly different distribution between stations, compared to Hex, which displayed different distributions between AKR and VAS. A difference in the percentage contribution of pico- and nanophytoplankton was also observed between AKR and VAS. Only Zea had a significantly higher concentration over the mixed period for the water column. For the 0 - 20 m layer, TChl-a, But and Zea had a significantly higher concentration over the mixed period. DVChl-a had a similar distribution throughout the sampling period, with almost undetectable values in the 0-20 m layer. Further, the percentage contribution of pico- and nanophytoplankton differed between the mixed and stratified periods over the 0-20 m layer. The concentrations of TChl-a, But, Hex and Fuc varied significantly between the entire water column and the 0-20 m depth. DVChl-a and Fuco had a similar distribution between the depth layers (Table II.***2***).

During the phytoplankton growth peak in January – February, the main pigment contribution to the TChl-a comes from Hex and Fuc, indicating a prevalence of nanophytoplankton and potentially the presence of larger cells during the peak (diatoms), even though Fuc is also found in prymnesiophytes (Figure II.***2***b - Figure II.***4***b).

Table II.2: Results of one-way ANOVA tests of differences between stations, between seasons and between depths (0-20 m, >20 m).

	Between stations		**Between seasons**				**Between depths**	
			Water column		**0-20 m**			
Variable	**F**	**p**	**F**	**p**	**F**	**p**	**F**	**p**
TChl-a	(2, 20) = 0.68		(1, 21) = 2.25		(1, 17) = 6.07	*	(1, 41) = 15.89	***
Zea	(2, 20) = 0.18		(1, 21) = 6.78	*	(1, 17) = 8.20	**	(1, 41) = 0.63	
DVChl-a	(2, 20) = 1.35		(1, 21) = 0.03		(1, 9) = 0.007		(1, 33) = 3.00	
But	(2, 20) = 1.30		(1, 21) = 1.42		(1, 17) = 6.02	*	(1, 41) = 10.16	**
Hex	(2, 20) = 6.81	**	(1, 21) = 0.69		(1, 17) = 2.12		(1, 41) = 19.17	***
Fuc	(2, 20) = 0.40		(1, 21) = 1.90		(1, 16) = 1.83		(1, 41) = 2.40	*
f_{pico}	(2, 20) = 4.65	*	(1, 21) = 0.32		(1, 17) = 4.60	*	(1, 41) = 2.40	
f_{nano}	(2, 20) = 5.67	**	(1, 21) = 0.75		(1, 17) = 5.56	*	(1, 41) = 9.57	**
f_{micro}	(2, 20) = 1.74		(1, 21) = 1.24		(1, 17) = 0.92		(1, 41) = 0.06	

p-values: 0.05*, 0.01**. 0.001***

2.3.3. Phytoplankton size structure

The weighted sum of the diagnostic pigments (ΣDP_w) was linearly related to TChl-a, making DP a valid estimator of the measured TChl-a (linear regression DP = 0.6629 TChl-a + 0.0023, r2 = 0.92, Fig. S4). The pigment-based estimations showed that during the mixed period, f_{pico} accounted for about half of the depth-integrated phytoplankton biomass in the water column and the 0 - 20 m layer in all stations, and f_{nano} for the remaining half in PYR and AKR and 39% in VAS. During the stratified period, the percentage of f_{nano} in all stations was higher (around 60%), with f_{pico} accounting for approximately 40% of the depth-integrated phytoplankton biomass. The percentage of f_{micro} did not exceed 7% in all stations, during both the mixed and stratified periods (Table II.***3***).

In general, the vertical distribution of total Chl-a associated with picophytoplankton followed the distribution of Zea and DVChl a, the distribution of total Chl-a associated with nanophytoplankton followed those of Hex and But, and the total Chl-a associated with microphytoplankton was driven by the distribution pattern of Fuco (Figure S2, Figure S3).

The phytoplankton community was mainly dominated by picophytoplankton and nanophytoplankton, both following the distribution of TChl-a. The very low concentrations of microphytoplankton could point to the scarcity of diatoms in the study area.

Table II.3: Mean (±SD) estimated contribution of pico- (f_{pico}), nano- (f_{nano}) and microphytoplankton (f_{micro}) as derived from pigment analysis, integrated over the water column and the surface layer (0-20 m), over the mixed (January – April) and stratified (May – December) periods.

			f_{pico} (%)		f_{nano} (%)		f_{micro} (%)	
Station	**Period**	**Depth**	**Range**	**Mean (±SD)**	**Range**	**Mean (±SD)**	**Range**	**Mean (±SD)**
PYR	Mixed	0-20	34-52	44±9	37-61	46±13	2-6	3±2
		0-100	38-50	44±6	46-57	51±6	2-5	3±1
	Stratified	0-20	35-54	43±6	45-59	52±5	3-10	5±4
		0-100	36-54	47±6	42-55	48±4	2-11	5±3
AKR	Mixed	0-20	38-54	46±7	45-54	49±4	4-10	7±3
		0-100	33-53	43±1	45-57	51±6	2-10	6±4
	Stratified	0-20	22-52	37±1	47-78	60±10	3-8	4±4
		0-100	26-57	39±13	42-73	58±13	1-7	3±2
VAS	Mixed	0-20	48-64	55±8	34-49	39±9	2-13	6±6
		0-50	47-64	55±9	32-49	39±8	4-10	6±4
	Stratified	0-20	30-58	40±10	38-62	54±9	4-10	6±3
		0-50	20-55	38±13	40-73	55±13	5-9	7±2

2.4. Discussion

Long-term timeseries of phytoplankton phenology based both on ocean colour remote sensing and *in situ* datasets can improve our understanding of phytoplankton seasonal succession. However, such a synergistic analysis for the coastal waters of Cyprus has not been carried out prior to the current study, primarily due to the lack of *in situ* timeseries on phytoplankton dynamics (on biomass and pigments). Therefore, this is the first attempt to characterise the phytoplankton dynamics in the coastal waters of Cyprus. The results from this study indicate that *in situ* data are consistent with the satellite-derived phytoplankton phenology in the coastal waters of Cyprus. The initiation of the phytoplankton growth period seen from the satellite in November, coincides with increased concentrations of the integrated total Chl-a calculated from HPLC and with an increase in Chl-a concentrations in the surface layer. The subsurface chlorophyll maximum (SCM) in the oligotrophic Levantine is a permanent feature (Barbieux *et al.* 2019), and the increase in surface Chl-a concentration captured by the satellite in November could be attributed to the redistribution of Chl-a following the erosion of the SCM after the winter mixing, as well as to the resulting enhanced nutrient availability within the mixed layer, which triggers phytoplankton growth. The termination of the growth period in March/April co-occurs with a shallowing of the MLD, the onset of the thermocline formation which in turn limits the amount of nutrients advected to shallower depths, and the re-establishment of the SCM. The maximum values of Chl-a have been recorded at 75 and 100 m depth, consistent with the SCM layer recorded in the Levantine, where the vertical distribution of Chl-a reaches maximum concentrations at around 90 – 110 m depth (Yacobi *et al.* 1995, Krom *et al.* 2005).

Based on satellite remote sensing data, the phytoplankton growth period in 2016 showed an earlier termination and thus a shorter duration compared to the Chl-a climatology (~23-year). This shorter duration of phytoplankton growth period was also evident in the open waters of eastern Mediterranean basin by the analysis of Salgado-Hermanz et al. (Salgado-Hernanz *et al.* 2019). Various factors, global and regional, can affect the phytoplankton growth periods, leading to cascading effects in the functioning of the ecosystem, since the shifting of the growth period could alter the entire food web structure (Cushing 1990). Earlier phytoplankton growth periods could be attributed to the limited nutrients in the eastern basin, leading to very low Chl-a concentrations. Further, the El Niño Southern Oscillation index (ENSO) has been found to impact Chl-a variability in the eastern Mediterranean during its positive phase (Salgado-Hernanz 2019). A correlation between Chl-a and nutrient rich Saharan dust deposition has been

found in the eastern Mediterranean (Gallisai *et al.* 2014), and ENSO has been found to control the export of Saharan dust in the summer (Deflorio *et al.* 2005). Therefore, the link between Chl-a and ENSO could possibly be explained by variations in atmospheric dust deposition.

The pattern of phytoplankton growth period in the coastal waters of Cyprus shows a higher biomass between November and April and lower values in the remaining period. This pattern is in accordance to the "no bloom" classification of the oligotrophic area of the open waters of eastern Mediterranean, were a smooth rise in Chl-a concentration has been observed in October and terminates in March, with higher concentrations in fall and winter and lower values in spring and summer (D'Ortenzio and Ribera d'Alcalà 2009).

Since the phytoplankton size is associated with the type of waters, i.e. small sized phytoplankton is more prominent in oligotrophic environments and larger cells are associated with more productive waters, investigating the size structure of phytoplankton community could provide more information than the composition of the phytoplankton community itself (Vidussi *et al.* 2001). Pigment-based estimations of the relative contribution of phytoplankton size classes can be used to determine the size distribution of phytoplankton, as an alternative to the often complicated and time-consuming various cell counting methods (flow cytometry, inverted microscopy). Based on our HPLC pigments analysis, the pico- and nanoplanktonic cells represent the most significant part of the community, consistent with oligotrophic Levantine open waters, and other Mediterranean areas where a dominance of small-sized phytoplankton up to 80 – 100% of TChl-a has been recorded (Li *et al.* 1993, Yacobi *et al.* 1995, Vidussi *et al.* 2001, Siokou-Frangou *et al.* 2010, Yücel 2013). During the mixed season (January – April), pico- and nanophytoplankton percentages are almost of equal importance, each one accounting for approximately 50% of the total biomass. Picophytoplankton seems to dominate slightly more in VAS station in the southeast. This station is located next to a fish farm cage and the increased picophytoplankton contribution to the total Chl-a is in agreement with Tsagaraki *et al.* (Tsagaraki *et al.* 2013). During the stratified period (May – December) in southern stations AKR and VAS, the percentage of nanophytoplankton is higher, thus nanophytoplankton dominates over picophytoplankton. In general, it has been found that picoplankton dominates the eastern Mediterranean surface layers during most of the year (Yacobi *et al.* 1995, Zohary *et al.* 1998, Tanaka *et al.* 2007), with the exception of the dynamic mesoscale structures were nanophytoplankton seems to be the dominant size class (Psarra *et al.* 2005, Tanaka *et al.* 2007). More specifically, when the microbial food web within and outside the Cyprus Eddy was analysed, nanoplankton were dominant followed by picoplankton

and then ciliates (Tanaka *et al.* 2007). Nanophytoplankton was also found to be dominant throughout the year in the Mediterranean, with a relative constant contribution to the total primary production (Uitz *et al.* 2012). Other studies carried out in the eastern Mediterranean found that the most dominant size class in the northern Levantine was picophytoplankton (Yücel 2018), which was also found to be dominant off the coast of Israel during the summer and fall, whereas nanoplankton was dominant during spring (Azov 1986).

Akrotiri station had the highest TChl-a concentration. The southwestern coast of Cyprus, around Akrotiri peninsula, is characterized by cooler waters, most likely due to a combination of upwelling and advection from the Rhodes Gyre (Zodiatis *et al.* 2008). This coastal upwelling feature, evident during the summer, is caused by persistent westerly winds that affect the near-surface layers. The advection of cool water from the Rhodes Gyre to the southern coast of Cyprus is modelled by the Cyprus Coastal Ocean Forecasting and Observing System (CYCOFOS - http://www.oceanography.ucy.ac.cy/cycofos) (Zodiatis *et al.* 2008). The use of drifters and gliders to monitor the water masses properties of the Levantine during September 2016 and August 2017 (Mauri *et al.* 2019) confirmed this strong upwelling during the summer months in the south of Cyprus.

The extremely low chlorophyll-a values recorded in the coastal waters of Cyprus reflect the ultra-oligotrophy of the eastern Mediterranean. Eddies and currents in the area control the distribution of nutrients in the surface waters (Ediger and Yilmaz 1996), whereas atmospheric depositions provide a considerable nutrient input in an otherwise nutrient depleted area with limited input from external sources (Markaki *et al.* 2003, 2010, Krom *et al.* 2004, Herut *et al.* 2005). Even though studies conducted in the coastal waters of Turkey, north of Cyprus, recorded some of the highest total primary production values in the Mediterranean (Yücel 2013, 2018), such values are not observed in the northernmost PYR station, indicating that the exchange of productive coastal waters with oligotrophic offshore waters in the northeastern Levantine is limited.

The current study provides for the first time a complete seasonal cycle of phytoplankton phenology in the coastal waters of Cyprus, using a combination of ocean colour remote sensing observations and analysis of *in situ* phytoplankton pigments. This *in situ* dataset is the first such dataset of phytoplankton pigments in this area, and the fact that the phenology indicators derived from the *in situ* Chl-a data closely match the satellite derived phenology metrics, indicates that ocean colour remote sensing can be used to monitor and observe the marine ecosystem of Cyprus and effectively that of the eastern Levantine, where *in situ* observations

are scarce. For instance, phytoplankton size classes (PSCs) can be derived using satellite ocean colour observations. We anticipate that future work will entail the re-parameterision of an abundance-based PSC model (e.g., (Brewin *et al.* 2010)) with the in situ pigment dataset utilised in this study, in order to investigate variability of specific phytoplankton size classes. This approach has already been successfully applied in several oligotrophic oceanic regions like the Red Sea (Brewin *et al.* 2019, Gittings *et al.* 2019a, 2021) and the Mediterranean Sea (Sammartino *et al.* 2015). Ultimately, this could enable a deeper understanding of how oceanic warming is affecting phytoplankton phenology and the seasonal succession of phytoplankton pigments. Considering that climate change impacts the timing of phytoplankton growth periods (Gittings *et al.* 2018), this could alter the balance between food availability and the fitness and recruitment of higher trophic levels.

2.5. Conclusions

To the best of our knowledge, the present study is the first attempt to provide information on the phytoplankton seasonal succession in Cyprus, utilising a synergistic analysis of ocean colour remote sensing and in situ data. Further, it is demonstrated that the coastal waters of Cyprus reflect the ultra-oligotrophic open waters of the Levantine, as evident from the extremely low chlorophyll-a values recorded in the study area.

The overall mean duration of the phytoplankton growth period in the coastal waters of Cyprus is approximately 4 months, initiating in November and terminating in April. The higher Chl-a concentrations observed between November and April classify the coastal waters of Cyprus under the "no bloom" category of the open waters of the oligotrophic eastern Mediterranean (D'Ortenzio and Ribera d'Alcalà 2009). The phytoplankton community in the coastal waters of Cyprus is dominated by pico- and nanoplankton cells. Nanophytoplakton is dominant during the growth peak in February, whereas the rest of the year, picoplanktonic cells dominate the community, consistent with oligotrophic Levantine open waters.

The current study demonstrates the importance of ocean colour remote sensing in regions with limited in situ datasets, such as Cyprus and the eastern Levantine. The close match observed between the in situ derived phenology indicators and the satellite derived phenology metrics, indicates the suitability of ocean colour remote sensing in monitoring the marine ecosystem in the study area. This analysis paves the way for further investigation of the variability of specific phytoplankton size classes through the re-parameterisation of an abundance-based PSC model

(Brewin *et al.* 2010), as well as for assessing the impact of oceanic warming on phytoplankton phenology. Such work will be paramount for developing a better understanding on phytoplankton dynamics and seasonal succession in the coastal waters of Cyprus, with implications on fisheries and the marine environment in general.

III. Seasonal phytoplankton variability in relation to environmental parameters in the coastal waters of Cyprus (eastern Mediterranean)

3.1. Introduction

Phytoplankton, the main primary producers of the marine ecosystem, play an essential role in the ocean biogeochemical cycles, linking atmospheric and oceanic processes. A major component of the global carbon cycle, the biological carbon pump, transfers carbon as the net result of phytoplankton photosynthesis, calcification and respiration of phytoplankton to the deep ocean, where it is made available to other trophic levels (Falkowski *et al.* 1998, Field *et al.* 1998, Robinson 2017). The biological pump's efficiency is determined by phytoplankton physiology and community structure, which in turn are influenced by the ocean's physico-chemical conditions (Basu and Mackey 2018).

The biogeochemical cycling of carbon, nitrogen and phosphorus is greatly affected by phytoplankton community composition, since different functional groups have different requirements for the above elements, for example diatoms sink faster due to their heavy silica frustule, thus being very efficient in sequestering carbon to the deep ocean (Falkowski *et al.* 1998, 2004). Grouping phytoplankton in functional groups, based on common traits, can be used to predict community composition in various environments (Litchman and Klausmeier 2008). Cell size is one such trait, correlated with other traits such a nutrients utilization and grazer pressure (Litchman and Klausmeier 2008). The higher surface to volume ratio of small cells makes them more efficient in acquiring limiting nutrients, in the expense of being more vulnerable to grazing (Thingstad *et al.* 2005). The traditional phytoplankton classification method that involves microscope observations is the only method that can estimate biodiversity through species identification, however, it is complicated and time consuming. On the other hand, alternative methods such as High Performance Liquid Chromatography (HPLC) and the application of the CHEMTAX algorithm (Mackey *et al.* 1996) can be used for bulk assessments of groups and size discriminations efficiently and reliably.

The Levantine basin of the eastern Mediterranean Sea is an ultra-oligotrophic marine area (Yacobi *et al.* 1995, Krom *et al.* 2003, Kress *et al.* 2014), with low nutrient and chlrophyll-a (chl-a) concentrations, low primary production and high contribution of small-sized

phytoplankton (Berman *et al.* 1984b, 1984a, Azov 1986, Li *et al.* 1993, Yacobi *et al.* 1995, Psarra *et al.* 2000, Christaki *et al.* 2001, Vidussi *et al.* 2001). Nitrogen and phosphorous are usually recorded in very low concentrations, which suggests that bacterial growth rates are severely nutrient limited (Siokou-Frangou *et al.* 2010). The atmospheric input of nutrients in the eastern Mediterranean Sea is of great importance since it exceeds the riverine inputs (Christodoulaki *et al.* 2013, Velaoras *et al.* 2019), and their distribution is mostly controlled by eddies and currents (Yücel 2013).

Cyprus is located in the Levantine Basin, eastern Mediterranean. Coastal physicochemical values are representative of open ocean values, mostly due to the exposed coastline and very narrow shelf region of the island (Petrou *et al.* 2012). Low nutrient concentrations have been recorded through the Department of Fisheries and Marine Research monitoring programme (EEA 2021), as well as extremely low Chl-a concentrations (0.01 – 0.09 μg / l) (Bianchi *et al.* 1996). The absence of permanent flow rivers on the island, together with the construction of dams on almost all rivers, limits the supply of coastal waters with nutrients (Sofroniou and Bishop 2014, WDD 2017).

The aim of this work was to assess the phytoplankton size fractions and chemotaxonomic groups in the coastal zone of Cyprus, and the seasonal phytoplankton variability in relation to physicochemical parameters. This is the first study to provide a unique, 12-month timeseries about phytoplankton in Cyprus.

3.2. Materials and Methods

3.2.1. Study site and sampling

Sampling was carried out monthly, between January and December 2016. Samples were collected from four coastal stations (Figure III.***1***). Pyrgos station (PYR) is located off Pygos village on the northwest of Cyprus. The area of Pyrgos is a relatively low impacted area, with very limited coastal development. Station Akrotiri (AKR) is located off Akrotiri peninsula in the south of the island, where upwelling is observed during the summer months. Station Vasilikos Fish Farm (VAS1) is located next to an aquaculture unit in Vasilikos bay and station Vasilikos Reference (VAS2) is approximately two nautical miles east of VAS1. Vasilikos bay is one of the most impacted areas on the island, posing a high environmental impact in terms of industrial effluents (cement company, power station, abandoned fertilizers chemical industry). Thermal effluents from the power plant of Vasilikos are discharged at sea, whereas

the desalination plan is discharging considerable amounts of brine to the sea (Kathijotes and Papatheodoulou 2013).

Conductivity – temperature – depth (CTD) measurements were collected with an SBE-19plus. Seawater for biogeochemical analyses was collected with a 5 L Niskin bottle at standard depths (surface, 2, 10, 20, 50, 75, 100 m), according to the bathymetry of each station (PYR and AKR 130 m, VAS1 and VAS2 55 m).

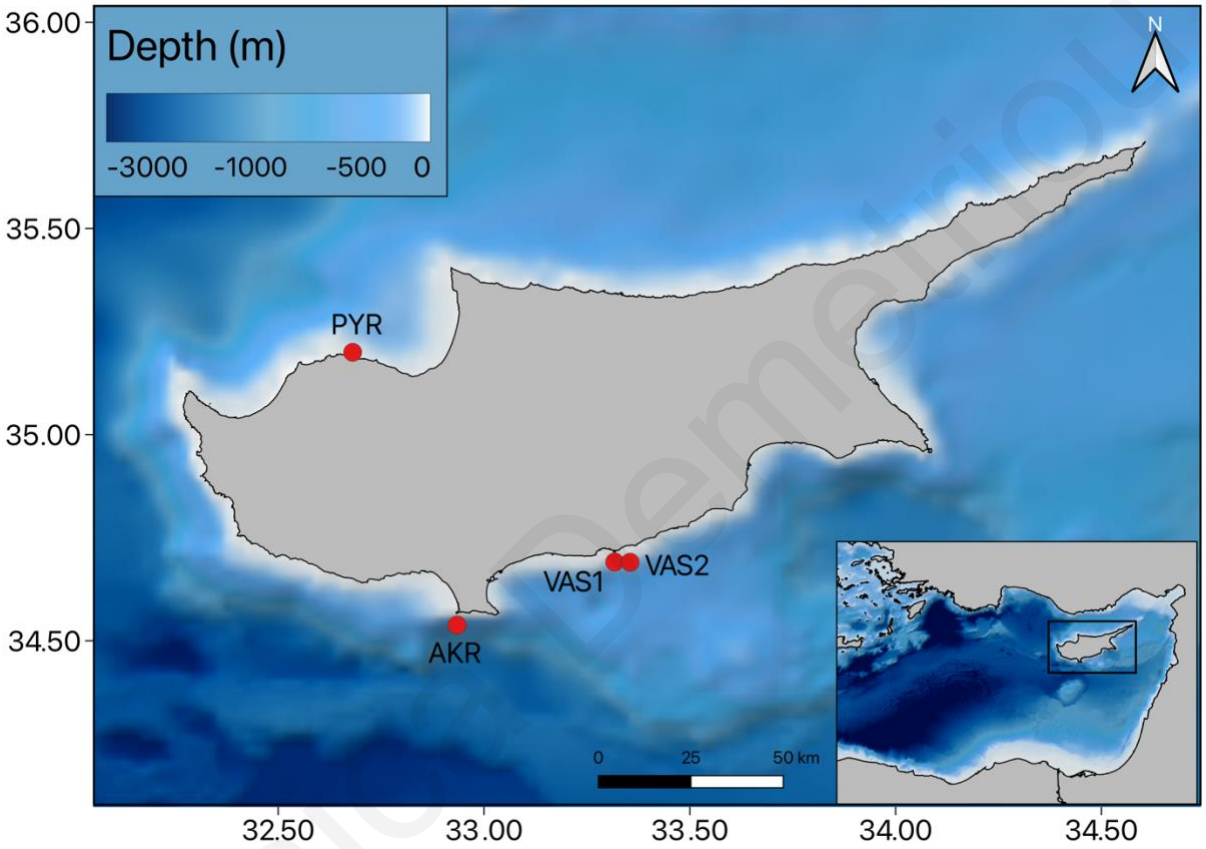

Figure III.1: The location of Cyprus at the eastern Mediterranean, indicating the bathymetry and the four sampling stations, Pyrgos (PYR), Akrotiri (AKR), Vasilikos Fish Farm (VAS1), and Vasilikos reference station (VAS2).

3.2.2. Nutrients

Water samples for nutrient analysis were collected in polyethylene bottles, prewashed with HCl. The samples were kept frozen until their analysis at the Department of Fisheries and Marine Research, using an OI Analytical Flow Solution IV+ autoanalyser. Samples were analysed for ammonium (NH4), nitrate (NO_3), nitrite (NO_2), and orthophosphate (PO_4), according to Strickland and Parsons (1972). Dissolved inorganic nitrogen (DIN) was calculated as the sum of NO_3, NO_2 and NH_4.

3.2.3. Phytoplankton pigments

For the HPLC pigment analysis, 4 L of seawater were filtered through Whatman GF/F filters (47 mm diameter) under low vacuum pressure (<150 mmHg). The filters were immediately frozen in liquid nitrogen and stored at -80 °C until analysis at the Hellenic Centre of Marine Research (HCMR). Filters were extracted in 3 ml acetone, sonicated (50% amplitude, 0.5 cycle) for 1.5 minutes and incubated overnight at -20 °C, and each filter was spiked with 20 µL of internal standard (β-apo-8′-carotenal 3 ng µl 1) and incubated. All extracts were clarified by centrifugation (5000 rpm for 10 min) and filtered through a 0.2 mm syringe filter (Whatman ReZist, PTFE, 0.2 mm pore size, 13 mm diameter). The above procedures were carried out under dim light conditions. An Agilent 1260 Infinity Binary Pump HPLC system (Agilent Technologies) equipped with a Poroshell 120 column (EC-C18, 150 mm 3 mm, 2.7 mm particles; Agilent Technologies) was used to analyse the extracts, according to Van Heukelem and Thomas (2001), as modified by Lagaria *et al.* (2017). Twenty (20) µl of extract were mixed with 30 µl of aqueous 28 mM tetrabutyl ammonium acetate (TBAA) and remained in the autosampler loop for 5 min, before being injected into the column. The temperature of the column was set at 45 °C and the flow rate at 0.45 ml min^{-1}. Pigments were separated by applying a binary gradient of solvent A (70:30 methanol:water with 28 mM TBAA, pH 6.5) and solvent B (methanol), as follows; 0 min: 10% B, 50 min: 100% B, 74 min: 100% B, 76 min: 10% B, 81 min: 10% B. Pigments were detected with a continuous recording of absorbance at 440 nm (8 nm bandwidth) and identified by comparing the retention times and the UV/Vis spectra of the chromatographic peaks with those of authentic standards (DHI Water & Environment, Hørsholm, Denmark). A total of 17 pigments were identified and their concentrations were calculated using the internal standard method. The detection limit was approximately 1 ngL^{-1}. The pigment abbreviations and calculated pigment sums are presented in Table III.***1***.

Table III.1: Pigment names, abbreviations, taxonomic significance and pigment sums (from Jeffrey *et al.* (2011) and Lagaria *et al.* (2017)

Pigment	**Abbreviation**	**Taxonomic significance**
19′-butanoyloxyfucoxanthin	But	Pelagophytes, prymnesiophytes
19′-hexanoyloxyfucoxanthin	Hex	Prymnesiophytes
Astaxanthin	Asta	
Alloxanthin	Allo	Cryptophytes
Chlorophyll-a	Chla	All – except Prochlorophytes
Chlorophyll-b	Chlb	Green algae
Crocoxanthin	Crocox	
Diadinoxanthin	Diadino	Various
Divinyl Chlorophyll-a	DVChla	Prochlorophytes
Divinyl Chlorophyll-b	DVChlb	Prochlorophytes
Fucoxanthin	Fuco	Diatoms, prymnesiophytes, some Dinoflagellates
Lutein	Lut	Chlorophytes
Neoxanthin	Neo	Green algae
Peridinin	Peri	Dinoflagellates
Pheophytin	Phe	Degradation product of Chl-a
Prasinoxanthin	Prasino	Prasinophytes
Zeaxanthin	Zea	Cyanobacteria, Prochlorophytes
a-Carotene	α-Car	Various
β-Carotene	β-Car	Various
Pigment Sums	**Abbreviation**	**Formula**
Total chlorophyll-a	TChla	Chla + DVChla
Total chlorophyll-b	TChlb	Chlb + DVChlb
Weighted sum of diagnostic pigments	DP	0.86[Zea]+1.01[Chlb]+[DVChla]+0.60[Allo]+1.27[Hex]+0.35 [But]+1.41[Fuco]+1.41[Peri]
Relative contribution of picoplankton	f_{pico}	(0.86 [Zea]+1.01[Chlb]+[DVChla])/DP
Relative contribution of nanoplankton.	f_{nano}	(0.60 [Allo]+0.35 [But]+1.27 [Hex])/DP
Relative contribution of microplankton.	f_{micro}	(1.41 [Fuco]+1.41 [Peri])/DP

3.2.4. Analysis of Chl-a using a fluorescence microplate reader

The potential to utilize a microplate-based assay for the quantification of Chl-a in phytoplankton extracts has been proposed by Mandalakis et al. (2017). The above method is simple, has a high throughput and a short analysis time. To demonstrate the efficiency of the microplate method in analysing Chl-a, all pigment extracts were loaded on a microplate together with Chl-a standard solutions. The results from the microplate method were compared

with the concentrations of the chlorophyll pigments measured using HPLC (Chl-a, DVChl-a). For a detailed analysis of the microplate reader method see Mandalakis et al. (2017).

3.2.5. Pigment-based estimation of phytoplankton size classes

The relative contribution of pico- (0.2 – 2.0 μm), nano- (2.0-20μm), and microphytoplankton (>20μm) to the total Chl-a was estimated using the approach of Vidussi et al. (2001), as refined by Uitz et al. (2015) (Table III.***2***).

Table III.2: Equations used to derive the relative proportions of the phytoplankton size classes (fpico, fnano, fmicro). ΣDPw is the total Chl-a concentration estimated from the concentration of seven diagnostic pigments ((Vidussi et al. 2001, Uitz et al. 2015)

Size class	Equations
f_{pico}	$(1.01[TChlb] + 0.86[Zea])/DP_w$
f_{nano}	$(1.27[Hex] + 0.35[But] + 0.60[Allo])/DP_w$
f_{micro}	$(1.41[Fuc] + 1.41[Peri])/DP_w$
ΣDP_w	$1.41[Fuc] + 1.41[Peri] + 1.27[Hex] + 0.35[But] + 0.60[Allo] + 1.01[TChlb] + 0.86[Zea]$

An estimate of the TChl-a concentration is obtained from the weighted sum of seven major diagnostic pigments (DP_w), associated with phytoplankton size classes, under the following assumptions: (1) green flagellates, prochlorophytes and cyanobacteria (zeaxanthin and TChlb) make up picophytoplankton (f_{pico}), (2) nanophytoplankton (f_{nano}) is composed of cryptophytes, chromophytes prymnesiophytes and various and nanoflagellates like small dinoflagellates (alloxanthin, 19' hex- and 19' butanoyloxyfucoxanthin, fucoxanthin), and (3) microphytoplankton (f_{micro}) is comprised of diatoms and dinoflagellates, which are characterized by fucoxanthin and peridinin (Table III.***3***) (Lagaria *et al.* 2017, Brewin *et al.* 2019, Gittings *et al.* 2019a, Nunes *et al.* 2019).

Table III.3: Phytoplankton diagnostic pigments, abbreviations, taxonomic significance and size classes (from Jeffrey et al. *2011)*.

Pigments	**Abbreviations**	**Taxonomic significance**	**Size μm**
Zeaxanthin	Zea	Cyanobacteria and Prochlorophytes	< 2
Divinyl-chlorophyll a	DVChl-a	Prochlorophytes	< 2
19' hexanoyloxyfucoxanthin	Hex	Prymnesiophytes (major)	2-20
19' butanoyloxyfucoxanthin	But	Pelagophytes (major), Prymnesiophytes	2-20
Fucoxanthin	Fuc	Diatoms (major), Prymnesiophytes	> 20

3.2.6. CHEMTAX analysis

The relative contribution of different phytoplankton groups to total Chl-a was calculated from the main pigment markers, using the software CHEMTAX V 1.95 (Mackey *et al.* 1996). CHEMTAX uses an initial matrix of Chl-a:pigment ratios for selected phytoplankton groups and it then derives the contribution of each pigmentary class to the total Chl-a. CHEMTAX was run following the approach of Lagaria et al. (2017), with initial pigment ratios calculated by Anna Lagaria. Based on the main pigment markers detected by HPLC, five functional groups were uploaded to CHEMTAX: CYANO-2 for Synechococcus sp., CYANO-4 for Prochlorococcus sp., PRYMNE for Prymnesiophytes, PELAGO for Pelagophytes and Chrysophytes, and DIATOMS. The data matrix included concentrations of Fuco, But, Hex, DVChl-a, and Zea. Sixty ratio matrices were generated by adjusting each of the pigment ratios according to a random function (Wright *et al.* 2009), in order to avoid potentially unreliable initial pigment:Chl-a ratios. The contribution of each class to the TChl-a concentration was determined by selecting the best 10% of the outputs, based on lower Root Mean Square (RMS) errors.

3.2.7. Statistical analyses

At each station, all phytoplankton related parameters were depth-integrated using the trapezoid rule (Laws 1997). In order to compare stations and seasons, integrations were performed over the 0-100 or 0-50 depth layer, depending on the station's depth. For comparing depths, integrations were carried out over the 0-20 m and >20 m depth layers. A mean weighted value (m^{-3}) for each selected layer was calculated by normalising the integrated values per surface area (m^{-2}) over the respective integration depth.

Spearman's correlation was used to examine the spatiotemporal relationships among environmental variables salinity, temperature, nitrate, phosphate, and TChl-a. A Generalised Linear Model (GLM) was used to test for differences among sampling dates, among stations at each sampling date and between the surface and the deeper layers.

Statistical analyses were carried out in R 4.1.0 (R Core Team 2021), using packages stats 3.6.2 (R Core Team 2021), dplyr 1.0.7 (Wickman *et al.* 2021), cmocean 0.3-1 (Thyng *et al.* 2016), MBA 0.0-9 (Finley *et al.* 2017), and ggplot2 3.3.5 (Wickham 2016).

3.3. Results

3.3.1. Hydrography

A strong stratification was observed in all stations, starting in spring (April) and lasting until December, while in winter the water column is well mixed (Figure III.***3*** - Figure III.***6***). A sharp thermocline was located at 20 – 50 m in PYR and AKR and at 10 – 40 m in VAS1 and VAS2 stations. Temperatures at the top 20 m peaked in August, with the highest temperature of 29.5 °C recorded at the surface in PYR. The lowest temperature (17.1 °C) was recorded at 20 m depth, in January 2016 at AKR. Salinity was high throughout the year (>38.7), representative of the high salinity Levantine waters. The halocline followed the distribution of the thermocline in all sampled stations (Figure III.***3*** - Figure III.***6***).

3.3.2. Nutrients

Concentrations of DIN and PO_4^{3-} did not vary significantly with depth, or among seasons and stations. No correlation was found between mineral nutrients and salinity or temperature. Considering the entire water column, DIN ranged from 0.02 – 3.45 μM, and PO_4^{3-} ranged between 0.007 – 0.38 μM (Table III.***6*** - Table III.*7*).

The mean N:P ratio ranged 0.2-48 in winter, 0.3-52 in spring, 0.6-50 in summer, and 0.6-13 in autumn. The lowest N:P ratio was recorded in station VAS1 in March (Figure III.***2***).

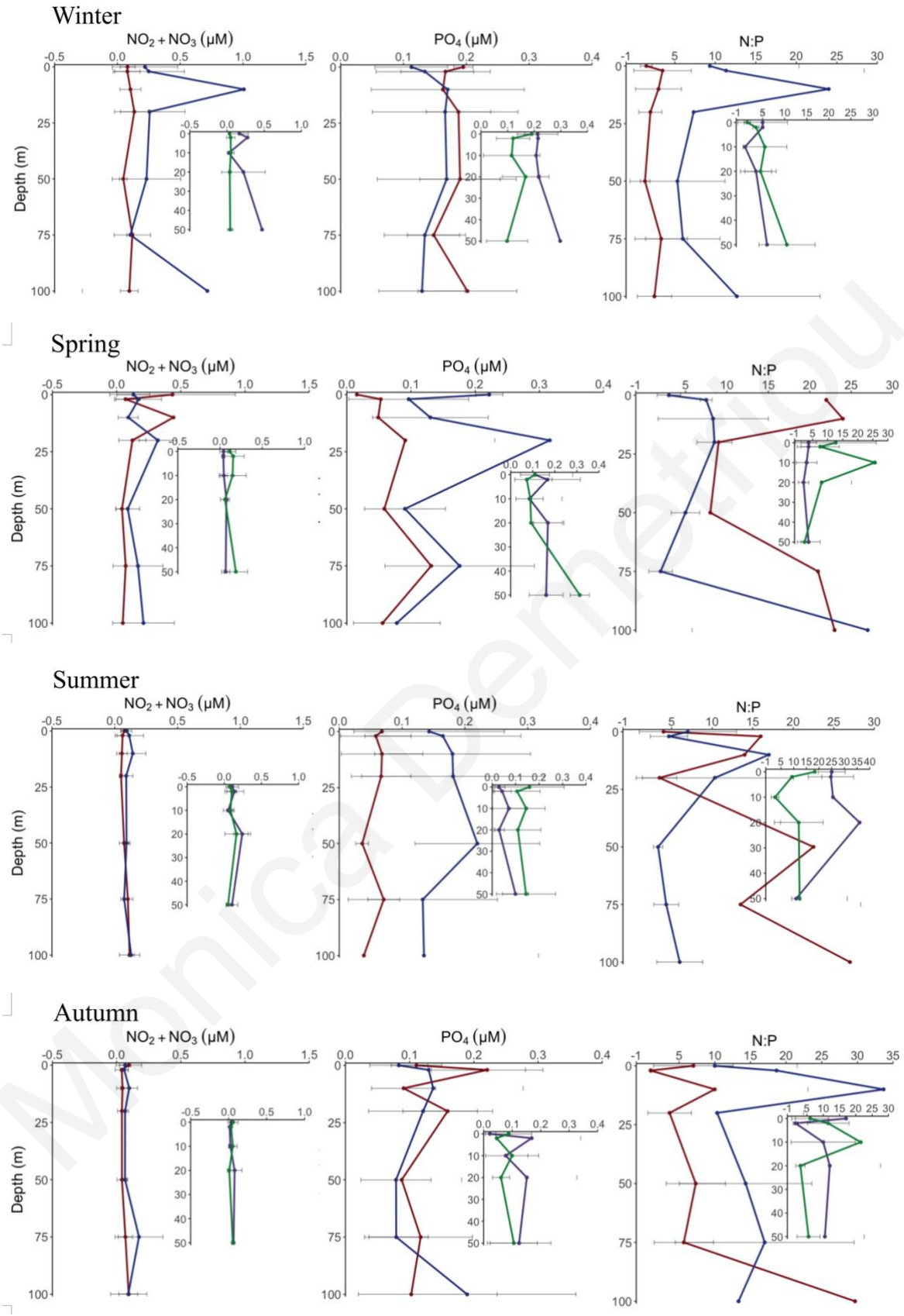

Figure III.2: Vertical profiles of phosphate and DIN in all stations, during winter (January-March), spring (April-June), summer(July-September), and autumn (October-December). The values are the average of the sampling stations.

3.3.3. Concentrations and spatial distribution of phytoplankton pigments

During the stratified period (May to November), TChl-a had a homogenous distribution in all stations ((Figure III.***3*** - Figure III.***6***)), with the lowest TChl-a value in the upper 0-20 m layer (0.005 μg L-1 in VAS2 surface), and maximum values below the thermocline, at 100 m depth in AKR in April (0.23 μg L-1). Maximum concentrations of Chl-a were more prominent during spring (April-June) and summer (July-September), indicating the presence of a subsurface chlorophyll maximum (SCM) layer. Only in the shallow layer, did the total Chl-a, DVChl-a, But, and Hex correlate with phosphate concentration. All pigments were corelated with temperature (Table III.***5***).

Other diagnostic pigments typically detected in all stations were DVChl-a, Zea, But, Hex and Fuc (Table III.***1*** for abbreviations, Figure III.***3*** - Figure III.***6***). Hex (prymnesiophytes) and But (pelagophytes and chrysophytes) showed a similar distribution pattern to Chl-a. Zea (cyanobacteria) showed a decreasing trend with depth during the mixed period (January – April) in VAS1 and VAS2 stations, whereas highest values of Zea were recorded in the deepest layers in PYR during the stratified period (May – December). Zea and DVChl-a had minimal concentrations during the stratified period in all stations (Figure III.***3*** - Figure III.***6***).

The highest values for all pigments were recorded at AKR, at 75 and 100 m depth, with the exception of Zea (20 m). The shallow layer (0 – 20 m) at VAS2 station had the lowest values for Hex, But, and Zea. DVChla and Fuc had minimum recorded values at PYR (50 m), VAS1 (10 m) and AKR (10 m), respectively.

Table III.4: GLM table between stations, between seasons and between depths (0-20 m, >20 m).

Variables	Factors		GLM		
			Exp(Beta)	95% CI	p-value
TChl-a	Station	VAS2	0.98	0.97, 0.99	**
	Season	Spring	0.97	0.96, 0.98	***
		Summer	0.98	0.96, 0.99	**
		Autumn	1.02	1.01, 1.04	**
	Depth	<20 m	0.98	0.96, 0.99	**
Zea	Season	Spring	0.99	0.99, 0.99	***
		Summer	0.99	0.98, 0.99	***
		Autumn	0.99	0.99, 1.00	**
DVChl-a	Station	PYR	0.99	0.99, 1.00	*
		VAS2	0.99	0.99, 1.00	**
	Season	Autumn	1.02	1.01, 1.03	***
	Depth	<20 m	0.99	0.98, 1.00	*
But	Station	VAS1	1.00	1.00, 1.00	**
		VAS2	1.00	1.00, 1.00	**
	Season	Spring	0.99	0.99, 1.00	***
		Summer	1.00	0.99, 1.00	**
		<20 m	1.00	0.99, 1.00	*
Hex	Station	PYR	0.99	0.99, 1.00	**
		VAS1	0.99	0.98, 0.99	***
		VAS2	0.99	0.99, 1.00	***
	Season	Spring	0.98	0.98, 0.99	***
		Summer	0.98	0.98, 0.99	***
	Depth	<20 m	0.99	0.98, 0.99	***
Fuc	Season	Spring	1.00	1.00, 1.00	***
		Summer	1.00	1.00, 1.00	**
f_{pico}	Station	PYR	1.06	1.00, 1.12	*
		VAS1	1.06	1.00, 1.13	*
	Season	Summer	0.89	0.84, 0.95	***
	Depth	<20 m	0.90	0.85, 0.95	***
f_{nano}	Station	PYR	0.93	0.88, 0.99	0.016
	Season	Summer	1.14	1.07, 1.21	<0.001
	Depth	<20 m	0.90	0.85, 0.94	<0.001
f_{micro}	Station	VAS1	1.03	1.01, 1.05	0.001
		VAS2	1.02	1.00, 1.04	0.042

The seasonal changes in the phytoplankton community structure are revealed by the dynamics of HPLC diagnostic pigments data. TChl-a, But, Hex, and DVChl-a showed a significantly different distribution between stations, and specifically between stations PYR and VAS (Table III.***4***).

Among the sampling stations, the water-column average concentrations of TChl-a, (0.023-0.132 μg L^{-1}), But (0.0006–0.023 μg L^{-1}), Hex (0.007–0.056 μg L^{-1}), Zea (0.005–0.029 μg L^{-1}), DVChl-a (0.0004–0.045 μg L^{-1}), and Fuc (0.0005-0.008 μg L^{-1}) had highest values during winter (January-March).

The concentrations of all pigments varied significantly between the shallow (0-20 m) and deeper layers (> 20 m) (Table III.***4***).

Table III.5: Spearman correlations between pigments, size classes, and abiotic parameters.

0 – 20 m		
Variables	**Factors**	**Spearman (Rho)**
TChl-a	Temperature	-0.62***
	Phosphate	0.42**
Zea	Temperature	-0.60***
DVChl-a	Salinity	0.73***
	Temperature	0.42*
	Phosphate	0.41*
But	Temperature	-0.60***
	Phosphate	0.30*
Hex	Temperature	-0.45**
	Phosphate	0.28*
Fuc	Temperature	-0.45**
f_{pico}	Salinity	-0.35*
	Temperature	-0.53***
	Phosphate	0.31*
f_{nano}	Salinity	0.36**
	Temperature	0.58***

>20 m		
Variables	**Factors**	**Spearman (Rho)**
TChl-a	Temperature	-0.35*
Zea	Temperature	-0.46**
DVChl-a	Salinity	-0.34*
	Temperature	-0.32*
But	Salinity	-0.36*
	Temperature	-0.48**
Hex	Salinity	-0.40*
	Temperature	-0.42*
f_{pico}	Salinity	0.31*
	Phosphate	0.39*
f_{nano}	Temperature	0.55***
f_{micro}	Salinity	0.42**
	Temperature	0.31*

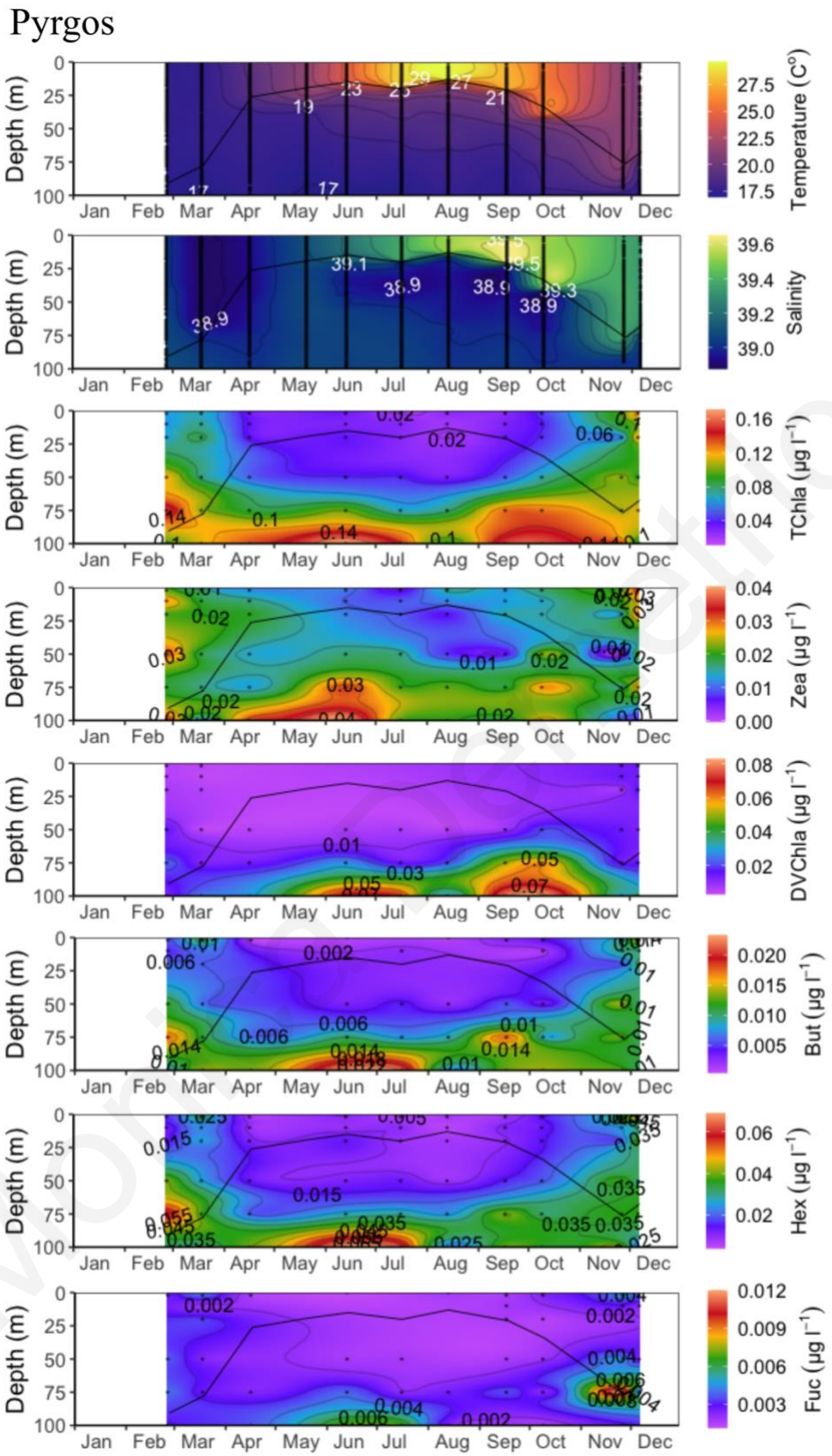

Figure III.3: Time series of vertical profiles of CTD temperature, salinity, and HPLC pigment concentrations (TChl-a, zeaxanthin, DVChl-a, 19'-but, 19'-hex, and fucoxanthin), in Pyrgos (PYR) station. The black line represents the Mixed Layer Depth (MLD).

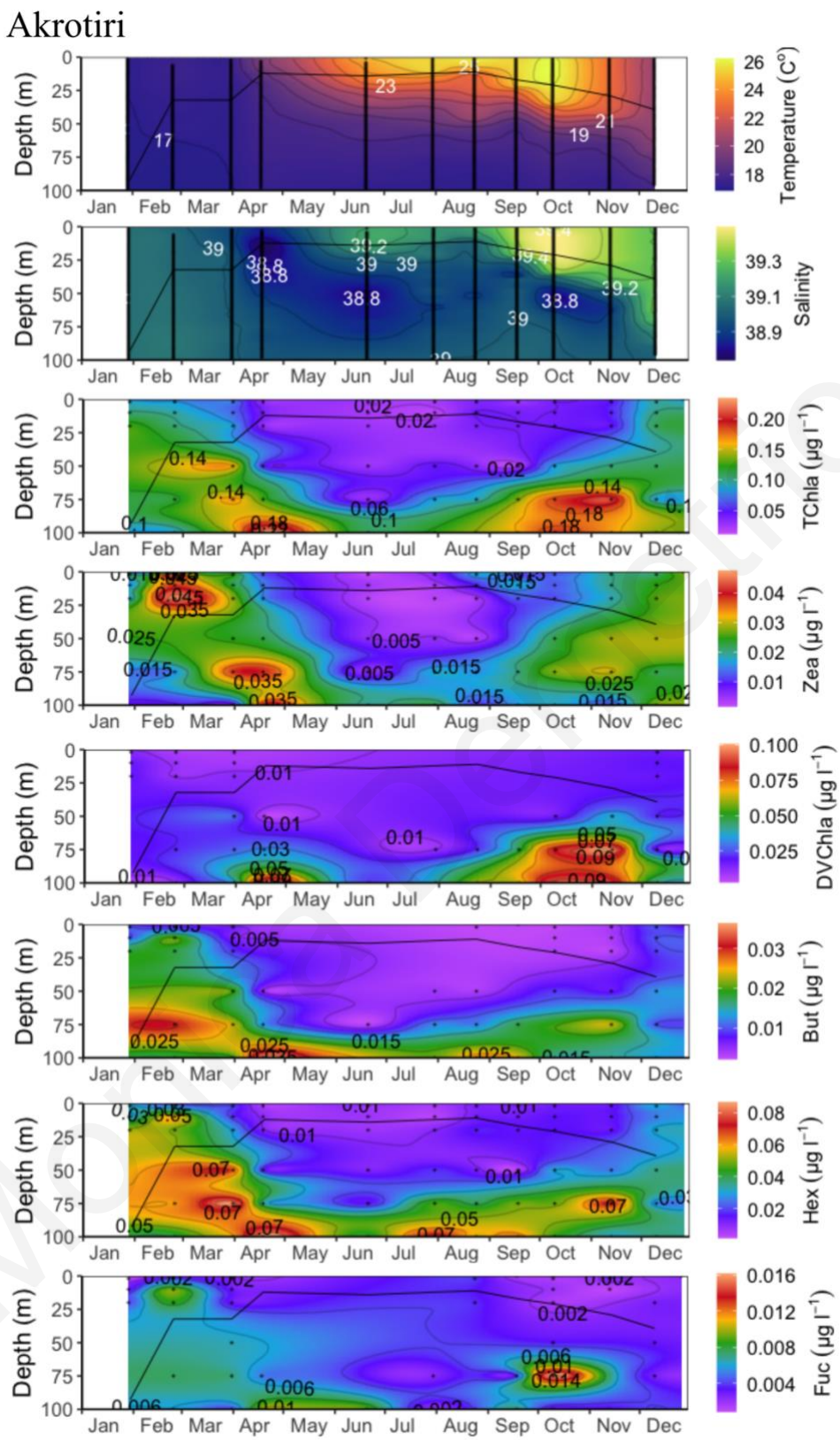

Figure III.4:Time series of vertical profiles of CTD temperature, salinity, and HPLC pigment concentrations (TChl-a, zeaxanthin, DVChl-a, 19'-but, 19'-hex, and fucoxanthin), in Akrotiri (AKR) station. The black line represents the Mixed Layer Depth (MLD).

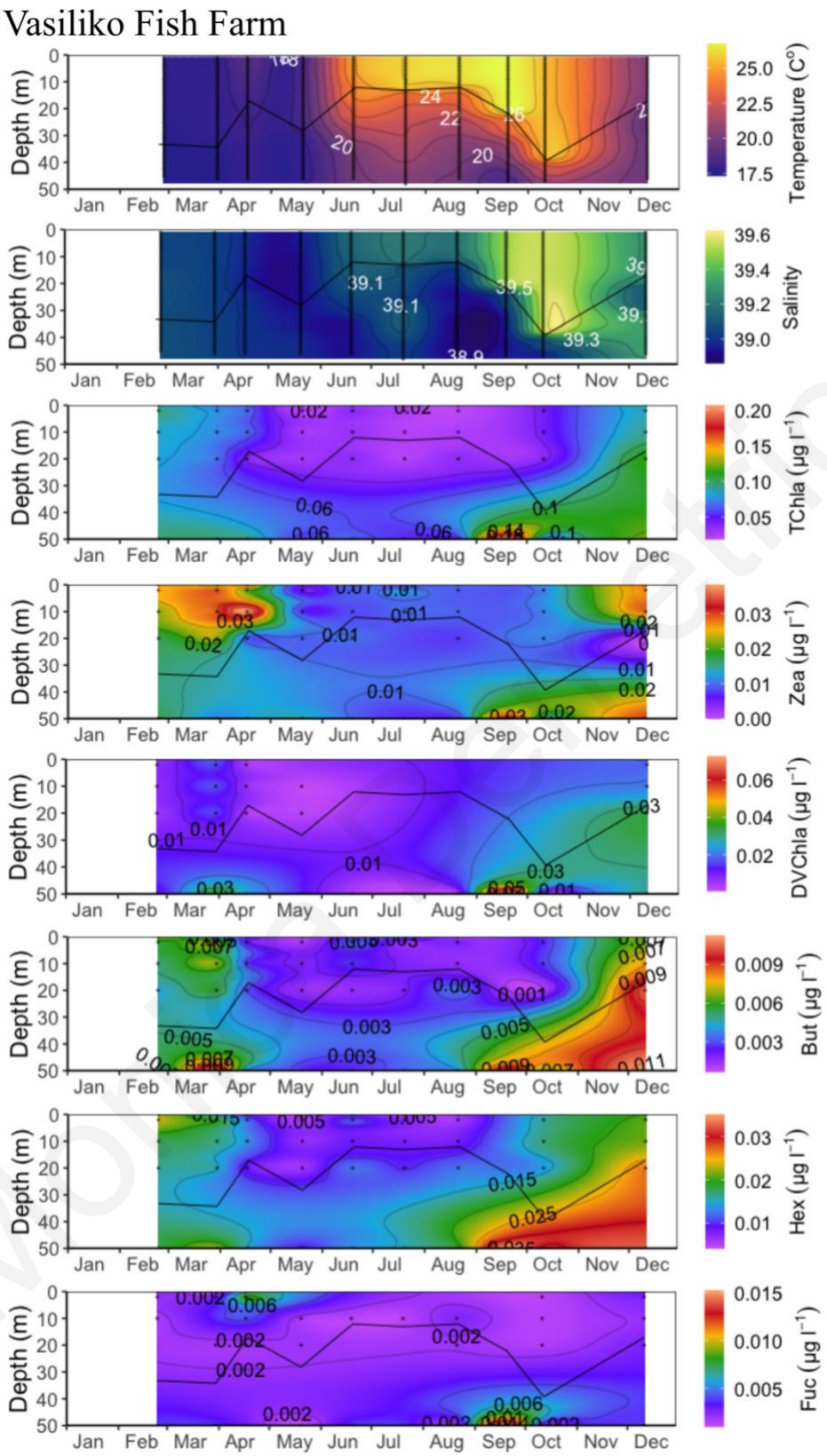

Figure III.5: Time series of vertical profiles of CTD temperature, salinity, and HPLC pigment concentrations (TChl-a, zeaxanthin, DVChl-a, 19'-but, 19'-hex, and fucoxanthin), in Vasilikos Fish Farm (VAS1) station. The black line represents the Mixed Layer Depth (MLD).

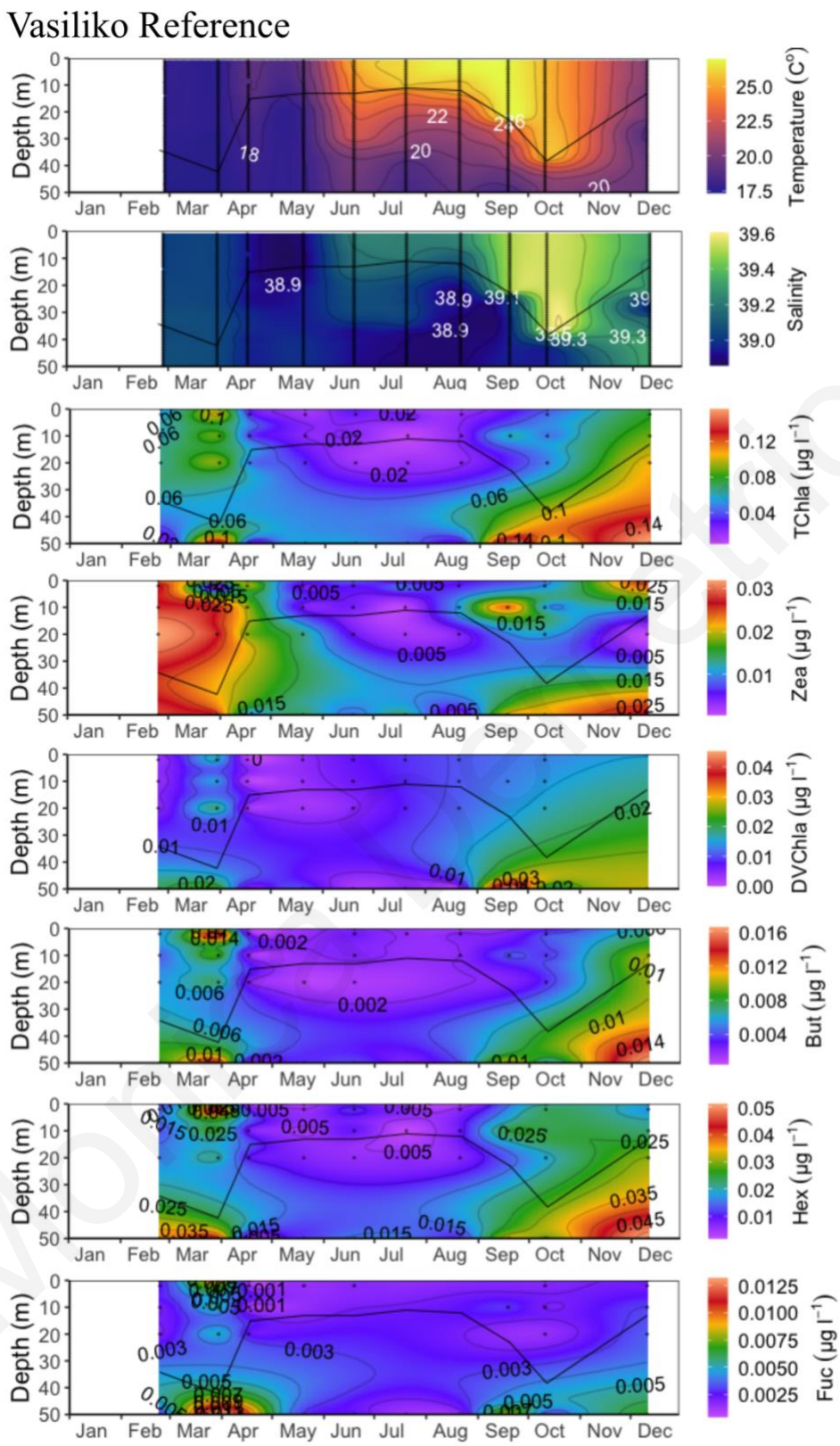

Figure III.6: Time series of vertical profiles of CTD temperature, salinity, and HPLC pigment concentrations (TChl-a, zeaxanthin, DVChl-a, 19'-but, 19'-hex, and fucoxanthin), in Vasilikos Reference (VAS2) station. The black line represents the Mixed Layer Depth (MLD)

Table III.6: Mean (and standard deviation) and range for temperature, salinity, phosphate, DIN, N:P ratio and HPLC pigments, for all four stations (AKR, PYR, VAS1, VAS2), in winter (January-March), spring (April-June), summer (July-September), and autumn (October-December), for the 0-20 m depth layer.

	Winter				Spring				Summer				Autumn			
	AKR	**PYR**	**VAS1**	**VAS2**	**AKR**	**PYR**	**VAS1**	**VAS2**	**AKR**	**PYR**	**VAS1**	**VAS2**	**AKR**	**PYR**	**VAS1**	**VAS2**
	Mean±SD (Range)	**Mean±SD (Range)**	**Mean±SD (Range)**	**Mean±SD (Range)**	**Mean±SD (Range)**	**Mean±SD (Range)**	**Mean±SD (Range)**	**Mean±SD (Range)**	**Mean±SD (Range)**	**Mean±SD (Range)**	**Mean±SD (Range)**	**Mean±SD (Range)**	**Mean±SD (Range)**	**Mean±SD (Range)**	**Mean±SD (Range)**	**Mean±SD (Range)**
Temperature	17.3±0.19 (17.09- 17.43)	17.17±0.45 (16.65- 17.45)	17.66±0.08 (17.6- 17.72)	17.66±0.1 (17.59- 17.73)	21.42±3.42 (19.01- 23.84)	21.57±2.42 (19.15- 23.98)	20.41±3.33 (18.46- 24.25)	20.7±3.2 (18.83- 24.39)	24.84±0.54 (24.33- 25.4)	27.48±0.06 (27.42- 27.54)	25.81±0.86 (25.21- 26.79)	25.77±0.91 (25.19- 26.81)	23.21±2.79 (20.55- 26.11)	22.63±2.73 (20.79- 25.77)	22.89±3.72 (20.26- 25.52)	22.96±3.68 (20.36- 25.56)
Salinity	39.01±0.06 (38.94- 39.06)	38.95±0.08 (38.9- 39.01)	39.03±0.02 (39.02- 39.05)	39.03±0 (39.03- 39.03)	38.99±0.28 (38.79- 39.19)	39.08±0.13 (38.94- 39.2)	39.01±0.11 (38.93- 39.13)	39±0.15 (38.9- 39.17)	39.21±0.16 (39.1- 39.4)	39.43±0.14 (39.32- 39.59)	39.27±0.2 (39.14- 39.5)	39.26±0.21 (39.12- 39.5)	39.38±0.09 (39.3- 39.47)	39.42±0.11 (39.34- 39.54)	39.41±0.2 (39.27- 39.55)	39.43±0.17 (39.31- 39.55)
PO_4-P	0.11±0.1 (0- 0.17)	0.16±0.11 (0.06- 0.27)	0.16±0.08 (0.1- 0.22)	0.14±0.04 (0.11- 0.16)	0.06± (0.06- 0.06)	0.1±0.09 (0.03- 0.2)	0.1±0.04 (0.05- 0.13)	0.09±0.14 (0- 0.25)	0.04±0.04 (0- 0.08)	0.12±0.13 (0.01- 0.26)	0.03±0.03 (0.01- 0.06)	0.12±0.08 (0.05- 0.21)	0.1±0.02 (0.08- 0.12)	0.13±0.1 (0.01- 0.21)	0.12±0.12 (0.03- 0.2)	0.07±0.05 (0.04- 0.11)
DIN	0.45±0.39 (0.03- 0.79)	2.53±3.93 (0.18- 7.06)	0.69±0.78 (0.14- 1.24)	0.18±0.13 (0.09- 0.28)	1.09 1.09	0.6±0.47 (0.32- 1.14)	0.19±0.08 (0.1- 0.26)	0.44±0.32 (0.19- 0.8)	0.23±0.11 (0.14- 0.35)	0.5±0.08 (0.44- 0.59)	0.48±0.46 (0.03- 0.94)	0.3±0.27 (0- 0.52)	0.21±0.04 (0.18- 0.23)	0.31±0.18 (0.19- 0.51)	0.14±0.15 (0.04- 0.25)	0.15±0.14 (0.05- 0.25)
N:P	1.57±1.96 (0.19- 2.96)	43.01±72.19 (1.26- 126.37)	1.98±2.3 (0.35- 3.6)	1.43±0.3 (1.22- 1.64)	29.29 29.29	3.63±2.62 (0.66- 5.61)	2.07±1.78 (0.74- 4.09)	58.28±61.03 (0.82- 122.35)	3.24±2.01 (1.82- 4.66)	9.82±6.92 (1.84- 14.08)	30.17±38.98 (0.34- 74.28)	6.5±5.39 (0.57- 11.1)	3.22±3.07 (1.05- 5.39)	9.51±13 (1.36- 24.5)	5.34±6.98 (0.4- 10.27)	1.81±0.54 (1.43- 2.19)
TChl-a	90.19±15.21 (73.75- 103.75)	65.24±12.83 (56.16- 74.31)	79.85±8.32 (73.97- 85.74)	74.67±22.82 (58.54- 90.81)	28.57±7.5 (23.27- 33.87)	31.7±0.16 (31.59- 31.81)	39.65±16.8 (26.66- 58.62)	26.7±10.36 (19.71- 38.61)	31.93±9.74 (20.79- 38.84)	25.47±4.11 (21.79- 29.91)	25.3±1.87 (23.98- 26.62)	19.17± (19.17- 19.17)	63.39±32.06 (40.46- 100.03)	79.69±36.69 (40.94- 113.9)	67.77±39.43 (39.89- 95.65)	67.72±30.09 (46.45- 89)
Zea	26.74±11.57 (16.56- 39.33)	20.13±2.85 (18.12- 22.15)	24.56±3.73 (21.92- 27.2)	24.42±5.49 (20.54- 28.3)	8.5±7.64 (3.1- 13.9)	12.5±2.79 (10.53- 14.48)	14.2±10.4 (7.38- 26.17)	10.31±7.41 (5.16- 18.81)	9.71±5.3 (4.15- 14.7)	10.92±2.74 (7.97- 13.39)	8.41±0.81 (7.84- 8.98)	7.65± (7.65- 7.65)	18.7±6.07 (12.25- 24.3)	21.31±7.54 (15.09- 29.69)	15.8±7.48 (10.51- 21.09)	6.05±6.51 (1.45- 10.65)
DVChl-a	10.75±4.07 (8.31- 15.45)	4.36±0.61 (3.93- 4.79)	11.46±6.88 (6.59- 16.32)	9.56±8.57 (3.5- 15.62)			2.94±2.63 (1.08- 4.8)	0.87±0.97 (0- 1.92)					17.18 17.18	13.29±1.29 (12.37- 14.2)	23.26 23.26	17.64 17.64
But	11.49±4.61 (6.67- 15.86)	6.18±1.96 (4.79- 7.56)	5.74±0.92 (5.09- 6.39)	7.32±3.39 (4.92- 9.72)		0.16±0.16 (0.05- 0.27)	2.22±0.65 (1.49- 2.71)	1.41±1.02 (0.23- 2.03)	0.35±0.31 (0.13- 0.57)	0.61±0.51 (0.06- 1.07)	1.52±0.74 (0.99- 2.04)	0.98±0.74 (0.46- 1.5)	5.17±3.71 (2.63- 9.43)	7.23±4.74 (1.95- 11.12)	5.14±4.19 (2.17- 8.1)	6.3±3.76 (3.64- 8.96)
Hex	33.86±11.87 (21.36- 44.98)	19.01±9.61 (12.21- 25.8)	18.05±1.53 (16.97- 19.13)	21.27±10.72 (13.69- 28.85)	7.73±0.74 (7.21- 8.25)	9.39±1.26 (8.5- 10.28)	9.22±2.86 (6.06- 11.62)	7.58±2.07 (5.19- 8.88)	10.37±4.07 (5.68- 12.97)	8.03±1.72 (6.27- 9.7)	8.29±0.35 (8.04- 8.53)	7.48 7.48	18.91±7.59 (14.5- 27.67)	25.62±11.48 (13.83- 36.77)	18.8±5.03 (15.24- 22.36)	22.54±0.45 (22.22- 22.85)
Fuc	4.26±2.7 (2.66- 7.38)	1.55±1.46 (0.52- 2.58)	1.29±0.2 (1.15- 1.43)	4.03±2.72 (2.1- 5.95)		0.18±0.18 (0.06- 0.31)	2.17±2.18 (0.58- 4.65)	0.75±0.62 (0.36- 1.46)	0.98±1.27 (0.08- 1.87)	0.85±1.08 (0.08- 1.61)	1.09±0.74 (0.57- 1.62)		1.19±0.45 (0.78- 1.67)	2±1.01 (1.03- 3.05)	1.88±0.81 (1.3- 2.45)	2.33±0.76 (1.79- 2.86)

Table III.7: Mean (and standard deviation) and range for temperature, salinity, phosphate, DIN, N:P ratio and HPLC pigments, for all four stations (AKR, PYR, VAS1, VAS2), in winter (January-March), spring (April-June), summer (July-September), and autumn (October-December), for the >20 m depth layer.

	Winter				Spring				Summer				Autumn			
	AKR	**PYR**	**VAS1**	**VAS2**	**AKR**	**PYR**	**VAS1**	**VAS2**	**AKR**	**PYR**	**VAS1**	**VAS2**	**AKR**	**PYR**	**VAS1**	**VAS2**
	Mean±SD (Range)	**Mean±SD (Range)**	**Mean±SD (Range)**	**Mean±SD (Range)**	**Mean±SD (Range)**	**Mean±SD (Range)**	**Mean±SD (Range)**	**Mean±SD (Range)**	**Mean±SD (Range)**	**Mean±SD (Range)**	**Mean±SD (Range)**	**Mean±SD (Range)**	**Mean±SD (Range)**	**Mean±SD (Range)**	**Mean±SD (Range)**	**Mean±SD (Range)**
Temperature	19.21±0.11 (19.09- 19.29)	18.42±1.38 (16.86- 19.48)	23.37±0.09 (23.3- 23.43)	23.37±0.06 (23.32- 23.41)	20.85±1.25 (19.97- 21.74)	20.89±0.74 (20.19- 21.66)	25.88±3.03 (24.01- 29.38)	25.9±2.88 (24.12- 29.22)	22.11±0.22 (21.97- 22.37)	22.47±0.69 (21.82- 23.2)	27.36±3.95 (22.8- 29.75)	29.67±1.69 (28.49- 31.61)	22.71±0.73 (22.15- 23.54)	23.02±0.66 (22.26- 23.5)	29.19±3.8 (26.5- 31.88)	29.04±3.39 (26.64- 31.43)
Salinity	43.92±0.04 (43.87- 43.94)	40.82±4.4 (37.71- 43.93)	52.06±0.04 (52.04- 52.09)	52.06±0.01 (52.05- 52.06)	43.77±0.04 (43.75- 43.8)	43.91±0.06 (43.84- 43.95)	51.98±0.07 (51.92- 52.05)	51.97±0.07 (51.92- 52.05)	43.9±0.08 (43.84- 43.99)	43.97±0.09 (43.89- 44.07)	47.76±7.4 (39.22- 52.09)	52.11±0.25 (51.93- 52.39)	44.02±0.1 (43.96- 44.13)	44.12±0.12 (44- 44.24)	52.4±0.06 (52.36- 52.44)	52.42±0.01 (52.41- 52.43)
PO_4-P	0.12±0.11 (0- 0.22)	0.16±0.08 (0.09- 0.25)	0.18±0 (0.18- 0.18)	0.23±0.08 (0.18- 0.29)	0.1± (0.1- 0.1)	0.11±0.1 (0.04- 0.22)	0.21±0.09 (0.11- 0.29)	0.12±0.2 (0- 0.35)	0.04±0.04 (0.01- 0.08)	0.17±0.14 (0.08- 0.33)	0.04±0.04 (0.01- 0.08)	0.17±0.13 (0.08- 0.32)	0.13±0.09 (0.07- 0.23)	0.1±0.07 (0.03- 0.17)	0.17±0.19 (0.04- 0.31)	0.11±0.07 (0.06- 0.16)
DIN	0.44±0.33 (0.07- 0.72)	1.49±1.89 (0.38- 3.67)	1.28±1.28 (0.38- 2.19)	0.21±0.07 (0.16- 0.26)	0.3± (0.3- 0.3)	0.68±0.63 (0.29- 1.4)	0.35±0.08 (0.26- 0.42)	0.6±0.22 (0.35- 0.76)	0.39±0.1 (0.32- 0.51)	0.43±0.09 (0.33- 0.5)	0.54±0.52 (0- 1.04)	0.45±0.47 (0- 0.93)	0.26±0.22 (0.1- 0.41)	0.47±0.23 (0.22- 0.68)	0.38±0.28 (0.18- 0.57)	0.17±0.01 (0.16- 0.18)
N:P	1.69±1.14 (0.54- 2.81)	16.44±24.59 (2.05- 44.84)	4.24±5.65 (0.25- 8.24)	1.73±0.14 (1.63- 1.83)	4.39± (4.39- 4.39)	4.63±3.86 (0.31- 7.76)	2.82±2.06 (1.27- 5.16)	30.25±25.2 (2.9- 52.52)	6.8±3.2 (4.54- 9.07)	10.06±7.38 (1.6- 15.16)	15.85±16.38 (1.76- 33.82)	7.48±5.76 (0.84- 11.19)	2.98±1.58 (1.86- 4.1)	6.46±3.29 (3.71- 10.1)	10.09±13.06 (0.86- 19.33)	2.44±1.64 (1.28- 3.6)
TChl-a	138.18±25 (120.5- 155.86)	112.72±14.56 (102.42- 123.01)	111.45±6.99 (106.51- 116.39)	100.6±60.36 (57.92- 143.28)	73.47±43.06 (43.02- 103.91)	79.63±3.83 (76.92- 82.34)	65.68±14.99 (52.98- 82.21)	48.83±8.07 (39.52- 53.72)	76.84±9.43 (69.15- 87.36)	71.76±17.31 (58- 91.2)	51.36±6.31 (46.9- 55.83)	31.92± (31.92- 31.92)	130.32±9.91 (120.98- 140.72)	109.83±7.79 (101.61- 117.11)	112.22±57.06 (71.87- 152.56)	126.18±52 (89.41- 162.95)
DVChl-a	21.52±7.11 (16.5- 26.55)	13.12±3.92 (10.35- 15.89)	20.32±14.62 (9.99- 30.66)	14.54±15.94 (3.27- 25.81)	14.97±15.99 (3.66- 26.28)	15.75±7.93 (10.15- 21.36)	8.62±6.57 (2.09- 15.23)	4.34±2.83 (1.2- 6.69)	16.78±7.93 (9.34- 25.13)	20.18±9.29 (12.8- 30.61)	1.7±1.43 (0.69- 2.71)	1.64± (1.64- 1.64)	42.44±16.11 (24.84- 56.44)	24.75±11.28 (17.02- 37.7)	21.82±25.46 (3.81- 39.82)	20.57±13.9 (10.74- 30.4)
But	23.31±4.57 (20.08- 26.55)	11.19±2.02 (9.76- 12.62)	8.09±3.03 (5.94- 10.23)	10.79±3.05 (8.63- 12.95)	6±7.33 (0.82- 11.18)	5.92±2.62 (4.07- 7.77)	3.31±1.11 (2.6- 4.59)	2.75±0.36 (2.36- 3.08)	8.88±0.37 (8.48- 9.22)	7.24±2.24 (4.91- 9.38)	3.75±1.17 (2.92- 4.58)	1.84±0.87 (1.23- 2.46)	10.66±3.7 (6.4- 13.05)	10.03±3.38 (6.24- 12.71)	9.29±6.38 (4.78- 13.8)	11.42±7.09 (6.41- 16.43)
Hex	63.92±4.89 (60.47- 67.38)	37.43±5.87 (33.28- 41.58)	23.46±0.74 (22.94- 23.98)	34.95±5.73 (30.9- 39)	25.47±11.31 (17.47- 33.47)	23.72±4.53 (20.52- 26.92)	14.07±3.44 (10.15- 16.61)	11.82±1.19 (10.93- 13.17)	31.54±2.24 (29.85- 34.08)	23.41±5.36 (17.25- 27.03)	17.44±2.67 (15.55- 19.32)	12.05± (12.05- 12.05)	37.71±2.15 (35.92- 40.09)	33.38±5.97 (26.5- 37.22)	32.31±7.45 (27.04- 37.58)	40.5±12.68 (31.53- 49.46)
Zea	30.16±0.28 (29.96- 30.36)	24.3±6.4 (19.77- 28.82)	24.78±1.48 (23.73- 25.83)	37.8±3.08 (35.62- 39.97)	18.94±16.5 (7.28- 30.61)	22.43±3.84 (19.72- 25.15)	15.48±3.12 (12.9- 18.95)	15.5±6.34 (8.69- 21.24)	11.29±2.01 (9.15- 13.14)	16.78±1.63 (15.24- 18.48)	8.07±3.92 (5.3- 10.85)	6.18± (6.18- 6.18)	26.42±3.32 (22.79- 29.29)	20.7±8.99 (10.36- 26.67)	18.8±2.11 (17.31- 20.29)	16.8±4.23 (13.81- 19.79)
Fuc	7.36±1.83 (6.06- 8.65)	2.77±0.3 (2.56- 2.98)	2.58±0.57 (2.17- 2.98)	6.9±5.35 (3.12- 10.69)	2.27±1.24 (1.39- 3.15)	2.04±1.07 (1.28- 2.8)	2.48±0.71 (2.05- 3.3)	1.51±0.3 (1.19- 1.79)	1.66±0.65 (1.08- 2.36)	1.95±0.67 (1.18- 2.4)	2.37±0.44 (2.06- 2.68)	0.84± (0.84- 0.84)	3.67±3.32 (0.59- 7.18)	3.41±2.47 (1.94- 6.26)	3.41±0.95 (2.74- 4.08)	4.59±2.12 (3.09- 6.09)

To evaluate the overall performance of the microplate reader method, the pigment extracts collected from all sampling sites were analysed and compared with the results obtained by the HPLC analysis. The sum of Chl-a and DVChl-a from HPLC was used to calculate total Chl-a, which was compared to the values obtained from the microplate reader.

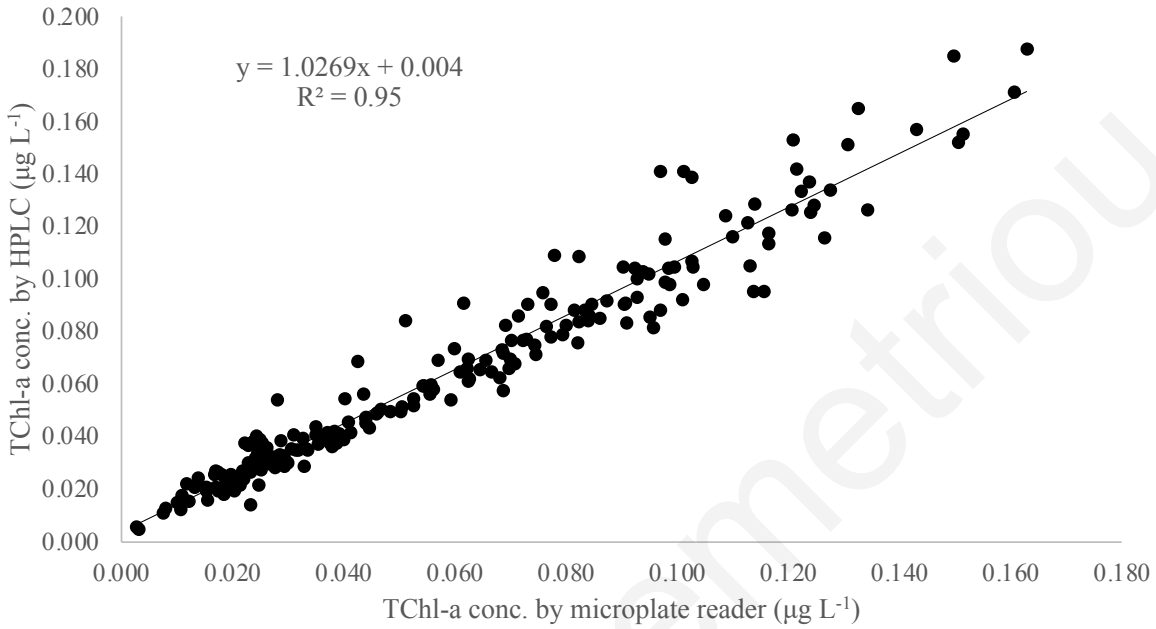

Figure III.7: Linear regression between TChl-a concentrations (sum of Chl-a and DVChl-a) measured in seawater samples by HPLC and respective Chl-a levels obtained by fluorescence microplate reader.

TChl-a concentrations obtained from the HPLC analysis ranged between 0.005 - 0.188 µg L^{-1} with an average of 0.064 ± 0.003 µg L^{-1}.

The microplate reader produced a similar range of Chl-a values, between 0.003 - 0.163 µg L^{-1} with an average of 0.058 ± 0.003 µg L^{-1}. The linear regression analysis between the two datasets provided a positive correlation (R^2 = 0.95) (Figure III.7).

3.3.4. Phytoplankton size structure

Estimations from pigment data were used to calculate the relative contribution of the phytoplankton size classes to the total Chl-a. TChl-a was lineary related to the weighted sum of the diagnostic pigments (ΣDP_w), therefore DP can be used as a valid estimator of the measured TChl-a (linear regression DP = 0.6629 TChl-a + 0.0023, r2 = 0.92).

The phytoplankton community was mainly dominated by picophytoplankton and nanophytoplankton, both following the distribution of TChl-a. The pigment-based estimations showed that most of the year, f_{pico} accounted for about half of the depth-integrated

phytoplankton biomass in all depth layers, and f_{nano} for the remaining half (Table III.***8***). During summer, the percentage of f_{nano} was higher (around 60%), with f_{pico} accounting for approximately 35% of the depth-integrated phytoplankton biomass. The percentage of f_{micro} did not exceed 6% in all stations, throughout the year (Table III.***8***).

In general, the vertical distribution of total Chl-a associated with picophytoplankton followed the distribution of Zea and DVChl a, the distribution of total Chl-a associated with nanophytoplankton followed those of Hex and But, and the total Chl-a associated with microphytoplankton was driven by the distribution pattern of Fuco (Figure III.***3*** - Figure III.***6***).

Table III.8: Mean (±SD) estimated contribution of pico- (f_{pico}), nano- (f_{nano}) and microphytoplankton (f_{micro}) as derived from pigment analysis, integrated over the water column, the surface layer (0-20 m), and the deeper (>20 m), over winter (January-March), spring (April-June), summer (July-September), and autumn (October-December).

		f_{pico} (%)	f_{nano} (%)	f_{micro} (%)
Season	**Depth**	**Mean (±SD)**	**Mean (±SD)**	**Mean (±SD)**
Winter	0-20	48±9	46±9	5±3
	>20	46±10	48±9	6±3
	0-100	46±9	48±8	6±3
Spring	0-20	42±11	52±14	5±4
	>20	48±11	48±12	4±3
	0-100	47±11	48±12	5±3
Summer	0-20	39±7	56±7	5±4
	>20	34±12	61±12	5±4
	0-100	35±10	60±11	5±3
Autumn	0-20	41±10	54±9	5±2
	0-100	46±10	49±8	5±2
	0-50	45±10	50±8	5±2

3.3.5. Chemotaxonomy

The relative contribution of each chemotaxonomic group to TChl-a was calculated for the surface (0-20 m) and deeper layers (>20 m). *Synechococcus* sp. (CYANO-2) and Prymnesiophytes dominated the phytoplankton biomass throughout the year, in both depth layers. During spring and summer, *Synechococcus* sp. accounted for approximately 60% of the TChl-a, in the shallow layer (0-20 m). The contribution of *Prochlorococcus* sp. (cyano-4) during winter was equal (~13%) in both depth layers, and higher during spring and summer in the deeper layer. Pelagophytes and diatoms accounted for less than 3% each, in both depth layers (Figure III.***8***).

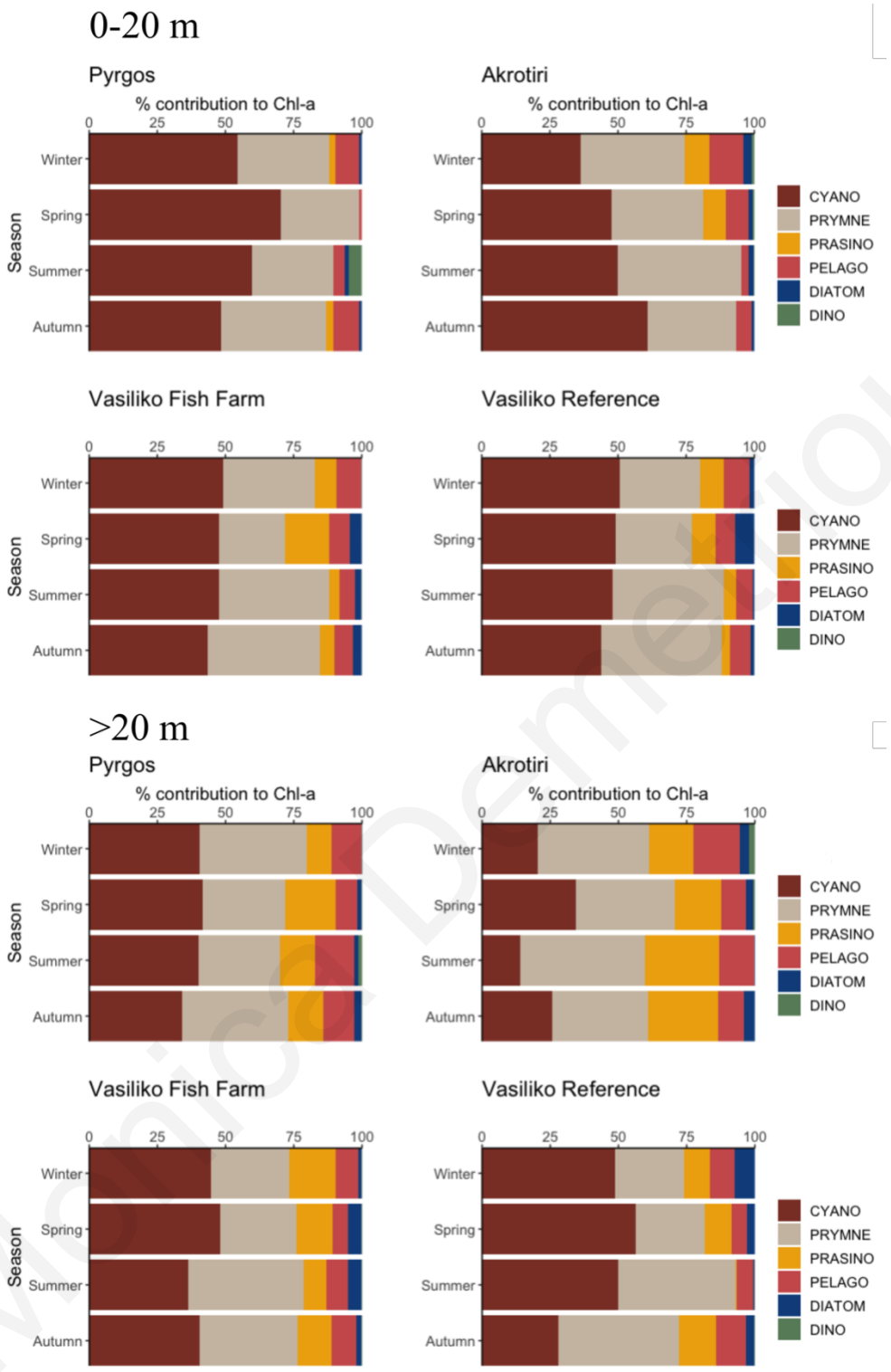

Figure III.8: Results of CHEMTAX analysis indicating the relative contribution of phytoplankton functional groups to total Chl-a at 0-20 m and >20 m depth layers, during winter (January-March), spring (April-June), summer (July-September) and autumn (October-December). CYANO is *Synechococcus* sp. and *Prochlorococcus* sp., PRYMNE is Prymnesiophytes, PRASINO is Chlorophytes and Prasinophytes, PELAGO is Pelagophytes, DIATOM is Diatoms and DINO and Dinoflagellates.

3.4. Discussion

Since phytoplankton form the base of aquatic food webs and are vital in the ocean's biogeochemical cycles, their seasonal dynamics are of paramount importance for the marine ecosystem, and fluctuations in phytoplankton community structure and abundance are linked to physical processes and nutrient inputs. In the present study, the seasonal dynamics of phytoplankton in the coastal waters of Cyprus have been studied for the first time, utilising a 12-month period timeseries.

The temperature profiles in all stations depict the mixed water-column lasting from December until April, while a strong stratification is observed for the rest of the year. Salinity is very high throughout the sampling period, consistent with high salinity Levantine waters. The lowest temperatures observed in AKR station, where the highest TChl-a concentration has also been recorded, could be attributed to a coastal upwelling present during the summer caused by persistent westerly winds that affect the near-surface layers, (Zodiatis *et al.* 2008, Mauri *et al.* 2019). However, despite the upwelling, no major blooming events may be triggered during summer. The upwelling depth in AKR could possibly be rather shallow and restricted above the thermocline within the nutrient depleted layer as is the case in the central and eastern Aegean (Androulidakis *et al.* 2017).

The concentrations of nutrients in the study area were not typical of the open waters of the Levantine, with N/P ratio being lower than the Redfield ratio of 16, and phosphate values particularly high in winter and spring. Similarly high values have been reported by DFMR's monitoring program (internal reports). When comparing the results of the present study with other coastal areas in the eastern Levantine, similar phosphate concentrations were recorded in Vasilikos bay in July 2008 (Tsagaraki *et al.* 2013). A transect of stations sampled off Mersin bay in the northeastern Levantine showed similarly low N/P ratios as the present study (Yücel 2018), and finally, compiled reference data for the establishment of nutrient thresholds in coastal stations in Israel exhibited similarly high phosphate values and N/P ratios below 16 (Kress *et al.* 2019). Even though coastal waters have higher concentrations of nutrients compared to the open sea waters, mostly due to occasional terrestrial runoff events, this is not the case in Cyprus, since input of water from land is very limited. Nutrient sources in coastal waters could be attributed to localised sources along the coast (Herut *et al.* 2000, 2002, Rahav *et al.* 2018, Kress *et al.* 2019). The area of Vasilikos bay, where stations VAS1 and VAS2 are located, is one of the most impacted coastal areas in Cyprus, where some of the largest heavy

industries in Cyprus are located. The largest power station of the island is located in the bay, as well as the largest desalination plant, producing about 60 000 cubic meters of water per day, and a cement factory. The area off PYR station is probably affected by untreated sewage since a central sewerage system has not been constructed yet., such as the heavy industry in Vasilikos bay and untreated sewage input in PYR. Microcosm experiments that have been carried out along the Israeli coast have confirmed the low N:P ratios, suggesting that coastal waters are N limited, in contrast to the open sea waters that are phosphate limited (Rahav *et al.* 2018). The relatively high nutrient concentrations are in contrast to the very low concentration of Chl-a in all stations. In oligotrophic environments, where small-sized cells are dominant, nutrient addition is not followed by a relative response of phytoplankton abundance, as was observed in fish farms in the eastern Mediterranean (Pitta *et al.* 2009). This is mainly attributed to grazing by microzooplankton, and specifically to ciliates transferring nutrients up the food web.

The small phytoplanktonic cells that dominate the eastern Mediterranean basin have large surface area to volume ratios and this allows them to utilize the low nutrient concentrations faster than larger diatoms and dinoflagellates (Litchman *et al.* 2007, Edwards *et al.* 2012). Since the phytoplankton size is associated with the type of waters, investigating the size structure of phytoplankton community could provide more information than the composition of the phytoplankton community itself (Vidussi *et al.* 2001). Based on the HPLC pigments analysis, the pico- and nanoplanktonic cells represent the most significant part of the community, consistent with oligotrophic Levantine open waters, and other Mediterranean areas where a dominance of small-sized phytoplankton up to 80 – 100% of TChl-a has been recorded (Li *et al.* 1993, Yacobi *et al.* 1995, Vidussi *et al.* 2001, Siokou-Frangou *et al.* 2010, Yücel 2013). During winter, spring, and autumn, pico- and nanophytoplankton percentages are almost of equal importance, each one accounting between 40-50% of the total biomass. In the summer, nanophytoplankton seems to dominate over picophytoplankton, with a contribution closer to 60%. This is consistent with previous studies in the eastern Mediterranean, where picophytoplankton was found to be dominant most of the year (Yacobi *et al.* 1995, Zohary *et al.* 1998, Tanaka *et al.* 2007, Yücel 2018), whereas nanophytoplankton was the dominant size class in dynamic mesoscale structures (Psarra *et al.* 2005, Tanaka *et al.* 2007).

The high nutrient concentrations recorded in the area are in contrast with the very low Chl-a concentrations and the small-sized cells that dominate the phytoplankton communities. Further work is needed to elucidate the nutrient profile of the area and to investigate further the

hydrological features. For example, wind systems and circulation patterns in the area could affect the mixing of the water-column and disperse localised high nutrient concentrations.

The use of HPLC pigment data analysis, together with the application of the CHMETAX algorithm, have been used here to characterise the phytoplankton community, as an alternative to the often complicated and time-consuming cell counting method via inverted microscopy. Previous studies have shown that the use of pigment biomarkers indicating phytoplankton size groups is a good proxy in determining phytoplankton biomass (Psarra *et al.* 2005, Lagaria *et al.* 2017). The results from the HPLC pigment signatures and CHMETAX analysis have shown that prymnesiophytes are abundant both in the shallow and in the deeper layers, throughout the year, confirming previous studies in the Mediterranean, where they were found in both mixed and stratified waters (Bustillos-Guzman *et al.* 1995, Marty *et al.* 2002, Lagaria *et al.* 2017, Yücel 2017). The cyanobacteria *Synechococcus* and *Prochlorococcus* have different spatial distributions, with *Synechococcus* more abundant in surface waters, and *Prochlorococcus* preferring deeper waters (Mella-Flores *et al.* 2011). This distribution is confirmed in this study, where the contribution of *Synechococcus* is higher in the surface layer, and this coincides with the distribution of zeaxanthin in all stations. *Prochlorococcus* on the other had had a higher contribution in the deeper layers, during spring and summer, particularly at AKR and PYR stations. This contribution is consistent with the distribution of DVChl-a, a unique biomarker pigment of *Prochlorococcus*, which had higher concentrations at deep waters.

Phytoplankton communities in the coastal waters of Cyprus demonstrate spatiotemporal variations, without significant differences in nutrient concentrations. This is the first study to demonstrate these variations, and to characterise the phytoplanktonic communities in the area. Further work is needed to elucidate the reasons of these variations, such as the effect of small grazers on phytoplankton (top-down control).

IV. Microphytoplankton species assemblages in the coastal waters of Cyprus

4.1. Introduction

Phytoplankton, as organisms at the base of food webs, support all marine life and play a critical role in maintaining biodiversity in the oceans (Field *et al.* 1998). Even though they represent less than 1% of the earth's photosynthetic biomass they are responsible for ~ 50% of the annual net primary production (Field *et al.* 1998). Given that phytoplankton are sensitive to environmental changes and have high turnover rates, they can be used as indicators of changes in the environment. Knowing the taxonomic composition of phytoplanktonic communities is of paramount importance since the community composition at any time affects the structure of marine food webs and the functioning of biogeochemical cycles (Azam *et al.* 1983).

One litre of seawater could contain up to a million algal cells, coming from over 100 different species (Hallegraeff *et al.* 2010). This has been demonstrated from various studies, which revealed that phytoplankton communities include a high number of species, most of them rare and only a small number of them dominating ecosystem functioning (Cermeño *et al.* 2014, Rodriguez-Ramos *et al.* 2014). The high number of species in a phytoplankton community, supported by a limited range of resources, consists the plankton paradox (Hutchinson 1961). The various theories trying to explain this paradox, such as that species richness positively affects the stability of the communities in the long run, require the quantification of the number of species in the phytoplankton communities (Branco *et al.* 2018). The fact that phytoplanktonic communities consist of many rare species, along with the dispersal in coastal environments, means that the structure of the communities changes quickly, with shifting conditions (Rodriguez-Ramos *et al.* 2014). Cermeño *et al*. (2014) have shown that over 40% of microplankton species are not accounted for with the use of traditional sampling methods. Therefore, the use of methods that infer species richness from small sample sizes is useful, especially for areas with limited *in situ* sampling and absence of long timeseries data, like the coastal waters of Cyprus.

Cyprus is located in the Levantine basin, eastern Mediterranean, one of the most oligotrophic marine areas with low nutrient availability and very low primary production (Krom *et al.* 1991). The coastal waters of Cyprus are characteristic of Levantine open waters, with high temperatures (up to 26 °C in the summer) and high salinity (39) (DFMR 2021a). The Department of Fisheries and Marine Research (DFMR) monitor various coastal stations for nutrients and Chl-a (DFMR 2021b), however, a long-term timeseries on phytoplankton species composition does not exist for the area. Given the fact that coastal stations are affected by localised nutrient input sources, such as untreated sewage, large factories, and desalination plants, knowing the composition of phytoplankton communities through time and seasons is very important, in order to establish trends and monitor any changes in the marine environment. Chao and Jost (2012) described how to interpolate and extrapolate diversity indices using one sample as reference. The datasets used for the rarefaction and extrapolation (R/E) curves designed by Chao and Jost (2012) are standardized by sample coverage.

This is the first attempt to record microphytoplankton species composition in Cyprus, through net samples and the recording of species present in each of the four sampling stations (AKR, PYR, VAS1, and VAS2) for a 12-month period in 2016.

4.2. Materials and Methods

Sampling was carried out monthly, between January and December 2016. Samples were collected from four coastal stations. Station PYR is located off Pyrgos on the northwest of Cyprus, whereas station AKR is located off Akrotiri peninsula. Stations VAS1 and VAS2 are located in Vasilikos bay, with station VAS1 next to an aquaculture cage and station VAS2 approximately 2 nautical miles east of VAS1.

Temperature and salinity were recorded with an SBE-19plus CTD profiler. Water was collected from standard depths (2, 10, 20, 50, 75, and 100 m) with a Niskin bottle and was used for nutrient analysis and HPLC pigment analysis.

Phytoplankton was collected from the water column at each station, with a vertical net haul (mesh size 36 microns) and preserved in buffered formalin, for qualitative analysis. The samples were viewed under a light microscope with phase contrast and photographs were taken. Where possible, phytoplankton was identified to species level. Identification of species was carried out using a large selection of taxonomic literature (Jörgensen 1920, Kofoid and Swezy 1921, Balech 1973, 1974, 1988, Taylor 1976, Sournia 1978, Tomas and Hasle 1997, Gómez

2003, 2003, 2005, Okolodkov and Gárate-Lizárraga 2006, Gomez 2007, Gómez and Furuya 2007, Hoppenrath *et al.* 2009, Okolodkov 2010, 2014).

The names in the taxonomic check-list were verified as accepted species and given the currently accepted name as defined by the World Register of Marine Species (WoRMS) database (www.marinespecies.org) (Costello *et al.* 2013). The identified taxa were recorded as presence records at each station and for each sampling month.

In order to evaluate if microphytoplankton communities from the four sampling stations were well represented and could be compared, rarefaction and extrapolation (R/E) curves were carried out using sample-size and coverage-based methods. These methodologies represent a unified sampling framework from which to make fair and meaningful comparisons of species richness among multiple assemblages (Chao and Chiu 2016).

Sample size-based R/E curves plot the diversity estimates with respect to sample size. Coverage-based R/E curves plot the diversity estimates with respect to sample coverage. The sample completeness curve depicts how the sample coverage varies as a function of sample size (Chao *et al.* 2014). In this case, the rarefaction curves were extrapolated to double the number of sampling sites of the sampling station with the lowest sampling units (Chao *et al.* 2014) (VAS stations, 9 samplings). The extrapolation was extended to a sample size of 18, configured at 40 knots and 100 replicate bootstrapping runs to estimate 95% confidence intervals (Hsieh *et al.* 2016).

Additionally, non-parametric estimators were calculated for incidence data, to estimate the total number of species that would be present in each station. The following non-parametric estimators were calculated:

- Homogenous model: this assumes that all species have the same incidence or detection probabilities (see eq. 12a in Chao and Chiu 2016).
- Chao2: this estimator uses the frequencies of uniques and duplicates to estimate the number of undetected species (see eq. 11a in Chao and Chiu 2016).
- Chao2-bc: a bias-corrected form for the Chao2 estimator (Chao 2005).
- iChao2: an improved Chao2 estimator (Chiu et al. 2014).
- ICE (Incidence-based Coverage Estimator): the observed species are separated as frequent and infrequent species groups and only data in the infrequent group are used to estimate the number of undetected species (see eq. 12b in Chao and Chiu 2016).

- ICE-1: a modified ICE for highly heterogeneous cases.
- 1st order Jacknife: uses the frequencies of uniques to estimate the number of undetected species (Burnham and Overton 1978).
- 2nd order jacknige: uses the frequencies of uniques and duplicate sto estimate the number of undetected species (Burnham and Overton 1978).

All above analyses were carried out in R R 4.1.0 (R Core Team 2021), using packages SpadeR 0.1.1 (Chao *et al.* 2016) for the calculation of the non-parametric estimators, and iNext 2.0.20 (Hsieh *et al.* 2016) for the construction of the R/E curves.

Non-metric Multidimensional Scaling (NMDS) analysis was used to compare the composition of the phytoplankton communities among seasons. NMDS was performed using species presence/absence per site/season matrix and the Jaccard similarity index. A Permutational Multivariate Analysis of Variance (PERMANOVA) was carried out to determine differences in the species composition among the four stations and seasons. The function adonis was used, with distance Jaccard similarity index and 999 random permutations (Oksanen *et al.* 2020). Adonis partitions dissimilarities and uses permutation tests to inspect the significance of the partitions (Oksanen *et al.* 2020). All analyses were carried out in R 4.1.0 (R Core Team 2021), using the packages dplyr 1.0.7 (Wickman *et al.* 2021) and vegan 2.5-7 (Oksanen *et al.* 2020).

4.3. Results

Twenty three (23) diatom and 85 dinoflagellate species were recorded, with a total of 50 taxa (Table IV.*2*).

The highest number of taxa was recorded in station PYR (45), followed by AKR (41), VAS2 (38) and VAS1 (35). This is confirmed by the incidence-based extrapolated curves, that showed PYR having the highest observed species richness followed by AKR, VAS2, and VAS1 (Figure IV.***1***). The coverage-based rarefaction curves suggest that species richness in all station is well represented, since the coverage percentage exceeds 90% (Figure IV.***1***b and Figure IV.***1***c).

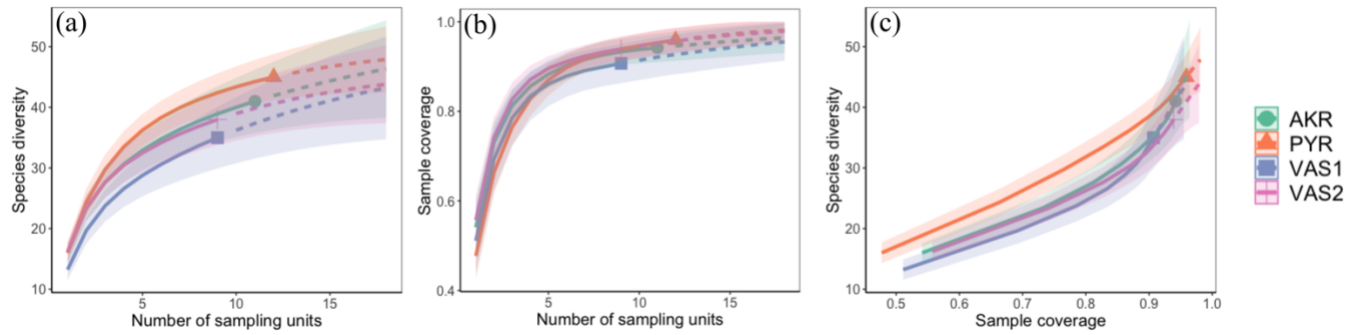

Figure IV.1: Rarefaction and Extrapolation (R/E) curves for each sampling station (AKR, PYR, VAS1, VAS2). (a) sample sized-based R/E curves, (b) coverage-based rarefaction curves, and (c) sample completeness curves. Solid lines represent rarefaction, dashed lines represent extrapolation (up to a maximum sample size of 18), and shaded areas represent the 95% confidence intervals, based on a bootstrap method with 100 replications.

The observed species richness in each station reached an important percentage of the species estimated using the non-parametric estimators. Specifically, the total number of taxa observed in PYR represented 82 – 96%, in AKR 71 – 93%, in VAS1 66 – 92%, and in VAS2 75 – 95% of expected species, respectively (Table IV.***1***).

Table IV.1: Observed taxa at each sampling station (PYR, AKR, VAS1, and VAS2) and incidence-based non-parametric estimators. Homogenous model: assumes that all species have the same incidence or detection probabilities (see eq. 12a in Chao and Chiu 2016); Chao2: uses the frequencies of uniques and duplicates to estimate the number of undetected species (see eq. 11a in Chao and Chiu 2016). Chao2-bc: bias-corrected form for the Chao2 estimator (Chao 2005). iChao2: an improved Chao2 estimator *(Chiu* et al. *2014)*. ICE (Incidence-based Coverage Estimator): the observed species are separated as frequent and infrequent species groups and only data in the infrequent group are used to estimate the number of undetected species (see eq. 12b in Chao and Chiu 2016). ICE-1: a modified ICE for highly heterogeneous cases. 1st order Jacknife: uses the frequencies of uniques to estimate the number of undetected species (Burnham and Overton 1978). 2nd order jacknige: uses the frequencies of uniques and duplicate sto estimate the number of undetected species (Burnham and Overton 1978).

Non-parametric estimators	PYR	AKR	VAS1	VAS2
Taxa observed	45	41	35	38
Homogenous Model	47±1.7	43.7 ± 2.0	38.6 ± 2.4	40.5 ± 1.9
Chao2	50.3 ± 4.7	54.7 ± 11.4	51.0 ± 12.9	46.9 ± 7.5
Chao2-bc	49.1 ± 3.8	51.0 ± 8.1	46.7 ± 9.1	44.7 ± 5.7
iChao2	50.9 ± 3.2	58.2 ± 6.8	53.2 ± 9.8	48.6 ± 5.2
ICE	50.4 ± 3.7	49.0 ± 4.9	45.2 ± 6.1	44.7 ± 4.4
ICE-1	51.4 ± 4.5	51.2 ± 6.7	48.7 ± 9.0	46.3 ± 5.7
1st order jackknife	53.3 ± 4.0	51.0 ± 4.4	45.7 ± 4.5	46.9 ± 4.1
2nd order jackknife	55.4 ± 6.5	57.1 ± 7.1	52.3 ± 7.2	51.3 ± 6.6

The NMDS ordination plot (Figure IV.***2***) shows the grouping of taxa into four seasons, winter (January – March), spring (April-June), summer (July – September), and autumn (October – December). Species composition differed significantly among stations PYR and AKR (Adonis, $F = 3.44^{e+16}$, $p<0.001$). The phytoplankton community composition was significantly related to salinity (Adonis, $F = 3.27$, $p<0.01$), temperature (Adonis, $F = 2.85$, $p<0.001$), and total Chl-a (Adonis, $F = 2.1$, $p<0.01$). The highest number of taxa (32) was recorded in spring in stations PYR and VAS2, and the lowest (13) was recorded in autumn in station VAS2.

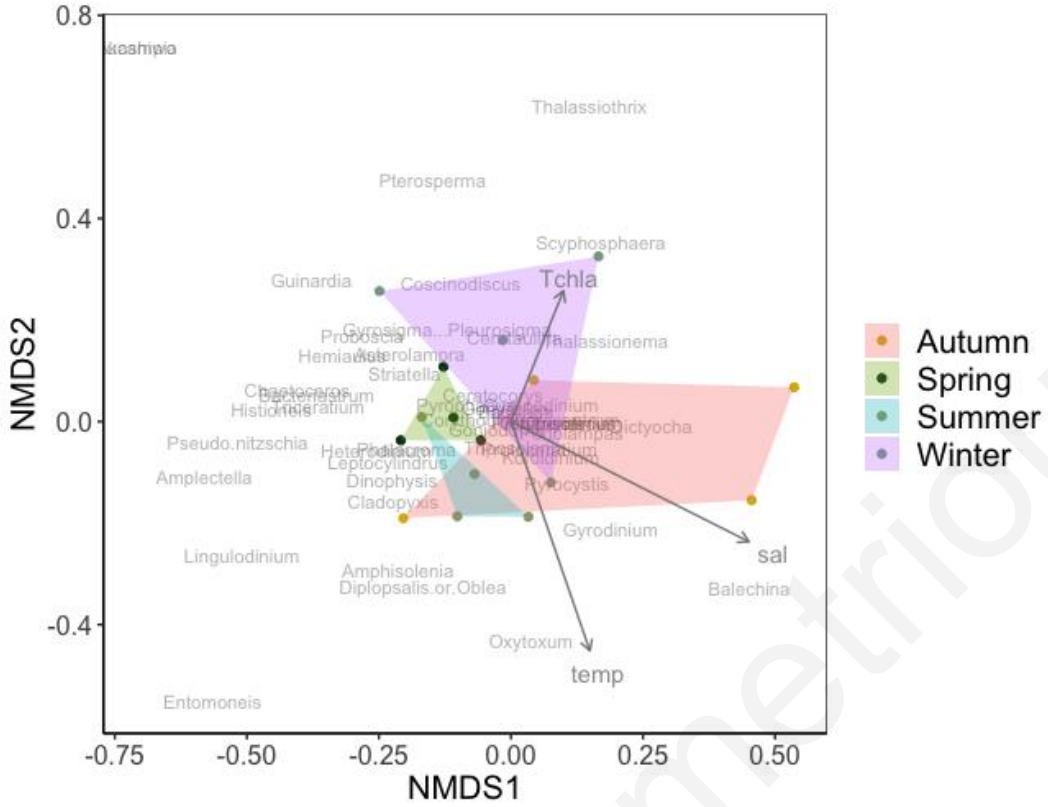

Figure IV.2: Ordination plot with the fitted surface of the three significant environmental factors (total Chl-a, temperature, and salinity), using NMDS of presence/absence data. Stress value was 0.17. Bullets are the four sampling stations at each season.

Further, a dendrogram constructed based on the Jaccard similarity index shows three distinct clusters (Figure IV.***3***). One cluster consists of stations VAS1 and VAS2 in autumn, the second groups together spring and summer of all stations, as well as winter of VAS2 and autumn of AKR, and the third cluster groups winter of stations PYR, AKR, and VAS1 and autumn PYR.

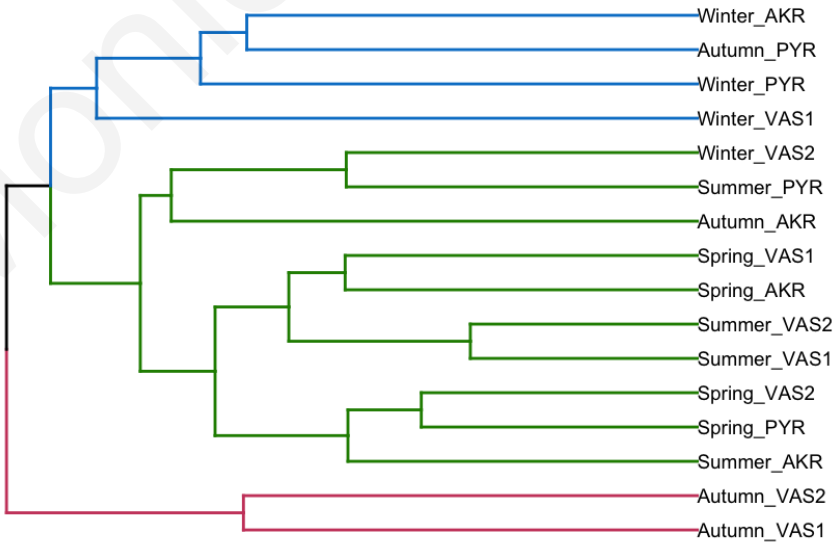

Figure IV.3: Dendrogram of species composition per station and season, based on the Jaccard similarity index.

Given that the cells were identified and counted in a known volume of sample, the net samples were converted to cell/L counts in a semi-quantitative way. The contribution of diatoms and dinoflagellates to the total biomass in all stations and seasons was trivial, as shown from the CHEMTAX results (Figure IV.***4***). The highest cell/L count was observed in stations VAS, and specifically in VAS2 (Figure IV.***5***).

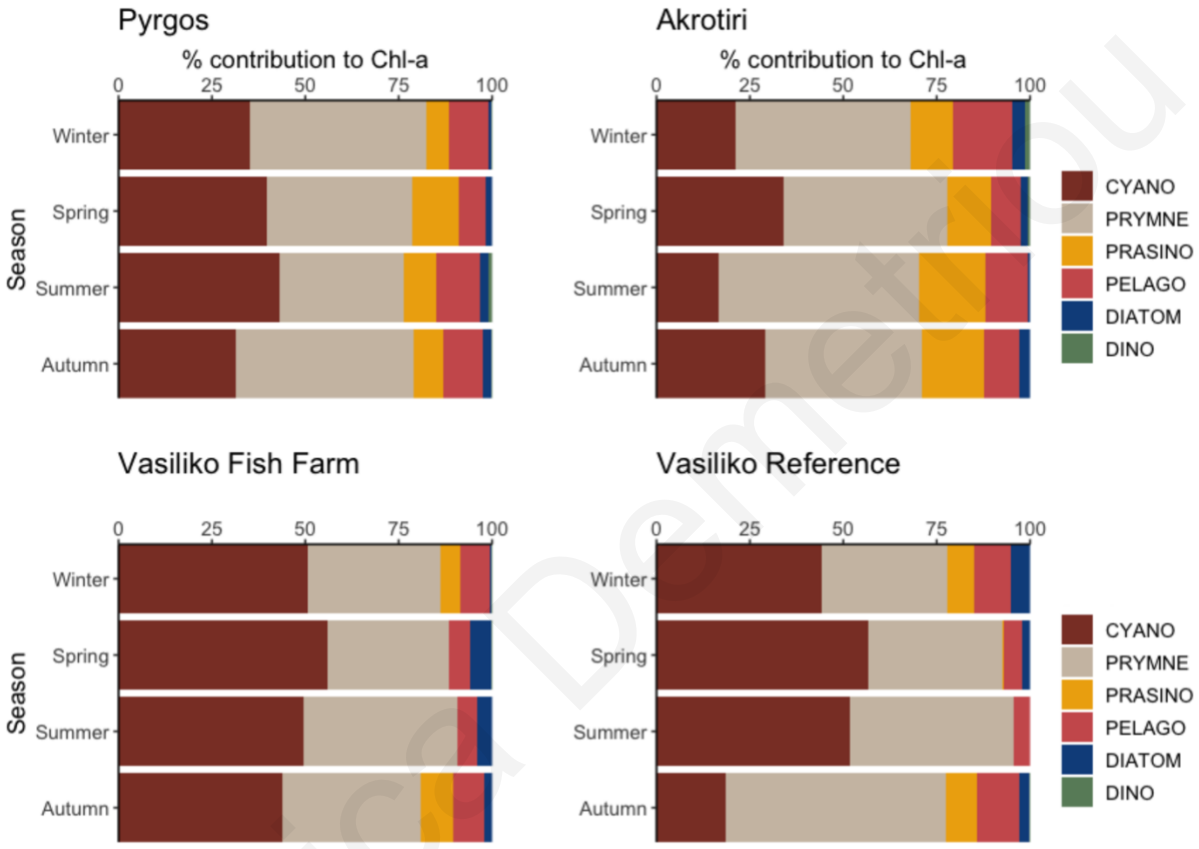

Figure IV.4: Results of CHEMTAX analysis indicating the relative contribution of phytoplankton functional groups to total Chl-a at the entire watercolumn, during winter (January-March), spring (April-June), summer (July-September) and autumn (October-December). CYANO is *Synechococcus* sp. and *Prochlorococcus* sp., PRYMNE is Prymnesiophytes, PRASINO is Chlorophytes and Prasinophytes, PELAGO is Pelagophytes, DIATOM is Diatoms and DINO and Dinoflagellates.

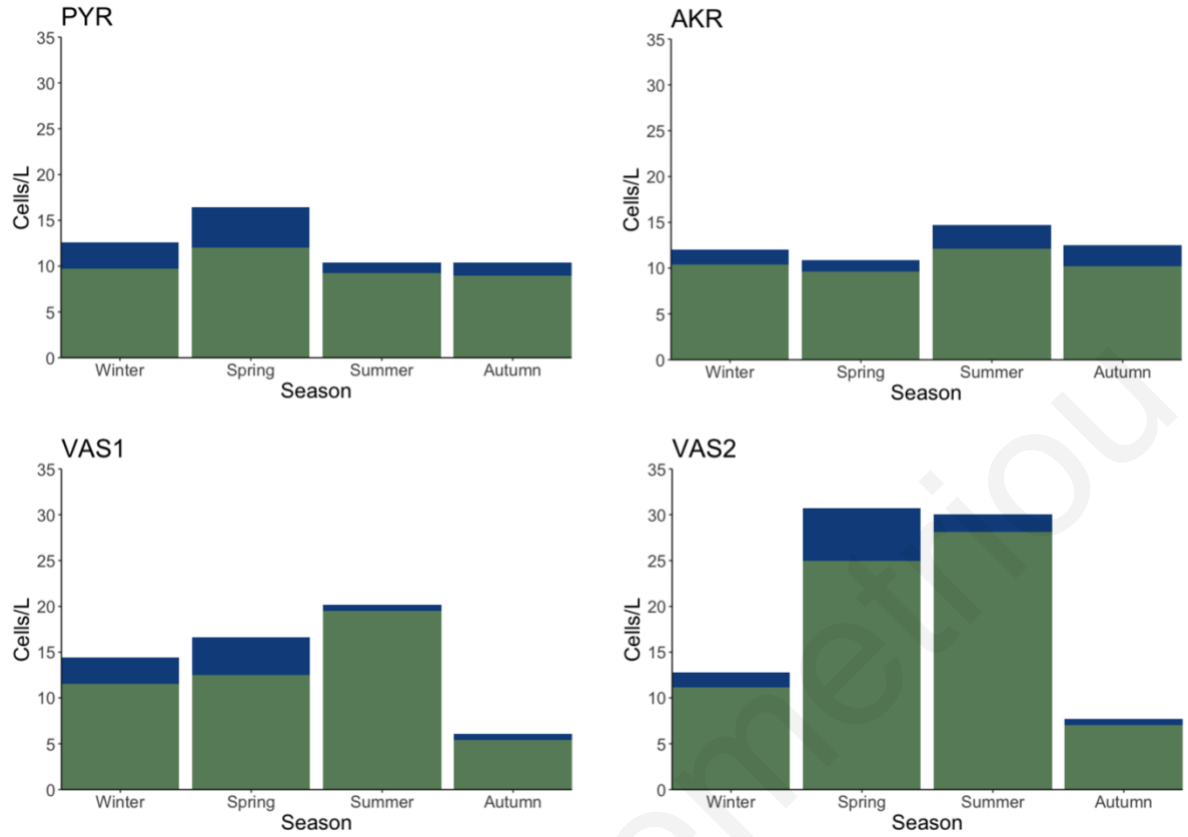

Figure IV.5: Cell/L counts per season, for stations PYR, AKR, VAS1, and VAS2.

4.4. Discussion

The results from this study offer a first recording of the larger phytoplankton taxa (mostly diatoms and dinoflagellates) in the coastal waters of Cyprus, as observed from net samples. All analysis carried out involved incidence-based methods.

Species richness in all stations seemed to be well represented (R/E curves). The analysis suggests that the Homogenous model, which assumes that all species have the same incidence or detection probabilities (Chao and Chiu 2016), was the best of the non-parametric species richness estimators, providing the most precise estimates. The lowest percentages of observed to expected taxa were recorded at stations VAS1 and VAS2, which had the lowest sampling effort (and the lowest number of recorded taxa) compared to AKR and PYR. The higher the sampling effort, the more precise the estimators were in providing species richness estimates. In a recent study that assessed the efficiency of non-parametric estimators of species richness for marine microplankton (Branco *et al.* 2018), it was found that non-parametric Jackknife estimators had a better performance compared to Chao's estimators, however, they all underestimated species richness. On the other hand, the rarefaction and extrapolation curves

showed that they can be used to compare diversity estimates for samples collected near in space and time (Branco *et al.* 2018), as is the case in the present study.

The community composition of phytoplankton in the four coastal stations was significantly related to the hydrology of the area (both temperature and salinity) and to the total Chl-a concentration. Since the community composition is related to temperature, stations are grouped into seasons, based on the taxa recorded. Grouped together and distant from the other stations, are VAS1 and VAS2 in autumn, where the lowest number of taxa has been recorded.

Future work should be carried out looking at phytoplankton abundance at the coastal waters of Cyprus, in order to have a complete picture of the phytoplankton community composition through space and time. Since the oligotrophic waters of the area support mostly pico- and nanoplanktonic cells, any future work should involve flow cytometry and molecular methods, in order to have a complete picture of the phytoplankton community in the area.

Table IV.2: List of ochrophyta, haptophyta, chlorophyta, diatoms and dinoflagellates reported in the coastal waters of Cyprus. Stations are Akrotiri (AKR), Pyrgos (PYR), Vasilikos Fish farm (VAS1) and Vasilikos reference (VAS2).

	AKR	PYR	VAS1	VAS2
Dictyochophyceae				
Dictyocha Ehrenberg, 1837	■	■	■	■
Prymnesiophyceae				
Scyphosphaera apsteinii Lohmann, 1902	■	■	■	■
Prasinophyceae				
Pterosperma Pouchet, 1893	■	■		
Bacillariophyceae				
Asterolampra sp. C.G. Ehrenberg, 1844	■	■	■	■
Asterolampra marylandica Ehrenberg, 1844	■	■	■	■
Bacteriastrum sp. G. Shadbolt, 1854	■	■	■	■
Cerataulina pelagica (Cleve) Hendey, 1937	■	■	■	■
Chaetoceros sp. C.G. Ehrenberg, 1844	■	■	■	■
Chaetoceros messanensis Castracane, 1875	■	■		
Coscinodiscus sp. C.G. Ehrenberg, 1839	■	■	■	■
Entomoneis sp. Ehrenberg, 1845	■			
Eucampia sp. C.G. Ehrenberg, 1839		■	■	
Guinardia striata (Stolterfoth) Hasle, 1996	■	■	■	■
Gyrosigma sp. A.H. Hassall, 1845 / *Pleurosigma* sp. W. Smith, 1852	■	■	■	■
Hemiaulus hauckii Grunow ex Van Heurck, 1882	■	■	■	■
Leptocylindrus sp. P.T. Cleve in C.G.J. Petersen, 1889	■	■	■	■
Proboscia alata (Brightwell) Sundström, 1986	■	■	■	■
Pseudo-nitzschia sp. H. Peragallo in H. Peragallo & M. Peragallo, 1900	■	■	■	■
Rhizosolenia sp. T. Brightwell, 1858	■	■	■	■
Rhizosolenia bergonii H.Peragallo, 1892	■	■	■	
Rhizosolenia castracanei H.Peragallo, 1888		■	■	
Rhizosolenia temperei H.Peragallo, 1888	■			
Striatella unipunctata (Lyngbye) C.Agardh, 1832				■
Thalassionema sp. A. Grunow ex C. Mereschkowsky, 1902	■	■	■	■
Triceratium sp. C.G. Ehrenberg, 1839		■	■	
Vibrio paxillifer O.F.Müller, 1786				■
Dinophyceae				
Amphisolenia sp. Stein, 1883	■	■	■	■
Balechina sp. Loeblich Jr. & Loeblich III, 1968		■	■	■
Ceratocorys gourretii Paulsen, 1937	■		■	
Ceratocorys horrida Stein, 1883	■	■	■	■
Ceratocorys sp. Stein, 1883	■	■	■	■
Cladopyxis sp. Stein, 1883	■	■	■	
Corythodinium diploconus (F.Stein) F.J.R.Taylor, 1976	■	■	■	■
Corythodinium sp. Loeblich Jr. & Loeblich III, 1966	■	■	■	■
Dinophysis caudata Saville-Kent, 1881	■	■	■	■
Dinophysis hastata F.Stein, 1883	■			
Dinophysis schuettii Murray & Whitting, 1899	■	■	■	■
Goniodoma polyedricum (Pouchet) Dodge, 1981	■	■	■	■
Goniodoma sp. Stein, 1883	■	■	■	■
Gonyaulax sp. Diesing, 1866	■	■	■	■
Gonyaulax pacifica Kofoid, 1907		■	■	

Gonyaulax spinifera (Claparède & Lachmann) Diesing, 1866
Gymnodinium sp. F. Stein, 1878
Gyrodinium sp. Kofoid & Swezy, 1921
Heterodinium sinistrum Kofoid & Adamson, 1933
Histioneis sp. Stein, 1883
Kofoidinium sp. Pavillard, 1928
Lingulodinium sp. D.Wall, 1967
Ornithocercus francescae (Murray) Balech, 1962
Ornithocercus magnificus Stein, 1883
Ornithocercus quadratus Schütt, 1900
Ornithocercus steinii Schütt, 1900
Oxytoxum sp. Stein, 1883
Phalacroma doryphorum Stein, 1883
Phalacroma mitra F.Schütt, 1895
Phalacroma rapa Jorgensen, 1923
Podolampas bipes Stein, 1883
Podolampas elegans Schütt, 1895
Podolampas palmipes Stein, 1883
Podolampas spinifera Okamura, 1912
Protoceratium sp. Bergh, 1881
Protoceratium reticulatum (Claparède & Lachmann) Bütschli, 1885
Protoceratium spinulosum (Murray & Whitting) Schiller, 1937
Protoperidinium sp. Bergh, 1881
Pyrocystis elegans Pavillard, 1931
Pyrocystis fusiformis C.W.Thomson, 1876
Pyrocystis fusiformis f. detruncata Matzen., 1933
Pyrocystis fusiformis f. lanceolata (Schröder) F.J.R.Taylor, 1976
Pyrocystis hamulus Cleve, 1900
Pyrocystis hamulus var. inaequalis Schröder, 1900
Pyrocystis pseudonoctiluca Wyville-Thompson, 1876
Pyrophacus horologium F.Stein, 1883
Pyrophacus steinii (Schiller) Wall & Dale, 1971
Pyrophacus vancampoae (R.Rossignol) Wall & Dale, 1971
Tripos arietinus (Cleve) F.Gómez, 2013
Tripos arietinus f. gracilentus (Jörgensen) F.Gómez, 2013
Tripos azoricus (Cleve) F.Gómez, 2013
Tripos belone (Cleve) F.Gómez, 2013
Tripos biceps (Claparède & Lachmann) F.Gómez, 2013
Tripos candelabrum (Ehrenberg) F.Gómez, 2013
Tripos carriensis (Gourret) F.Gómez, 2013
Tripos coarctatus (Pavillard) F.Gómez, 2013
Tripos concilians (Jørgensen) F.Gómez, 2013
Tripos contrarius (Gourret) F.Gómez, 2013
Tripos declinatus (G.Karsten) F.Gómez, 2013
Tripos digitatus (F.Schütt) F.Gómez, 2013
Tripos euarcuatus (Jørgensen) F.Gómez, 2013
Tripos extensus (Gourret) F.Gómez, 2013
Tripos furca (Ehrenberg) F.Gómez, 2013
Tripos fusus (Ehrenberg) F.Gómez, 2013
Tripos gallicus (Kofoid) F.Gómez, 2013
Tripos gibberus (Gourret) F.Gómez, 1883
Tripos hexacanthus (Gourret) F.Gómez, 2013
Tripos horridus (Cleve) F.Gómez, 2013

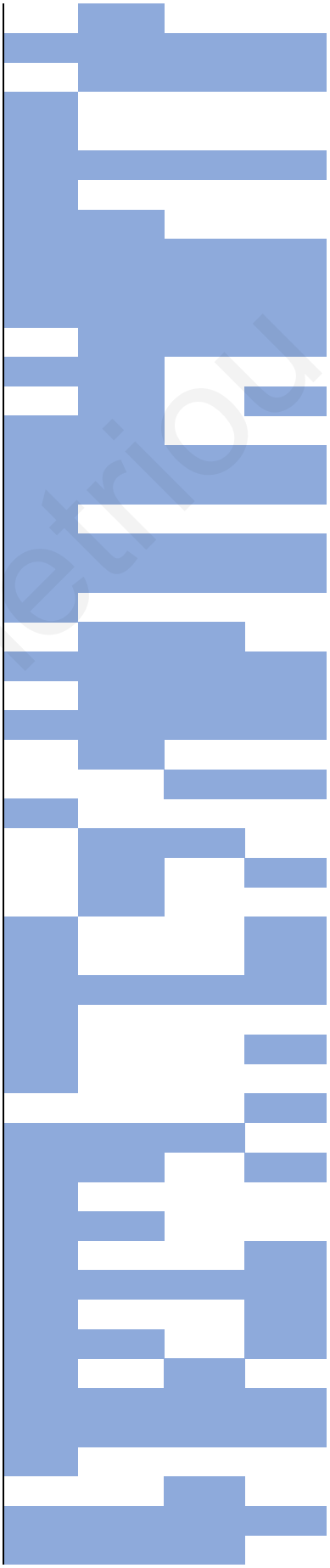

Tripos karstenii (Pavillard) F.Gómez, 1907
Tripos limulus (Pouchet) F.Gómez, 2013
Tripos macroceros (Ehrenberg) F.Gómez, 2013
Tripos massiliensis (Gourret) F.Gómez, 2013
Tripos muelleri Bory de Saint-Vincent, 1826
Tripos paradoxides (Cleve) F.Gómez, 2013
Tripos pentagonus (Gourret) F.Gómez, 2013
Tripos petersii (Steemann Nielsen) F.Gómez, 2013
Tripos platycornis (Daday) F.Gómez, 2013
Tripos pulchellus (Schröder) F.Gómez, 2013
Tripos ranipes (Cleve) F.Gómez, 2013
Tripos symmetricus (Pavill. 1905) F. Gómez, 2013
Tripos symmetricus var. coarctatus (Pavill. 1905) F. Gómez, 2013
Tripos teres (Kofoid) F.Gómez, 2013
Tripos trichoceros (Ehrenberg) Gómez, 2013
Tripos vultur (Cleve) F.Gómez, 2013
Triposolenia depressa Kofoid, 1906

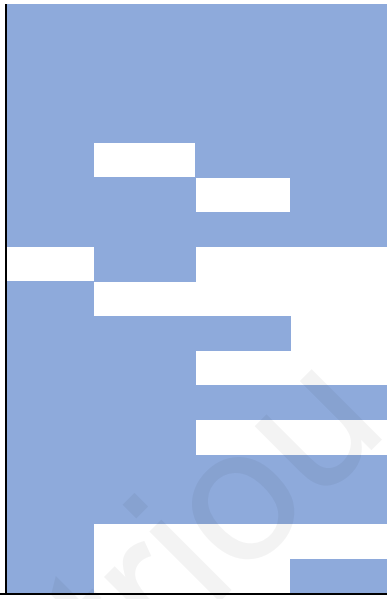

V. Conclusion and Future directions

5.1. Summary

This work provides, for the first time, insights on the phytoplankton community structure and dynamics in the coastal waters of Cyprus, using a combination of ocean colour remote sensing observations and a 12-month long timeseries of *in situ* biological and physiochemical data. Since phytoplankton play a vital role in biogeochemical cycles, and are at the base of food webs, studying the seasonal dynamics, community structure, and the taxonomy of their functional types, is crucial if we are to monitor the effect of environmental changes on phytoplankton dynamics. Any changes on the phytoplankton community structure can have implications in the functioning of the entire marine ecosystem, e.g., where effects of climate on the timing of phytoplankton growth periods can alter the balance between food availability and fitness and recruitment of higher trophic levels.

Chapter II provides the first complete seasonal cycle of phytoplankton phenology in the coastal waters of Cyprus, by applying both remote sensing observations and *in situ* phytoplankton pigments analysis. The results demonstrate that ocean colour remote sensing can be used to effectively monitor the marine ecosystem of Cyprus, and the eastern Levantine, where *in situ* data are scarce, and shows that by using a synergistic approach we can improve our understanding of phytoplankton seasonal succession. The phenology for the coastal waters of Cyprus agrees with D'Ortenzio and Ribera d'Alcalà (2009), where the open waters of the eastern Mediterranean are classified as "no bloom", with higher concentrations in fall and winter and lower values in spring and summer.

Chapter III explores the spatiotemporal dynamics of phytoplankton in the coastal waters of Cyprus, through the analysis of a 12-month long timeseries of *in situ* data. A combination of HPLC pigments analysis with the application of the CHEMTAX algorithm was carried out, to investigate the size structure of the phytoplankton community. The trait-based analysis of organisms can be used to predict the composition of the community in various environments.

Chapter IV provides the first description of microphytoplankton comunities from the coastal waters of Cyprus and a preliminary checklist of species present. Rarefaction and extrapolation (R/E) curves can be used to compare diversity estimates in this case, where samples are collected near in space and time.

5.2. Chapter II overview:

- Results show that *in situ* data are consistent with the satellite-derived phytoplankton phenology in the coastal waters of Cyprus.
- Satellite observations place the initiation of the phytoplankton growth period in November. This coincides with increased concentrations of the integrated total Chl-a calculated from HPLC data. The growth period terminates in March/April, when the MLD becomes shallower.
- Compared to the 23-year climatology, the remote sensing data for the sampling period of 2016 showed an earlier termination and thus, a shorter duration.
- Pico- and nanophytoplankton had the highest contribution in the phytoplankton communities, consistent with oligotrophic Levantine open waters.
- The coastal waters of Cyprus reflect the ultra-oligotrophic conditions of the eastern Mediterranean, evident from the extremely low Chl-a values recorded in the study area.

5.3. Chapter III overview:

- The mixed water column period lasts from December to April, and for the rest of the year the water column is stratified. Salinity in the area is very high, consistent with Levantine waters. A coastal upwelling feature reported in the area of AKR during the summer could explain the cold waters and higher total Chl-a concentrations.
- Nutrient concentrations in the coastal waters of Cyprus were generally low, with some exceptionally high values of phosphate concentrations in winter and spring. Possible reasons for these high values are the localised sources of nutrient inputs along the coast, such as a power station, a cement factory, a desalination plant, and untreated sewage.
- The contribution of nanophytoplankton during the summer was closer to 60%, whereas the rest of the year, the contribution of both pico- and nanophytoplankton was equal and between 40-50%.

- CHEMTAX and HPLC analysis results confirm previous studies in the Mediterranean. Prymnesiophytes were the most abundant group in both the shallow and deeper layers, throughout the year. *Synechococcus* had a higher distribution in the surface layer, coinciding the distribution of zeaxanthin. The contribution of *Prochlorococcus* was higher in the deeper layers, consistent with the distribution of DVChl-a.
- The use of a fluorescence microplate reader in this study confirms that this can be used as an alternative method to the conventional fluorometric analysis or HPLC method, providing accurate total Chl-a readings, with a short analysis times and high sensitivity.

5.4. Chapter IV overview:

- A total of 50 taxa have been recorded, with PYR having the highest observed species richness followed by AKR, VAS2, and VAS1. This has also been confirmed by the rarefaction and extrapolation (R/E) curves.
- The use of non-parametric species estimators showed that the Homogenous Model performed the best, providing the most precise estimates of species richness.
- The community composition of microphytoplankton in the four coastal stations was significantly related to temperature, salinity and total Chl-a concentration, and the NMDS ordination plot revealed four groups, each one representing a season.

5.5. Future work

The results of this thesis provide a first picture of the composition and seasonal succession of phytoplankton communities in the coastal waters of Cyprus.

Future research should assess how oceanic warming is affecting phytoplankton phenology and the seasonal succession of phytoplankton pigments in the area. Another direction could be to investigate the suitability of applying methods that derive phytoplankton functional types through ocean colour remote sensing observations in the study area.

Identification of the smaller phytoplankton is often to a coarser taxonomic level as many cannot be distinguished to species using light microscopy. Given the dominance of pico- and nanoplanktonic cells in the study area, the use of other methods such as electron microscopy, flow cytometry, and molecular methods should be used to determine species and shed more light on the phytoplankton community structure of the area.

Finally, further work is needed to elucidate the reasons of observed spatiotemporal variations, such as the effect of small grazers on phytoplankton (top-down control).

References

AL-NAIMI, N., RAITSOS, D.E., BEN-HAMADOU, R. and SOLIMAN, Y., 2017. Evaluation of Satellite Retrievals of Chlorophyll-a in the Arabian Gulf. *Remote Sensing*. 9(3), pp. 301

AMANTE, C. and EAKINS, B.W., 2009. ETOPO1 1 Arc-Minute Global Relief Model: Procedures, Data Sources and Analysis [viewed 29 Nov 2021]. Available from: https://data.nodc.noaa.gov/cgi-bin/iso?id=gov.noaa.ngdc.mgg.dem:316

ANDROULIDAKIS, Y.S., KRESTENITIS, Y.N. and PSARRA, S., 2017. Coastal upwelling over the North Aegean Sea: Observations and simulations. *Continental Shelf Research*. 149, pp. 32–51

AZAM, F., FENCHEL, T., FIELD, J., GRAY, J., MEYER-REIL, L. and THINGSTAD, F., 1983. The Ecological Role of Water-Column Microbes in the Sea. *Marine Ecology Progress Series*. 10, pp. 257–263

AZOV, Y., 1986. Seasonal patterns of phytoplankton productivity and abundance in nearshore oligotrophic waters of the Levant Basin (Mediterranean). *Journal of Plankton Research*. 8(1), pp. 41–53

AZOV, Y., 1991. Eastern Mediterranean—a marine desert? *Marine Pollution Bulletin*. 23, pp. 225–232

BALECH, E., 1973. *Segunda Contribución al Conocimiento Del Microplancton Del Mar de Bellingshausen*. Direccion Nacional del Antartico

BALECH, E., 1974. *El Género Protoperidinium Bergh, 1881 (Peridinium Ehrenberg, 1831, Partim)*

BALECH, E., 1988. *Los Dinoflagelatos Del Atlantico Sudoccidental*. Madrid

BARBIEUX, M., UITZ, J., GENTILI, B., PASQUERON DE FOMMERVAULT, O., MIGNOT, A., POTEAU, A., SCHMECHTIG, C., TAILLANDIER, V., LEYMARIE, E., PENKERC'H, C., D'ORTENZIO, F., CLAUSTRE, H. and BRICAUD, A., 2019. Bio-optical characterization of subsurface chlorophyll maxima in the Mediterranean Sea from a Biogeochemical-Argo float database. *Biogeosciences*. 16, pp. 1321–1342

BASU, S. and MACKEY, K., 2018. Phytoplankton as Key Mediators of the Biological Carbon Pump: Their Responses to a Changing Climate. *Sustainability*. 10(3), pp. 869

BEAUGRAND, G., 2005. Monitoring pelagic ecosystems using plankton indicators. *ICES Journal of Marine Science*. 62(3), pp. 333–338

BENGIL, F. and MAVRUK, S., 2018. Bio-optical trends of seas around Turkey: An assessment of the spatial and temporal variability. *Oceanologia*. 60(4), pp. 488–499

BERMAN, T., AZOV, Y. and TOWNSEND, D., 1984a. Understanding Oligotrophic Oceans : Can the Eastern Mediterranean be a Useful Model? *In*: D.O. HOLM-HANSEN, P.L. BOLIS, and P.R. GILLES, eds. *Marine Phytoplankton and Productivity*. Springer Berlin Heidelberg, pp. 101–112

BERMAN, T., TOWNSEND, D.W., ELSAYED, S.Z., TREES, C.C. and AZOV, Y., 1984b. Optical transparency, chlorophyll and primary productivity in the Eastern Mediterranean near the Israeli coast. *Oceanologica Acta*. 7(3), pp. 367–372

BERTHON, J.-F. and ZIBORDI, G., 2004. Bio-optical relationships for the northern Adriatic Sea. *International Journal of Remote Sensing*. 25(7–8), pp. 1527–1532

BETHOUX, J.P., GENTILI, B., MORIN, P., NICOLAS, E., PIERRE, C. and RUIZ-PINO, D., 1999. The Mediterranean Sea: a miniature ocean for climatic and environmental studies and a key for the climatic functioning of the North Atlantic. *Progress in Oceanography*. 44, pp. 131–146

BIANCHI, T.S., DEMETROPOULOS, A., HADJICHRISTOPHOROU, M., ARGYROU, M., BASKARAN, M. and LAMBERT, C., 1996. Plant pigments as biomarkers of organic matter sources in sediments and coastal waters of Cyprus (eastern Mediterranean). *Estuarine, Coastal and Shelf Science*. 42(1), pp. 103–115

BJØRRISEN, P.K., 1988. Phytoplankton exudation of organic matter: *Why* do healthy cells do it?1. *Limnology and Oceanography*. 33(1), pp. 151–154

DE BOYER MONTÉGUT, C., 2004. Mixed layer depth over the global ocean: An examination of profile data and a profile-based climatology. *Journal of Geophysical Research*. 109(C12), pp. C12003

BRANCO, M., FIGUEIRAS, F.G. and CERMEÑO, P., 2018. Assessing the efficiency of non-parametric estimators of species richness for marine microplankton. *Journal of Plankton Research*. 40(3), pp. 230–243

BREWIN, R.J.W., MORÁN, X.A.G., RAITSOS, D.E., GITTINGS, J.A., CALLEJA, M.Ll., VIEGAS, M., ANSARI, M.I., AL-OTAIBI, N., HUETE-STAUFFER, T.M. and HOTEIT, I., 2019. Factors Regulating the Relationship Between Total and Size-Fractionated Chlorophyll-a in Coastal Waters of the Red Sea. *Frontiers in Microbiology*. 10, pp. 1964

BREWIN, R.J.W., RAITSOS, D.E., PRADHAN, Y. and HOTEIT, I., 2013. Comparison of chlorophyll in the Red Sea derived from MODIS-Aqua and in vivo fluorescence. *Remote Sensing of Environment*. 136, pp. 218–224

BREWIN, R.J.W., SATHYENDRANATH, S., HIRATA, T., LAVENDER, S.J., BARCIELA, R.M. and HARDMAN-MOUNTFORD, N.J., 2010. A three-component model of phytoplankton size class for the Atlantic Ocean. *Ecological Modelling*. 221(11), pp. 1472–1483

BRICAUD, A., BOSC, E. and ANTOINE, D., 2002. Algal biomass and sea surface temperature in the Mediterranean Basin. *Remote Sensing of Environment*. 81(2–3), pp. 163–178

BURNHAM, K.P. and OVERTON, W.S., 1978. Estimation of the size of a closed population when capture probabilities vary among animals. *Biometrika*. 65(3), pp. 625–633

BUSTILLOS-GUZMAN, J., CLAUSTRE, H. and MARTY, J.-C., 1995. Specific phytoplankton signatures and their relationship to hydrographic conditions in the coastal northwestern Mediterranean Sea. *Marine ecology progress series. Oldendorf*. 124(1), pp. 247–258

CASTELLANI, C. and EDWARDS, M., eds., 2017. *Marine Plankton: A Practical Guide to Ecology, Methodology, and Taxonomy*. First edition.. Oxford: Oxford University Press

CERMEÑO, P., TEIXEIRA, I.G., BRANCO, M., FIGUEIRAS, F.G. and MARANON, E., 2014. Sampling the limits of species richness in marine phytoplankton communities. *Journal of Plankton Research*. 36(4), pp. 1135–1139

CHAO, A., 2005. Species estimation and applications. *In*: *Encyclopedia of Statistical Sciences*. New York: Wiley, pp. 7907–7916

CHAO, A. and CHIU, C.-H., 2016. Nonparametric Estimation and Comparison of Species Richness. *In*: JOHN WILEY & SONS, LTD, ed. *ELS*. Wiley [viewed 25 Nov 2021]. Available from: https://onlinelibrary.wiley.com/doi/book/10.1002/047001590X

CHAO, A., GOTELLI, N.J., HSIEH, T.C., SANDER, E.L., MA, K.H., COLWELL, R.K. and ELLISON, A.M., 2014. Rarefaction and extrapolation with Hill numbers: a framework for sampling and estimation in species diversity studies. *Ecological Monographs*. 84(1), pp. 45–67

CHAO, A. and JOST, L., 2012. Coverage-based rarefaction and extrapolation: standardizing samples by completeness rather than size. *Ecology*. 93(12), pp. 2533–2547

CHAO, A., MA, K.H., HSIEH, T.C. and CHIU, C.-H., 2016. *SpadeR: Species-Richness Prediction and Diversity Estimation with R*

CHIU, C.-H., WANG, Y.-T., WALTHER, B.A. and CHAO, A., 2014. An improved nonparametric lower bound of species richness via a modified good-turing frequency formula: An Improved Nonparametric Lower Bound of Species Richness. *Biometrics*. 70(3), pp. 671–682

CHRISTAKI, U., GIANNAKOUROU, A., VAN WAMBEKE, F. and GRÉGORI, G., 2001. Nanoflagellate predation on auto- and heterotrophic picoplankton in the oligotrophic Mediterranean Sea. *Journal of Plankton Research*. 23(11), pp. 1297–1310

CHRISTODOULAKI, S., PETIHAKIS, G., KANAKIDOU, M., MIHALOPOULOS, N., TSIARAS, K. and TRIANTAFYLLOU, G., 2013. Atmospheric deposition in the Eastern Mediterranean. A driving force for ecosystem dynamics. *Journal of Marine Systems*. 109–110, pp. 78–93

CLAUSTRE, H., MOREL, A., HOOKER, S.B., BABIN, M., ANTOINE, D., OUBELKHEIR, K., BRICAUD, A., LEBLANC, K., QUÉGUINER, B. and MARITORENA, S., 2002. Is desert dust making oligotrophic waters greener? *Geophysical Research Letters*. 29(10), pp. 107-1-107–4

COLL, M., PIRODDI, C., STEENBEEK, J., KASCHNER, K., BEN RAIS LASRAM, F., AGUZZI, J., BALLESTEROS, E., BIANCHI, C.N., CORBERA, J., DAILIANIS, T., DANOVARO, R., ESTRADA, M., FROGLIA, C., GALIL, B.S., GASOL, J.M., GERTWAGEN, R., GIL, J., GUILHAUMON, F., KESNER-REYES, K., KITSOS, M.-S., KOUKOURAS, A., LAMPADARIOU, N., LAXAMANA, E., LÓPEZ-FÉ DE LA CUADRA, C.M., LOTZE, H.K., MARTIN, D., MOUILLOT, D., ORO, D., RAICEVICH, S., RIUS-BARILE, J., SAIZ-SALINAS, J.I., SAN VICENTE, C., SOMOT, S., TEMPLADO, J., TURON, X., VAFIDIS, D., VILLANUEVA, R. and VOULTSIADOU, E., 2010. The Biodiversity of the Mediterranean Sea: Estimates, Patterns, and Threats. *PLoS ONE*. 5(8), pp. e11842

COSTELLO, M.J., BOUCHET, P., BOXSHALL, G., FAUCHALD, K., GORDON, D., HOEKSEMA, B.W., POORE, G.C.B., VAN SOEST, R.W.M., STÖHR, S., WALTER, T.C., VANHOORNE, B., DECOCK, W. and APPELTANS, W., 2013. Global Coordination and Standardisation in Marine Biodiversity through the World Register of Marine Species (WoRMS) and Related Databases. *PLoS ONE*. 8(1), pp. e51629

CUSHING, D.H., 1990. Plankton Production and Year-class Strength in Fish Populations: an Update of the Match/Mismatch Hypothesis. *Advances in Marine Biology*. 26, pp. 249–293

DE BAAR, H.J.W., 1994. von Liebig's law of the minimum and plankton ecology (1899–1991). *Progress in Oceanography*. 33(4), pp. 347–386

DEFLORIO, M., APREA, A., CORRIERO, A., SANTAMARIA, N. and DE METRIO, G., 2005. Incidental captures of sea turtles by swordfish and albacore longlines in the Ionian sea. *Fisheries Science*. 71(5), pp. 1010–1018

DFMR, 2021a. *The Marine Environment of Cyprus* [online] [viewed 24 Nov 2021]. Available from: http://www.moa.gov.cy/moa/dfmr/dfmr.nsf/All/6561CB64C528ECFA42257F370041F296?OpenDocument

DFMR, 2021b. *Activities of Marine Environment Division* [online] Available from: http://www.moa.gov.cy/moa/dfmr/dfmr.nsf/All/ABF40A7AB7C59E3842257F3700418786?OpenDocument

DOMINGUES, R.B., BARBOSA, A. and GALVÃO, H., 2008. Constraints on the use of phytoplankton as a biological quality element within the Water Framework Directive in Portuguese waters. *Marine Pollution Bulletin*. 56(8), pp. 1389–1395

D'ORTENZIO, F., MARULLO, S., RAGNI, M., RIBERA D'ALCALÀ, M. and SANTOLERI, R., 2002. Validation of empirical SeaWiFS algorithms for chlorophyll-a retrieval in the Mediterranean Sea: A case study for oligotrophic seas. *Remote Sensing of Environment*. 82(1), pp. 79–94

D'ORTENZIO, F. and RIBERA D'ALCALÀ, M., 2009. On the trophic regimes of the Mediterranean Sea: a satellite analysis. *Biogeosciences*. 6(2), pp. 139–148

D'ORTENZIO, F., SANTOLERI, R., MARULLO, S., RAGNI, M. and RIBERA D'ALCALA, M., 2000. Empirical SeaWiFS chlorophyll algorithm validation for the Mediterranean Sea. *In*: C.R. BOSTATER, JR. and R. SANTOLERI, eds.. Presented at the Europto Remote Sensing, Barcelona, Spain, pp. 124–131 [viewed 5 Dec 2021]. Available from: http://proceedings.spiedigitallibrary.org/proceeding.aspx?articleid=924299

EDIGER, D. and YILMAZ, A., 1996. Characteristics of deep chlorphyll maximum in the Northeastern Mediterranean with respect to environmental conditions. *Journal of Marine Systems*. 9(3–4), pp. 291–303

EDWARDS, K.F., THOMAS, M.K., KLAUSMEIER, C.A. and LITCHMAN, E., 2012. Allometric scaling and taxonomic variation in nutrient utilization traits and maximum growth rate of phytoplankton. *Limnology and Oceanography*. 57(2), pp. 554–566

EDWARDS, M. and RICHARDSON, A.J., 2004. Impact of climate change on marine pelagic phenology and trophic mismatch. *Nature*. 430(7002), pp. 881–884

EEA, 2021. *EIONET Central Data Repository* [online] [viewed 7 Jan 2021]. Available from: http://cdr.eionet.europa.eu/cy/eea/me1/

EL HOURANY, R., FADEL, A., GEMAYEL, E., ABBOUD-ABI SAAB, M. and FAOUR, G., 2017. Spatio-temporal variability of the phytoplankton biomass in the Levantine basin between 2002 and 2015 using MODIS products. *Oceanologia*. 59(2), pp. 153–165

FALKOWSKI, P.G., BARBER, R.T. and SMETACEK, V., 1998. Biogeochemical Controls and Feedbacks on Ocean Primary Production. *Science*. 281(5374), pp. 200–206

FALKOWSKI, P.G., KATZ, M.E., KNOLL, A.H., QUIGG, A., RAVEN, J.A., SCHOFIELD, O. and TAYLOR, F.J.R., 2004. The Evolution of Modern Eukaryotic Phytoplankton. *Science*. 305(5682), pp. 354–360

FALKOWSKI, P.G. and OLIVER, M.J., 2007. Mix and match: how climate selects phytoplankton. *Nature Reviews Microbiology*. 5(10), pp. 813–819

FALKOWSKI, P.G. and RAVEN, J.A., 2007. *Aquatic Photosynthesis*. 2nd ed.. Princeton: Princeton University Press

FIELD, C.B., BEHRENFELD, M.J., RANDERSON, J.T. and FALKOWSKI, P., 1998. Primary Production of the Biosphere: Integrating Terrestrial and Oceanic Components. *Science*. 281(5374), pp. 237–240

FINKEL, Z.V., BEARDALL, J., FLYNN, K.J., QUIGG, A., REES, T.A.V. and RAVEN, J.A., 2010. Phytoplankton in a changing world: cell size and elemental stoichiometry. *Journal of Plankton Research*. 32(1), pp. 119–137

FINLEY, A., BANERJEE, S. and HJELLE, Ø., 2017. *MBA: Multilevel B-Spline Approximation.* [online] Available from: https://CRAN.R-project.org/package=MBA

FOGG, G.E., 1983. The Ecological Significance of Extracellular Products of Phytoplankton Photosynthesis. *Botanica Marina* [online]. 26(1) [viewed 26 Nov 2021]. Available from: https://www.degruyter.com/document/doi/10.1515/botm.1983.26.1.3/html

FUHRMAN, J.A., 1999. Marine viruses and their biogeochemical and ecological effects. *Nature*. 399(6736), pp. 541–548

GALLISAI, R., PETERS, F., VOLPE, G., BASART, S. and BALDASANO, J.M., 2014. Saharan Dust Deposition May Affect Phytoplankton Growth in the Mediterranean Sea at Ecological Time Scales. *PLoS ONE*. 9(10), pp. e110762

GEORGIOU, A., 2002. *Assessment of Groundwater Resources of Cyprus*. Nicosia, Cyprus: Water Development Department - Ministry of Agriculture, Rural Development and Environment, No. TCP/CYP/8921

GITTINGS, J.A., BREWIN, R.J.W., RAITSOS, D.E., KHEIREDDINE, M., OUHSSAIN, M., JONES, B.H. and HOTEIT, I., 2019a. Remotely sensing phytoplankton size structure in the Red Sea. *Remote Sensing of Environment*. 234, pp. 111387

GITTINGS, J.A., RAITSOS, D.E., BREWIN, R.J.W. and HOTEIT, I., 2021. Links between Phenology of Large Phytoplankton and Fisheries in the Northern and Central Red Sea. *Remote Sensing*. 13(2), pp. 231

GITTINGS, J.A., RAITSOS, D.E., KHEIREDDINE, M., RACAULT, M.-F., CLAUSTRE, H. and HOTEIT, I., 2019b. Evaluating tropical phytoplankton phenology metrics using contemporary tools. *Scientific Reports*. 9(1), pp. 674

GITTINGS, J.A., RAITSOS, D.E., KROKOS, G. and HOTEIT, I., 2018. Impacts of warming on phytoplankton abundance and phenology in a typical tropical marine ecosystem. *Scientific Reports*. 8(1), pp. 2240

GÓMEZ, F., 2003. Checklist of Mediterranean Free-living Dinoflagellates. *Botanica Marina*. 46(3), pp. 215–242

GÓMEZ, F., 2005. A list of free-living dinoflagellate species in the world's oceans. *Acta Botanica Croatica*. 64(1), pp. 129–212

GOMEZ, F., 2007. Gymnodinioid Dinoflagellates (Gymnodiniales, Dinophyceae) in the Open Pacific Ocean. *Algae*. 22(4), pp. 273–286

GÓMEZ, F. and FURUYA, K., 2007. Kofoidinium, Spatulodinium and other kofoidiniaceans (Noctilucales, Dinophyceae) in the Pacific Ocean. *European Journal of Protistology*. 43(2), pp. 115–124

GROOM, S., HERUT, B., BRENNER, S., ZODIATIS, G., PSARRA, S., KRESS, N., KROM, M.D., LAW, C.S. and DRAKOPOULOS, P., 2005. Satellite-derived spatial and temporal biological variability in the Cyprus Eddy. *Deep Sea Research Part II: Topical Studies in Oceanography*. 52(22–23), pp. 2990–3010

GROOM, S., SATHYENDRANATH, S., BAN, Y., BERNARD, S., BREWIN, R., BROTAS, V., BROCKMANN, C., CHAUHAN, P., CHOI, J., CHUPRIN, A., CIAVATTA, S., CIPOLLINI, P., DONLON, C., FRANZ, B., HE, X., HIRATA, T., JACKSON, T., KAMPEL, M., KRASEMANN, H., LAVENDER, S., PARDO-MARTINEZ, S., MÉLIN, F., PLATT, T., SANTOLERI, R., SKAKALA, J., SCHAEFFER, B., SMITH, M., STEINMETZ, F., VALENTE, A. and WANG, M., 2019. Satellite Ocean Colour: Current Status and Future Perspective. *Frontiers in Marine Science*. 6, pp. 485

HALLEGRAEFF, G.M., AUSTRALIAN BIOLOGICAL RESOURCES STUDY, CSIRO (AUSTRALIA) and AUSTRALIA, eds., 2010. *Algae of Australia. Phytoplankton of Temperate Coastal Waters*. Collingwood, Vic: Australian Biological Resources Study and CSIRO Publishing

HAMAD, N., MILLOT, C. and TAUPIER-LETAGE, I., 2006. The surface circulation in the eastern basin of the Mediterranean Sea. *Scientia Marina*. 70(3), pp. 457–503

HATTAB, T., JAMET, C., SAMMARI, C. and LAHBIB, S., 2013. Validation of chlorophyll-α concentration maps from Aqua MODIS over the Gulf of Gabes

(Tunisia): comparison between MedOC3 and OC3M bio-optical algorithms. *International Journal of Remote Sensing*. 34(20), pp. 7163–7177
HAYES, D.R., ZODIATIS, G., KONNARIS, G., HANNIDES, A., SOLOVYOV, D. and TESTOR, P., 2011. Glider transects in the Levantine Sea: Characteristics of the warm core Cyprus eddy. *In*: *OCEANS 2011 IEEE - Spain*. Presented at the OCEANS 2011 IEEE - Spain, pp. 1–9
HERRERO, A. and FLORES, E., eds., 2008. *The Cyanobacteria: Molecular Biology, Genomics, and Evolution*. Norfolk, UK: Caister Academic Press
HERUT, B., ALMOGI-LABIN, A., JANNINK, N. and GERTMAN, I., 2000. The seasonal dynamics of nutrient and chlorophyll a concentrations on the SE Mediterranean shelf-slope. *Oceanologica Acta*. 23(7), pp. 771–782
HERUT, B., KRESS, N. and TIBOR, G., 2002. The use of hyper-spectral remote sensing in compliance monitoring of water quality (phytoplankton and suspended particles) at 'hot spot' areas (Mediterranean coast of Israel). *Fresenius Environmental Bulletin*. 11(10), pp. 782–787
HERUT, B., ZOHARY, T., KROM, M.D., MANTOURA, R.F.C., PITTA, P., PSARRA, S., RASSOULZADEGAN, F., TANAKA, T. and FREDE THINGSTAD, T., 2005. Response of East Mediterranean surface water to Saharan dust: On-board microcosm experiment and field observations. *Deep Sea Research Part II: Topical Studies in Oceanography*. 52(22–23), pp. 3024–3040
HOLLIDAY, N.P. and HENSON, S., 2017. The Marine Environment. *In*: *Marine Plankton: A Practical Guide to Ecology, Methodology, and Taxonomy*. Oxford: Oxford University Press, pp. 3–11
HOPPENRATH, M., ELBRÄCHTER, M. and DREBES, G., 2009. *Marine Phytoplankton: Selected Microphytoplankton Species from the North Sea around Helgoland and Sylt*. Stuttgart: E. Schweizerbart'sche Verlagsbuchh
HSIEH, T.C., MA, K.H. and CHAO, A., 2016. iNEXT: an R package for rarefaction and extrapolation of species diversity (H ill numbers). *Methods in Ecology and Evolution*. 7(12), pp. 1451–1456
HUTCHINSON, G.E., 1961. The paradox of the plankton. *American Naturalist*. pp. 137–145
IOCCG, 2000. *Remote Sensing of Ocean Colour in Coastal, and Other Optically-Complex, Waters*. [online]. 140pp.. Dartmouth, Canada: International Ocean-Colour Coordinating Group (IOCCG), No. 3 [viewed 20 Nov 2021]. Available from: https://www.oceanbestpractices.net/handle/11329/515
JEFFREY, S.W. and VESK, M., 1997. Introduction to marine phytoplankton and their pigment signatures. *In*: S.W. JEFFREY, R.F.C. MANTOURA, and S.W. WRIGHT, eds. *Phytoplankton Pigments in Oceanography Guidlines to Modern Methods*. UNESCO
JEFFREY, S.W., WRIGHT, S.W. and ZAPATA, M., 2011. Microalgal classes and their signature pigments. *In*: *Phytoplankton Pigments: Characterization, Chemotaxonomy, and Applications in Oceanography*. Cambridge, New York: Cambridge University Press
JÖRGENSEN, E., 1920. *Mediterranean Ceratia*
KARAGEORGIS, A.P., GARDNER, W.D., GEORGOPOULOS, D., MISHONOV, A.V., KRASAKOPOULOU, E. and ANAGNOSTOU, C., 2008. Particle dynamics in the Eastern Mediterranean Sea: A synthesis based on light transmission, PMC, and POC archives (1991–2001). *Deep Sea Research Part I: Oceanographic Research Papers*. 55(2), pp. 177–202
KATHIJOTES, N. and PAPATHEODOULOU, A., 2013. Integrated Coastal Zone Management - Preview and Evaluation of its Application on the Coast of Cyprus. *In*:

E. MOKSNESS, E. DAHL, and J.G. STØTTRUP, eds. *Global Challenges in Integrated Coastal Zone Management*. Ames, Iowa: Wiley-Blackwell

KIRK, J.T.O., 2011. *Light and Photosynthesis in Aquatic Ecosystems*. 3rd ed.. Cambridge, UK ; New York: Cambridge University Press

KLAUSMEIER, C.A., LITCHMAN, E., DAUFRESNE, T. and LEVIN, S.A., 2008. Phytoplankton stoichiometry. *Ecological Research*. 23(3), pp. 479–485

KOELLER, P., FUENTES-YACO, C., PLATT, T., SATHYENDRANATH, S., RICHARDS, A., OUELLET, P., ORR, D., SKÚLADÓTTIR, U., WIELAND, K., SAVARD, L. and ASCHAN, M., 2009. Basin-Scale Coherence in Phenology of Shrimps and Phytoplankton in the North Atlantic Ocean. *Science*. 324(5928), pp. 791–793

KOFOID, C.A. and SWEZY, O., 1921. *The Free-Living Unarmored Dinoflagellata*. Berkeley, California: University of California Press

KRESS, N., GERTMAN, I. and HERUT, B., 2014. Temporal evolution of physical and chemical characteristics of the water column in the Easternmost Levantine basin (Eastern Mediterranean Sea) from 2002 to 2010. *Journal of Marine Systems*. 135, pp. 6–13

KRESS, N., RAHAV, E., SILVERMAN, J. and HERUT, B., 2019. Environmental status of Israel's Mediterranean coastal waters: Setting reference conditions and thresholds for nutrients, chlorophyll-a and suspended particulate matter. *Marine Pollution Bulletin*. 141, pp. 612–620

KROM, M.D., BRENNER, S., ISRAILOV, L. and KRUMGALZ, B., 1991. Dissolved nutrients, preformed nutrients and calculated elemental ratios in the south-east mediterranean-sea. *Oceanologica Acta*. 14(2), pp. 189–194

KROM, M.D., GROOM, S. and ZOHARY, T., 2003. The Eastern Mediterranean. *In*: K.D. BLACK and G.B. SHIMMIELD, eds. *Biogeochemistry of Marine Systems*. Oxford: Blackwell, p. 384

KROM, M.D., HERUT, B. and MANTOURA, R.F.C., 2004. Nutrient budget for the Eastern Mediterranean: Implications for phosphorus limitation. *Limnology and Oceanography*. 49(5), pp. 1582–1592

KROM, M.D., THINGSTAD, T.F., BRENNER, S., CARBO, P., DRAKOPOULOS, P., FILEMAN, T.W., FLATEN, G.A.F., GROOM, S., HERUT, B., KITIDIS, V., KRESS, N., LAW, C.S., LIDDICOAT, M.I., MANTOURA, R.F.C., PASTERNAK, A., PITTA, P., POLYCHRONAKI, T., PSARRA, S., RASSOULZADEGAN, F., SKJOLDAL, E.F., SPYRES, G., TANAKA, T., TSELEPIDES, A., WASSMANN, P., WEXELS RISER, C., WOODWARD, E.M.S., ZODIATIS, G. and ZOHARY, T., 2005. Summary and overview of the CYCLOPS P addition Lagrangian experiment in the Eastern Mediterranean. *Deep Sea Research Part II: Topical Studies in Oceanography*. 52(22–23), pp. 3090–3108

LAGARIA, A., MANDALAKIS, M., MARA, P., FRANGOULIS, C., KARATSOLIS, B.-Th., PITTA, P., TRIANTAPHYLLOU, M., TSIOLA, A. and PSARRA, S., 2017. Phytoplankton variability and community structure in relation to hydrographic features in the NE Aegean frontal area (NE Mediterranean Sea). *Continental Shelf Research*. 149, pp. 124–137

LAWS, E.A., 1997. *Mathematical Methods for Oceanographers: An Introduction*. New York: Wiley

LI, W.K.W., ZOHARY, T., YACOBI, Y.Z. and WOOD, A.M., 1993. Ultraphytoplankton in the eastern Mediterranean Sea: towards deriving phytoplankton biomass from flow cytometric measurements of abundance, fluorescence and light scatter. *Marine Ecology Progress Series*. pp. 79–87

LITCHMAN, E. and KLAUSMEIER, C.A., 2008. Trait-Based Community Ecology of Phytoplankton. *Annual Review of Ecology, Evolution, and Systematics*. 39(1), pp. 615–639

LITCHMAN, E., KLAUSMEIER, C.A., SCHOFIELD, O.M. and FALKOWSKI, P.G., 2007. The role of functional traits and trade-offs in structuring phytoplankton communities: scaling from cellular to ecosystem level. *Ecology Letters*. 10(12), pp. 1170–1181

MACKEY, M.D., MACKEY, D.J., HIGGINS, H.W. and WRIGHT, S.W., 1996. CHEMTAX - a program for estimating class abundances from chemical markers: application to HPLC measurements of phytoplankton. *Marine Ecology Progress Series*. 144, pp. 265–283

MALANOTTE-RIZZOLI, P., 1994. Modeling the General Circulation of the Mediterranean. *In*: P. MALANOTTE-RIZZOLI and A.R. ROBINSON, eds. *Ocean Processes in Climate Dynamics: Global and Mediterranean Examples*. Springer Netherlands, pp. 307–321

MALANOTTE-RIZZOLI, P., ARTALE, V., BORZELLI-EUSEBI, G.L., BRENNER, S., CRISE, A., GACIC, M., KRESS, N., MARULLO, S., RIBERA D'ALCALÀ, M., SOFIANOS, S., TANHUA, T., THEOCHARIS, A., ALVAREZ, M., ASHKENAZY, Y., BERGAMASCO, A., CARDIN, V., CARNIEL, S., CIVITARESE, G., D'ORTENZIO, F., FONT, J., GARCIA-LADONA, E., GARCIA-LAFUENTE, J.M., GOGOU, A., GREGOIRE, M., HAINBUCHER, D., KONTOYANNIS, H., KOVACEVIC, V., KRASKAPOULOU, E., KROSKOS, G., INCARBONA, A., MAZZOCCHI, M.G., ORLIC, M., OZSOY, E., PASCUAL, A., POULAIN, P.-M., ROETHER, W., RUBINO, A., SCHROEDER, K., SIOKOU-FRANGOU, J., SOUVERMEZOGLOU, E., SPROVIERI, M., TINTORÉ, J. and TRIANTAFYLLOU, G., 2014. Physical forcing and physical/biochemical variability of the Mediterranean Sea: a review of unresolved issues and directions for future research. *Ocean Science*. 10(3), pp. 281–322

MALANOTTE-RIZZOLI, P. and EREMEEV, V.N., eds., 1999. *The Eastern Mediterranean as a Laboratory Basin for the Assessment of Contrasting Ecosystems*. Dordrecht: Springer Netherlands

MALANOTTE-RIZZOLI, P., MANCA, B.B., D'ALCALÀ, M.R., THEOCHARIS, A., BERGAMASCO, A., BREGANT, D., BUDILLON, G., CIVITARESE, G., GEORGOPOULOS, D., MICHELATO, A., SANSONE, E., SCARAZZATO, P. and SOUVERMEZOGLOU, E., 1997. A synthesis of the Ionian Sea hydrography, circulation and water mass pathways during POEM-Phase I. *Progress in Oceanography*. 39(3), pp. 153–204

MANDALAKIS, M., STRAVINSKAITĖ, A., LAGARIA, A., PSARRA, S. and POLYMENAKOU, P., 2017. Ultrasensitive and high-throughput analysis of chlorophyll a in marine phytoplankton extracts using a fluorescence microplate reader. *Analytical and Bioanalytical Chemistry*. 409(19), pp. 4539–4549

MARGALEF, R., 1985. Environmental Control of the Mesoscale Distribution of Primary Producers and its Bearing to Primary Production in the Western Mediterranean. *In*: P.M. MORAITOU-APOSTOLOPOULOU and P.V. KIORTSIS, eds. *Mediterranean Marine Ecosystems*. Springer US, pp. 213–229

MARKAKI, Z., LOŸE-PILOT, M.D., VIOLAKI, K., BENYAHYA, L. and MIHALOPOULOS, N., 2010. Variability of atmospheric deposition of dissolved nitrogen and phosphorus in the Mediterranean and possible link to the anomalous seawater N/P ratio. *Marine Chemistry*. 120(1–4), pp. 187–194

MARKAKI, Z., OIKONOMOU, K., KOCAK, M., KOUVARAKIS, G., CHANIOTAKI, A., KUBILAY, N. and MIHALOPOULOS, N., 2003. Atmospheric deposition of

inorganic phosphorus in the Levantine Basin, eastern Mediterranean: Spatial and temporal variability and its role in seawater productivity. *Limnology and Oceanography*. 48(4), pp. 1557–1568
MARTY, J.-C., CHIAVÉRINI, J., PIZAY, M.-D. and AVRIL, B., 2002. Seasonal and interannual dynamics of nutrients and phytoplankton pigments in the western Mediterranean Sea at the DYFAMED time-series station (1991–1999). *Deep Sea Research Part II: Topical Studies in Oceanography*. 49(11), pp. 1965–1985
MAURI, SITZ, GERIN, POULAIN, HAYES, and GILDOR, 2019. On the Variability of the Circulation and Water Mass Properties in the Eastern Levantine Sea between September 2016–August 2017. *Water*. 11(9), pp. 1741
MELLA-FLORES, D., MAZARD, S., HUMILY, F., PARTENSKY, F., MAHÉ, F., BARIAT, L., COURTIES, C., MARIE, D., RAS, J., MAURIAC, R., JEANTHON, C., MAHDI BENDIF, E., OSTROWSKI, M., SCANLAN, D.J. and GARCZAREK, L., 2011. Is the distribution of <i>Prochlorococcus</i> and <i>Synechococcus</i> ecotypes in the Mediterranean Sea affected by global warming? *Biogeosciences*. 8(9), pp. 2785–2804
MILLS, E.L., 2012. *Biological Oceanography: An Early History, 1870-1960*. Toronto ; Buffalo: University of Toronto Press
MØLLER, E.F., 2007. Production of dissolved organic carbon by sloppy feeding in the copepods Acartia tonsa, Centropages typicus, and Temora longicornis. *Limnology and Oceanography*. 52(1), pp. 79–84
MOURITSEN, L.T. and RICHARDSON, K., 2003. Vertical microscale patchiness innano- and microplankton distributions in a stratified estuary. *Journal of Plankton Research*. 25(7), pp. 783–797
NUNES, S., PEREZ, G.L., LATASA, M., ZAMANILLO, M., DELGADO, M., ORTEGA-RETUERTA, E., MARRASÉ, C., SIMÓ, R. and ESTRADA, M., 2019. Size fractionation, chemotaxonomic groups and bio-optical properties of phytoplankton along a transect from the Mediterranean Sea to the SW Atlantic Ocean. *Scientia Marina*. 83(2), pp. 87
OKOLODKOV, Y.B., 2010. Cearatium Schrank (Dinophyceae) of the national prak Sistema Arrecifal Veracruzano, Gulf of Mexico, with a key for identification. *Acta Botanica Mexicana*. pp. 61
OKOLODKOV, Y.B., 2014. Dinophysiales (Dinophyceae) of the national park Sistema Arrecifal Veracruzano, Gulf of Mexico, with a key for identification. *Acta Botanica Mexicana*. (106), pp. 9–71
OKOLODKOV, Y.B. and GÁRATE-LIZÁRRAGA, I., 2006. An annotated checklist of Dinoflagellates (Dinophyceae) from the Mexican Pacific. *Acta Botanica Mexicana*. 74, pp. 1–154
OKSANEN, J., BLANCHET, F.G., FRIENDLY, M., KINDT, R., LEGENDRE, P., MCGLINN, D., MINCHIN, P.R., O'HARA, R.B., SIMPSON, G.L., SOLYMOS, P., STEVENS, M.H.H., SZOECS, E. and WAGNER, H., 2020. *Vegan: Community Ecology Package* [online] Available from: https://CRAN.R-project.org/package=vegan
OVCHINNIKOV, I.M., 1984. The formation of Intermediate Water in the Mediterranean. *Oceanology*. 24(2), pp. 168–173
OVCHINNIKOV, L.M., ZATS, V.I., KRIVOSHEYA, V.G., NEMIROVSKY, M.S. and UDODOV, A.I., 1987. Winter convection in the Adriatic and formation of deep eastern Mediterranean waters. *Annales Geopysicae*. 5, pp. 89–92

ÖZSOY, E., HECHT, A. and ÜNLÜATA, ü., 1989. Circulation and hydrography of the Levantine Basin. Results of POEM coordinated experiments 1985–1986. *Progress in Oceanography*. 22(2), pp. 125–170

ÖZSOY, E., HECHT, A., ÜNLÜATA, Ü., BRENNER, S., SUR, H.I., BISHOP, J., LATIF, M.A., ROZENTRAUB, Z. and OĞUZ, T., 1993. A synthesis of the Levantine Basin circulation and hydrography, 1985–1990. *Deep Sea Research Part II: Topical Studies in Oceanography*. 40(6), pp. 1075–1119

PETROU, A., KALLIANIOTIS, A., HANNIDES, A.K., CHARALAMBIDOU, I., HADJICHRISTOFOROU, M., HAYES, D.R., LAMBRIDIS, C., LAMBRIDI, V., LOIZIDOU, X.I., ORFANIDIS, S., SCARCELLA, G., STAMATIS, N., TRIANTAFILLIDIS, G. and VIDORIS, P., 2012. *Initial Assessment of the Marine Environment of Cyprus: Part I - Characteristics*. Cyprus: Ministry of Agriculture, Natural Resources, And The Environment, Department of Fisheries and Marine Research, Implementation of Article 8 of the Marine Strategy Framework Directive (2008/56/EC)

PITTA, P., TSAPAKIS, M., APOSTOLAKI, E., TSAGARAKI, T., HOLMER, M. and KARAKASSIS, I., 2009. 'Ghost nutrients' from fish farms are transferred up the food web by phytoplankton grazers. *Marine Ecology Progress Series*. 374, pp. 1–6

PLATT, T., FUENTES-YACO, C. and FRANK, K.T., 2003. Spring algal bloom and larval fish survival. *Nature*. 423(6938), pp. 398–399

PLATT, T. and SATHYENDRANATH, S., 2008. Ecological indicators for the pelagic zone of the ocean from remote sensing. *Remote Sensing of Environment*. 112(8), pp. 3426–3436

POEM, 1992. General circulation of the Eastern Mediterranean. *Earth-Science Reviews*. 32(4), pp. 285–309

PSARRA, S., TSELEPIDES, A. and IGNATIADES, L., 2000. Primary productivity in the oligotrophic Cretan Sea (NE Mediterranean): seasonal and interannual variability. *Progress in Oceanography*. 46, pp. 187–204

PSARRA, S., ZOHARY, T., KROM, M.D., MANTOURA, R.F.C., POLYCHRONAKI, T., STAMBLER, N., TANAKA, T., TSELEPIDES, A. and FREDE THINGSTAD, T., 2005. Phytoplankton response to a Lagrangian phosphate addition in the Levantine Sea (Eastern Mediterranean). *Deep Sea Research Part II: Topical Studies in Oceanography*. 52(22–23), pp. 2944–2960

R CORE TEAM, 2021. *R: A Language and Environment for Statistical Computing* [online]. Vienna, Austria: R Foundation for Statistical Computing Available from: https://www.R-project.org/

RACAULT, M.-F., LE QUÉRÉ, C., BUITENHUIS, E., SATHYENDRANATH, S. and PLATT, T., 2012. Phytoplankton phenology in the global ocean. *Ecological Indicators*. 14(1), pp. 152–163

RACAULT, M.-F., PLATT, T., SATHYENDRANATH, S., A IRBA, E., MARTINEZ VICENTE, V. and BREWIN, R., 2014. Plankton indicators and ocean observing systems: support to the marine ecosystem state assessment. *Journal of Plankton Research*. 36(3), pp. 621–629

RACAULT, M.-F., RAITSOS, D.E., BERUMEN, M.L., BREWIN, R.J.W., PLATT, T., SATHYENDRANATH, S. and HOTEIT, I., 2015. Phytoplankton phenology indices in coral reef ecosystems: Application to ocean-color observations in the Red Sea. *Remote Sensing of Environment*. 160, pp. 222–234

RAHAV, E., RAVEH, O., HAZAN, O., GORDON, N., KRESS, N., SILVERMAN, J. and HERUT, B., 2018. Impact of nutrient enrichment on productivity of coastal water

along the SE Mediterranean shore of Israel - A bioassay approach. *Marine Pollution Bulletin*. 127, pp. 559–567
RAVEN, J., 2017. Phytoplankton productivity. *In*: *Marine Plankton: A Practical Guide to Ecology, Methodology, and Taxonomy*. Oxford: Oxford University Press, pp. 24–33
RAVEN, J.A., BEARDALL, J., FLYNN, K.J. and MABERLY, S.C., 2009. Phagotrophy in the origins of photosynthesis in eukaryotes and as a complementary mode of nutrition in phototrophs: relation to Darwin's insectivorous plants. *Journal of Experimental Botany*. 60(14), pp. 3975–3987
REDFIELD, A.C., 1958. The biological control of chemical factors in the environment. *American Scientist* [online] [viewed 22 Oct 2015]. Available from: http://people.uncw.edu/borretts/courses/BIO602/redfield%201954.pdf
REYNOLDS, C.S., 2006. *Ecology of Phytoplankton* [online]. Cambridge; New York: Cambridge University Press [viewed 16 Sep 2015]. Available from: http://public.eblib.com/choice/publicfullrecord.aspx?p=258503
REYNOLDS, C.S. and PADISÁK, J., 2013. Plankton, Status and Role of. *In*: *Encyclopedia of Biodiversity*. Elsevier, pp. 24–38 [viewed 19 Nov 2021]. Available from: https://linkinghub.elsevier.com/retrieve/pii/B9780123847195002926
RICHARDSON, K., BEARDALL, J. and RAVEN, J.A., 1983. Adaptation of Unicellular Algae to Irradiance: An Analysis of Strategies. *The New Phytologist*. 93(2), pp. 157–191
RICHARDSON, K. and BENDTSEN, J., 2019. Vertical distribution of phytoplankton and primary production in relation to nutricline depth in the open ocean. *Marine Ecology Progress Series*. 620, pp. 33–46
ROBINSON, A.R. and GOLNARAGHI, M., 1994. The Physical and Dynamical Oceanography of the Mediterranean Sea. *In*: P. MALANOTTE-RIZZOLI and A.R. ROBINSON, eds. *Ocean Processes in Climate Dynamics: Global and Mediterranean Examples*. Springer Netherlands, pp. 255–306
ROBINSON, A.R., GOLNARAGHI, M., LESLIE, W.G., ARTEGIANI, A., HECHT, A., LAZZONI, E., MICHELATO, A., SANSONE, E., THEOCHARIS, A. and ÜNLÜATA, Ü., 1991. The eastern Mediterranean general circulation: features, structure and variability. *Dynamics of Atmospheres and Oceans*. 15(3), pp. 215–240
ROBINSON, A.R., LESLIE, W.G., THEOCHARIS, A. and LASCARATOS, A., 2001. Mediterranean Sea Circulation. *In*: *Encyclopedia of Ocean Sciences*. Elsevier, pp. 1689–1705 [viewed 22 Apr 2017]. Available from: http://linkinghub.elsevier.com/retrieve/pii/B012227430X003767
ROBINSON, C., 2017. Phytoplankton biogeochemical cycles. *In*: *Marine Plankton: A Pracitcal Guide to Ecology, Methodology, and Taxonomy*. Oxford: Oxford University Press, pp. 42–51
ROBINSON, C., BENNETT, C., BLISS, J., GARCÍA-MARTÍN, E., GARDNER, J. and NG, M., 2015. *Interactions between the Marine Biogeochemical Cycles of Carbon, Nitrogen and Phosphorus.* [online]. figshare [viewed 19 Nov 2021]. Available from: https://figshare.com/articles/figure/Interactions_between_the_marine_biogeochemical_cycles_of_carbon_nitrogen_and_phosphorus_/1585741/1
RODRIGUEZ-RAMOS, T., DORNELAS, M., MARANON, E. and CERMENO, P., 2014. Conventional sampling methods severely underestimate phytoplankton species richness. *Journal of Plankton Research*. 36(2), pp. 334–343
SALGADO-HERNANZ, P.M., 2019. Patterns of Phytoplankton and Primary Production Variability in the Mediterranean Sea Based on Remote Sensing Data. PhD. Universitat de les Illes Balears

SALGADO-HERNANZ, P.M., RACAULT, M.-F., FONT-MUÑOZ, J.S. and BASTERRETXEA, G., 2019. Trends in phytoplankton phenology in the Mediterranean Sea based on ocean-colour remote sensing. *Remote Sensing of Environment*. 221, pp. 50–64

SAMMARTINO, M., DI CICCO, A., MARULLO, S. and SANTOLERI, R., 2015. Spatio-temporal variability of micro-, nano- and pico-phytoplankton in the Mediterranean Sea from satellite ocean colour data of SeaWiFS. *Ocean Science*. 11(5), pp. 759–778

SIOKOU-FRANGOU, I., CHRISTAKI, U., MAZZOCCHI, M.G., MONTRESOR, M., RIBERA D'ALCALÁ, M., VAQUÉ, D. and ZINGONE, A., 2010. Plankton in the open Mediterranean Sea: a review. *Biogeosciences*. 7(5), pp. 1543–1586

SKLIRIS, N., 2014. Past, Present and Future Patterns of the Thermohaline Circulation and Characteristic Water Masses of the Mediterranean Sea. *In*: *The Mediterranean Sea: Its History and Present Challenges*. Dordrecht: Springer, pp. 29–48

SOFRONIOU, A. and BISHOP, S., 2014. Water Scarcity in Cyprus: A Review and Call for Integrated Policy. *Water*. 6(10), pp. 2898–2928

SOURNIA, A., ed., 1978. *Phytoplankton Manual*. Paris: Unesco

SOURNIA, A., CHRDTIENNOT-DINET, M.-J. and RICARD, M., 1991. Marine phytoplankton: how many species in the world ocean? *Journal of Plankton Research*. 13(5), pp. 1093–1099

TANAKA, T., ZOHARY, T., KROM, M.D., LAW, C.S., PITTA, P., PSARRA, S., RASSOULZADEGAN, F., THINGSTAD, T.F., TSELEPIDES, A., WOODWARD, E.M.S., FLATEN, G.A.F., SKJOLDAL, E.F. and ZODIATIS, G., 2007. Microbial community structure and function in the Levantine Basin of the eastern Mediterranean. *Deep Sea Research Part I: Oceanographic Research Papers*. 54(10), pp. 1721–1743

TAYLOR, F.J.R., 1976. *Dinoflagellates from the International Indian Ocean Expedition: A Report on Material Collected by the R. V. 'Anton Bruun' 1963-1964*. Stuttgart

THINGSTAD, T.F., KROM, M.D., MANTOURA, R.F.C., FLATEN, G.F., GROOM, S., HERUT, B., KRESS, N., LAW, C.S., PASTERNAK, A., PITTA, P., and OTHERS, 2005. Nature of phosphorus limitation in the ultraoligotrophic eastern Mediterranean. *Science*. 309(5737), pp. 1068–1071

THYNG, K., GREENE, C., HETLAND, R., ZIMMERLE, H. and DIMARCO, S., 2016. True Colors of Oceanography: Guidelines for Effective and Accurate Colormap Selection. *Oceanography*. 29(3), pp. 9–13

TOMAS, C.R. and HASLE, G.R., eds., 1997. *Identifying Marine Phytoplankton*. San Diego: Academic Press

TSAGARAKI, T., PITTA, P., FRANGOULIS, C., PETIHAKIS, G. and KARAKASSIS, I., 2013. Plankton response to nutrient enrichment is maximized at intermediate distances from fish farms. *Marine Ecology Progress Series*. 493, pp. 31–42

TSIMPLIS, M.N., ZERVAKIS, V., JOSEY, S.A., PENEVA, E.L., STRUGLIA, M.V., STANEV, E.V., THEOCHARIS, A., LIONELLO, P., MALANOTTE-RIZZOLI, P., ARTALE, V., TRAGOU, E. and OGUZ, T., 2006. Changes in the oceanography of the Mediterranean Sea and their link to climate variability. *In*: P. LIONELLO, P. MALANOTTE-RIZZOLI, and R. BOSCOLO, eds. *Developments in Earth and Environmental Sciences*. pp. 227–282

UITZ, J., CLAUSTRE, H., MOREL, A. and HOOKER, S.B., 2006. Vertical distribution of phytoplankton communities in open ocean: An assessment based on surface chlorophyll. *Journal of Geophysical Research: Oceans*. 111(C8), pp. C08005

UITZ, J., STRAMSKI, D., GENTILI, B., D'ORTENZIO, F. and CLAUSTRE, H., 2012. Estimates of phytoplankton class-specific and total primary production in the

Mediterranean Sea from satellite ocean color observations. *Global Biogeochemical Cycles*. 26(2), pp. GB2024

UITZ, J., STRAMSKI, D., REYNOLDS, R.A. and DUBRANNA, J., 2015. Assessing phytoplankton community composition from hyperspectral measurements of phytoplankton absorption coefficient and remote-sensing reflectance in open-ocean environments. *Remote Sensing of Environment*. 171, pp. 58–74

VAN HEUKELEM, L. and THOMAS, C.S., 2001. Computer-assisted high-performance liquid chromatography method development with applications to the isolation and analysis of phytoplankton pigments. *Journal of Chromatography. A*. 910(1), pp. 31–49

VELAORAS, D., GOGOU, A., ZERVOUDAKI, S., CIVITARESE, G., GIANI, M. and RAHAV, E., 2019. Revisiting the Eastern Mediterranean: Recent knowledge on the physical, biogeochemical and ecosystemic states and trends (Volume I). *Deep Sea Research Part II: Topical Studies in Oceanography*. 164, pp. 1–4

VIDUSSI, F., CLAUSTRE, H., MANCA, B.B., LUCHETTA, A. and MARTY, J.-C., 2001. Phytoplankton pigment distribution in relation to upper thermocline circulation in the eastern Mediterranean Sea during winter. *Journal of Geophysical Research*. 106(C9), pp. 19939–19956

VIOLLE, C., NAVAS, M.-L., VILE, D., KAZAKOU, E., FORTUNEL, C., HUMMEL, I. and GARNIER, E., 2007. Let the concept of trait be functional! *Oikos*. 116(5), pp. 882–892

VOLPE, G., COLELLA, S., BRANDO, V.E., FORNERIS, V., LA PADULA, F., DI CICCO, A., SAMMARTINO, M., BRACAGLIA, M., ARTUSO, F. and SANTOLERI, R., 2019. Mediterranean ocean colour Level 3 operational multi-sensor processing. *Ocean Science*. 15(1), pp. 127–146

VOLPE, G., SANTOLERI, R., VELLUCCI, V., RIBERA D'ALCALÀ, M., MARULLO, S. and D'ORTENZIO, F., 2007. The colour of the Mediterranean Sea: Global versus regional bio-optical algorithms evaluation and implication for satellite chlorophyll estimates. *Remote Sensing of Environment*. 107(4), pp. 625–638

WDD, 2017. *Water Resources - Introduction* [online] [viewed 15 Dec 2020]. Available from: http://www.moa.gov.cy/moa/wdd/Wdd.nsf/page08_en/page08_en?opendocument

WICKHAM, H., 2016. *Ggplot2: Elegant Graphics for Data Analysis*. 2nd ed. 2016.. New York: Springer

WICKMAN, H., FRANÇOIS, R., HENRY, L. and MÜLLER, K., 2021. *Dplyr: A Grammar of Data Manipulation* [online]. R package version 1.0.7 Available from: https://CRAN.R-project.org/package=dplyr

WRIGHT, S.W., ISHIKAWA, A., MARCHANT, H.J., DAVIDSON, A.T., VAN DEN ENDEN, R.L. and NASH, G.V., 2009. Composition and significance of picophytoplankton in Antarctic waters. *Polar Biology*. 32(5), pp. 797–808

WRIGHT, S.W. and JEFFREY, S.W., 2006. Pigment Markers for Phytoplankton Production. *In*: J.K. VOLKMAN, ed. *Marine Organic Matter: Biomarkers, Isotopes and DNA*. Berlin/Heidelberg: Springer-Verlag, pp. 71–104 [viewed 31 May 2016]. Available from: http://link.springer.com/10.1007/698_2_003

WÜST, G., 1961. On the vertical circulation of the Mediterranean Sea. *Journal of Geophysical Research*. 66(10), pp. 3261–3271

YACOBI, Y.Z., ZOHARY, T., KRESS, N., HECHT, A., ROBARTS, R.D., WAISER, M., WOOD, A.M. and LI, W.K.W., 1995. Chlorophyll distribution throughout the southeastern Mediterranean in relation to the physical structure of the water mass. *Journal of Marine Systems*. 6(3), pp. 179–190

YÜCEL, N., 2013. Monthly Changes in Primary and Bacterial Productivity in the North-Eastern Mediterranean Shelf Waters. PhD. Middle East Technical University, Turkey

YÜCEL, N., 2017. Variability in phytoplankton pigment composition in Mersin Bay. *Turkish Journal of Aquatic Sciences*. pp. 49–70

YÜCEL, N., 2018. Spatio-temporal variability of the size-fractionated primary production and chlorophyll in the Levantine Basin (northeastern Mediterranean). *Oceanologia*. 60(3), pp. 288–304

ZODIATIS, G., DRAKOPOULOS, P., BRENNER, S. and GROOM, S., 2005. Variability of the Cyprus warm core Eddy during the CYCLOPS project. *Deep Sea Research Part II: Topical Studies in Oceanography*. 52(22–23), pp. 2897–2910

ZODIATIS, G., LARDNER, R., HAYES, D.R., GEORGIOU, G., SOFIANOS, S., SKLIRIS, N. and LASCARATOS, A., 2008. Operational ocean forecasting in the Eastern Mediterranean: implementation and evaluation. *Ocean Science*. 4(1)

ZODIATIS, G., THEODOROU, A. and DEMETROPOULOS, A., 1998. Hydrography and circulation south of Cyprus in late summer 1995 and in spring 1996. *Oceanologica Acta*. 21(3), pp. 447–458

ZOHARY, T., BRENNER, S., KROM, M., ANGEL, D., KRESS, N., LI, W., NEORI, A. and YACOBI, Y., 1998. Buildup of microbial biomass during deep winter mixing in a Mediterranean warm-core eddy. *Marine Ecology Progress Series*. 167, pp. 47–57

Appendix I

Supplementary data to Chapter II

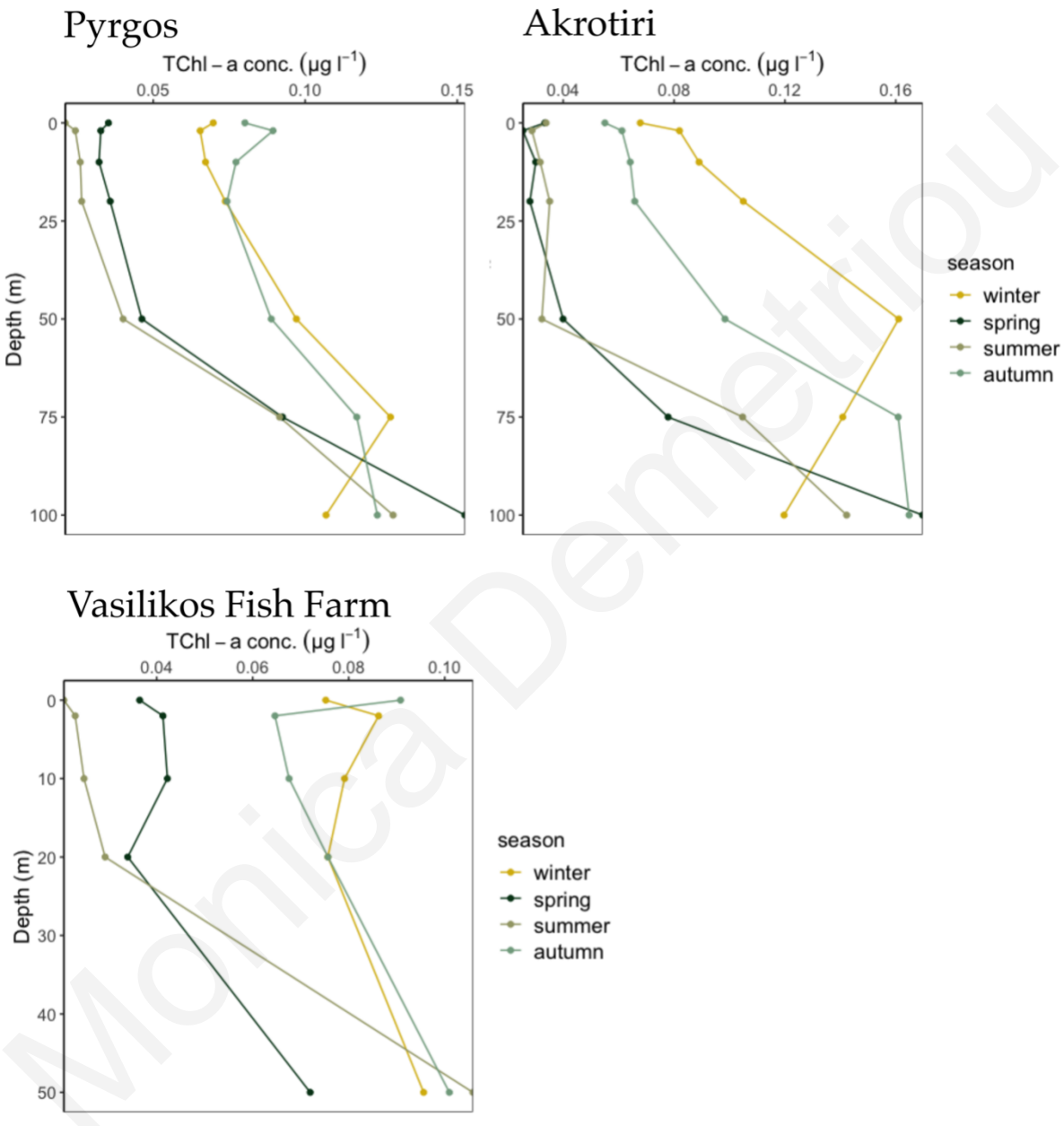

Figure S1: Vertical distribution of average total Chl-a per season, for the four sampling stations, PYR, AKR, and VAS.

Pyrgos

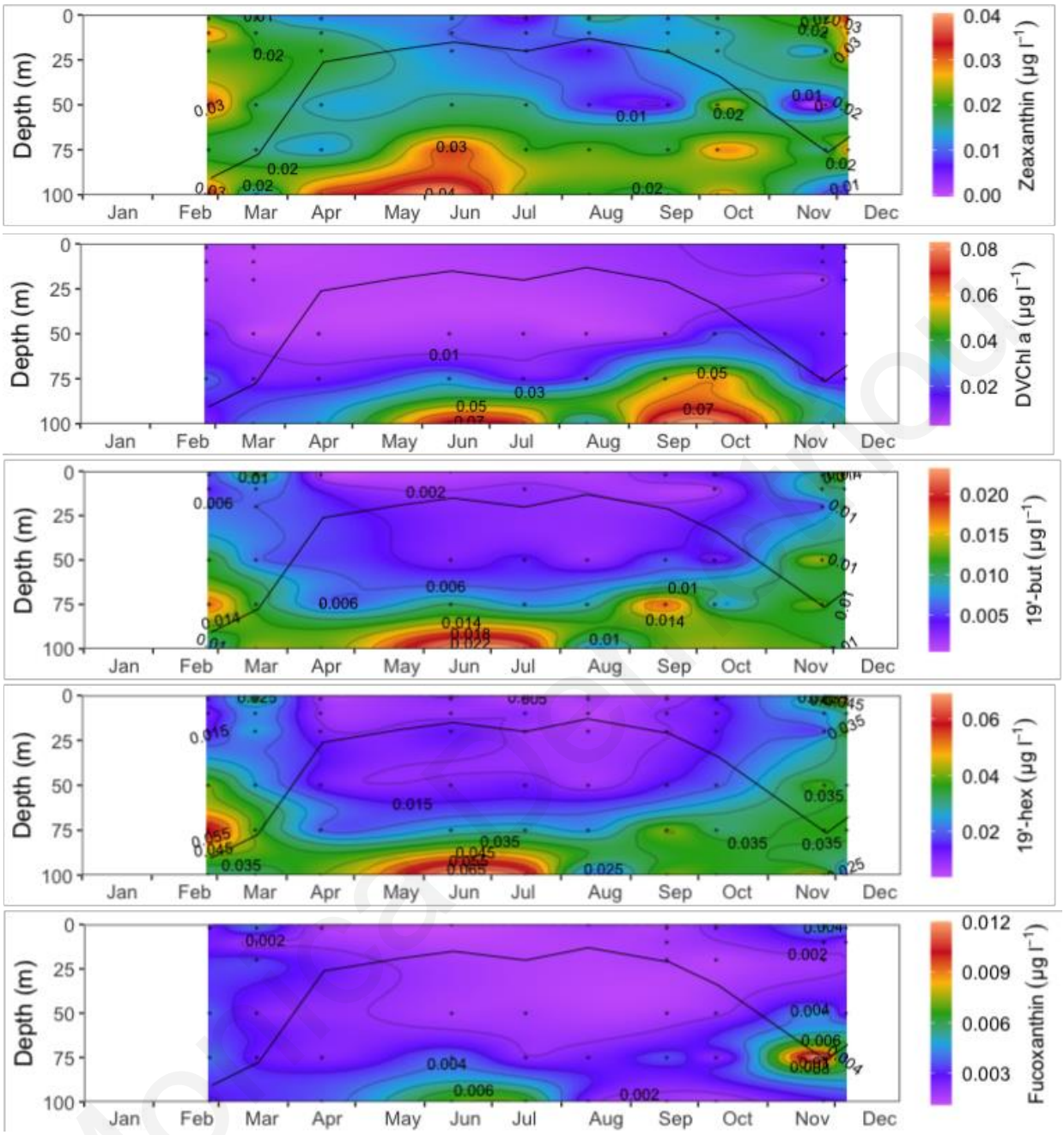

Akrotiri

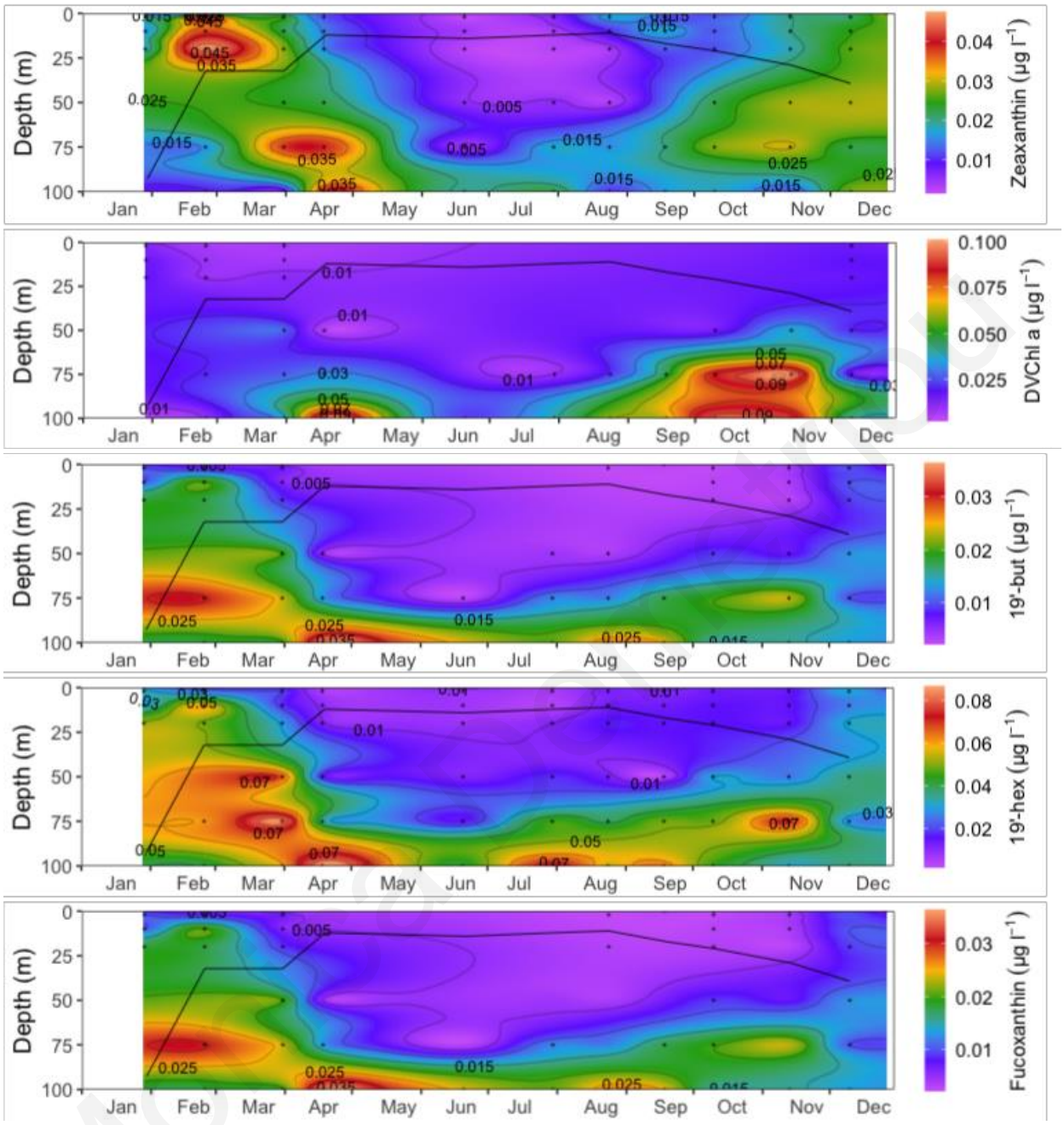
Depth (m)
0
25
50
75
100
Jan
Feb
Mar
Apr
May
Jun
Jul
Aug
Sep
Oct
Nov
Dec
Zeaxanthin (μg l⁻¹)
0.04
0.03
0.02
0.01
DVChl a (μg l⁻¹)
0.100
0.075
0.050
0.025
19'-but (μg l⁻¹)
19'-hex (μg l⁻¹)
0.08
0.06
0.04
0.02
Fucoxanthin (μg l⁻¹)

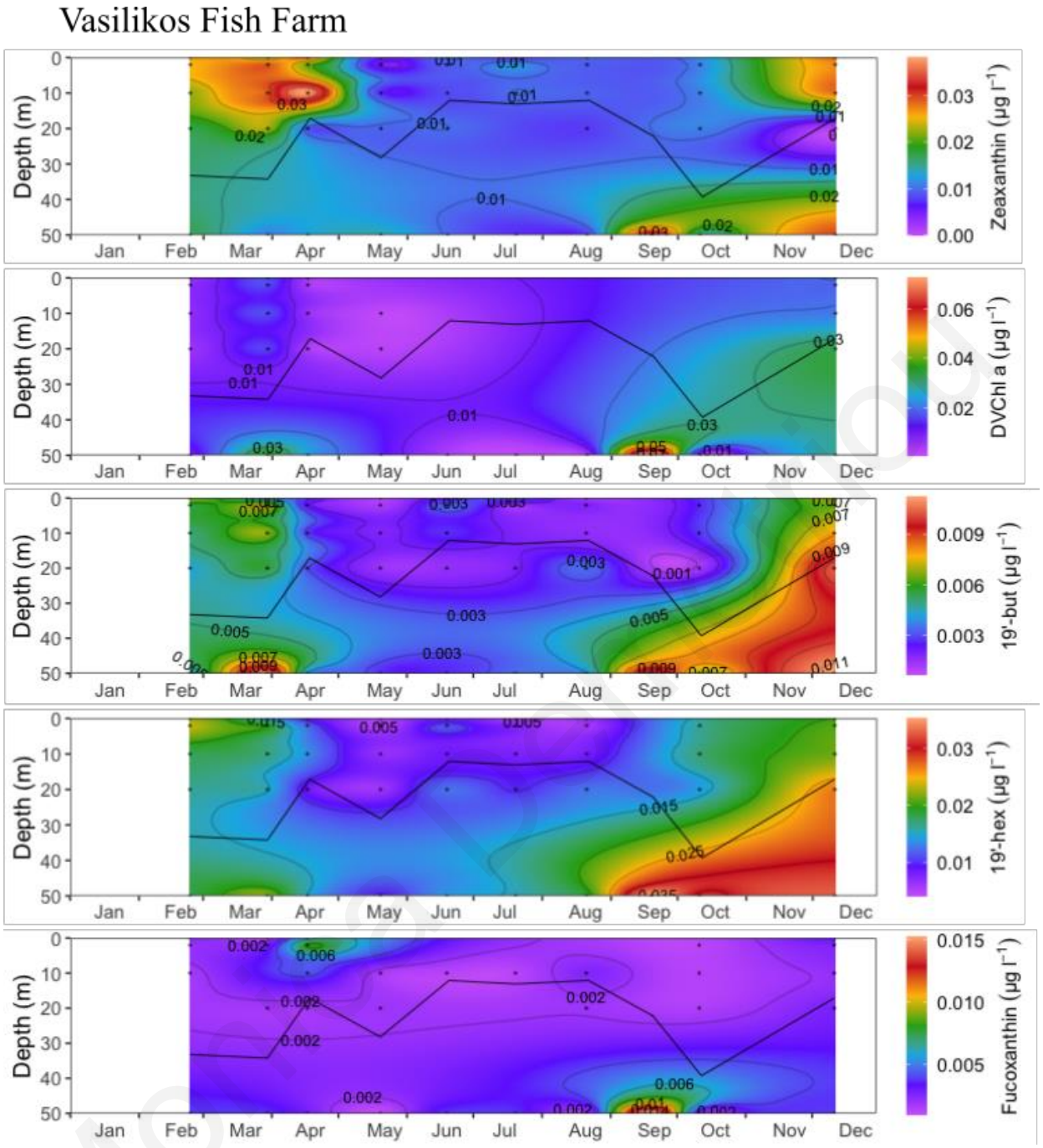

Figure S2: Contour plots of major accessory pigments (Zeaxanthin and Divinil-chlorophyll a (picoplankton), 19'butanoyloxyfucoxanthin and 19'hexanoyloxyfucoxanthin (nanoplankton) and Fucoxanthin (microplankton), for PYR, AKR and VAS.

Pyrgos

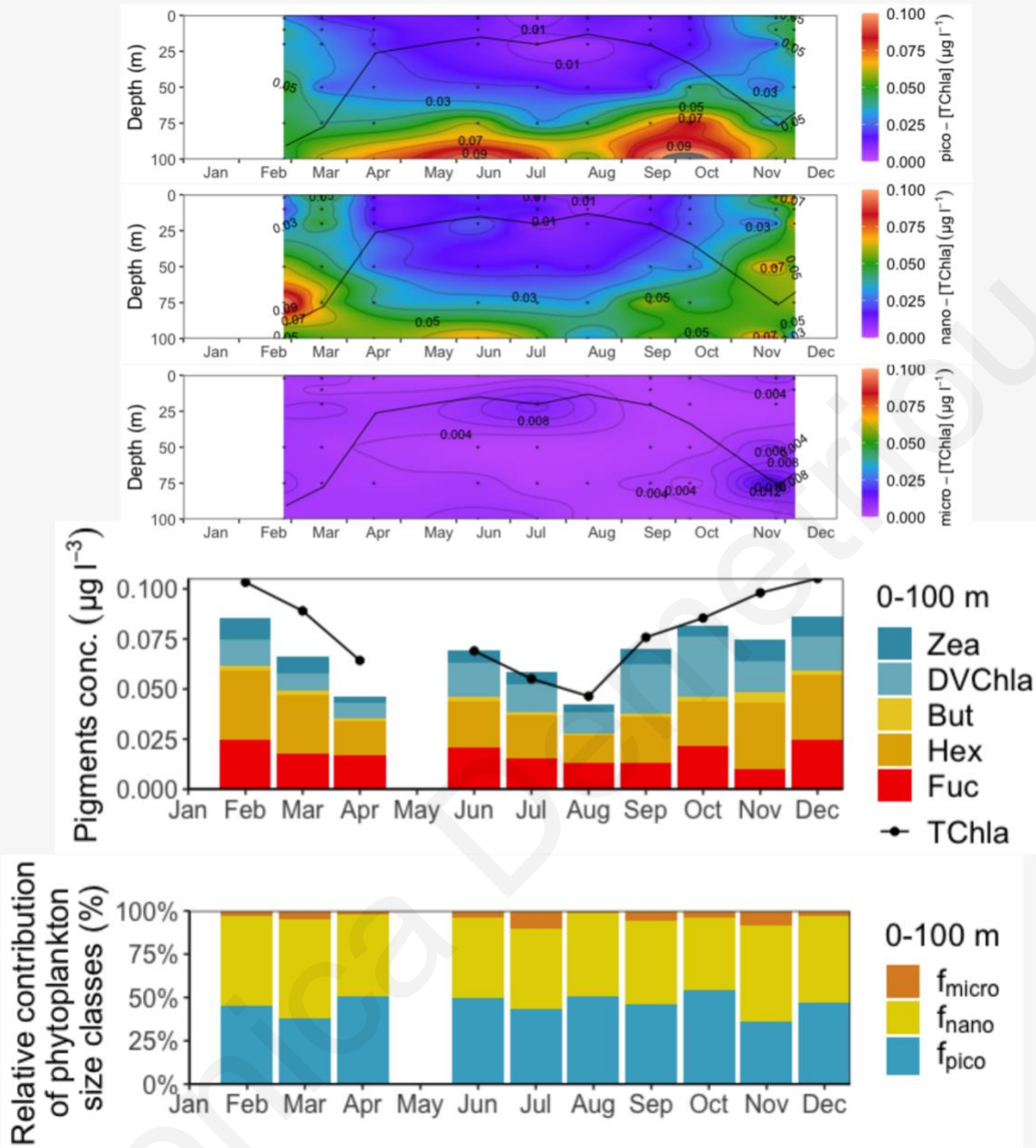

Akrotiri

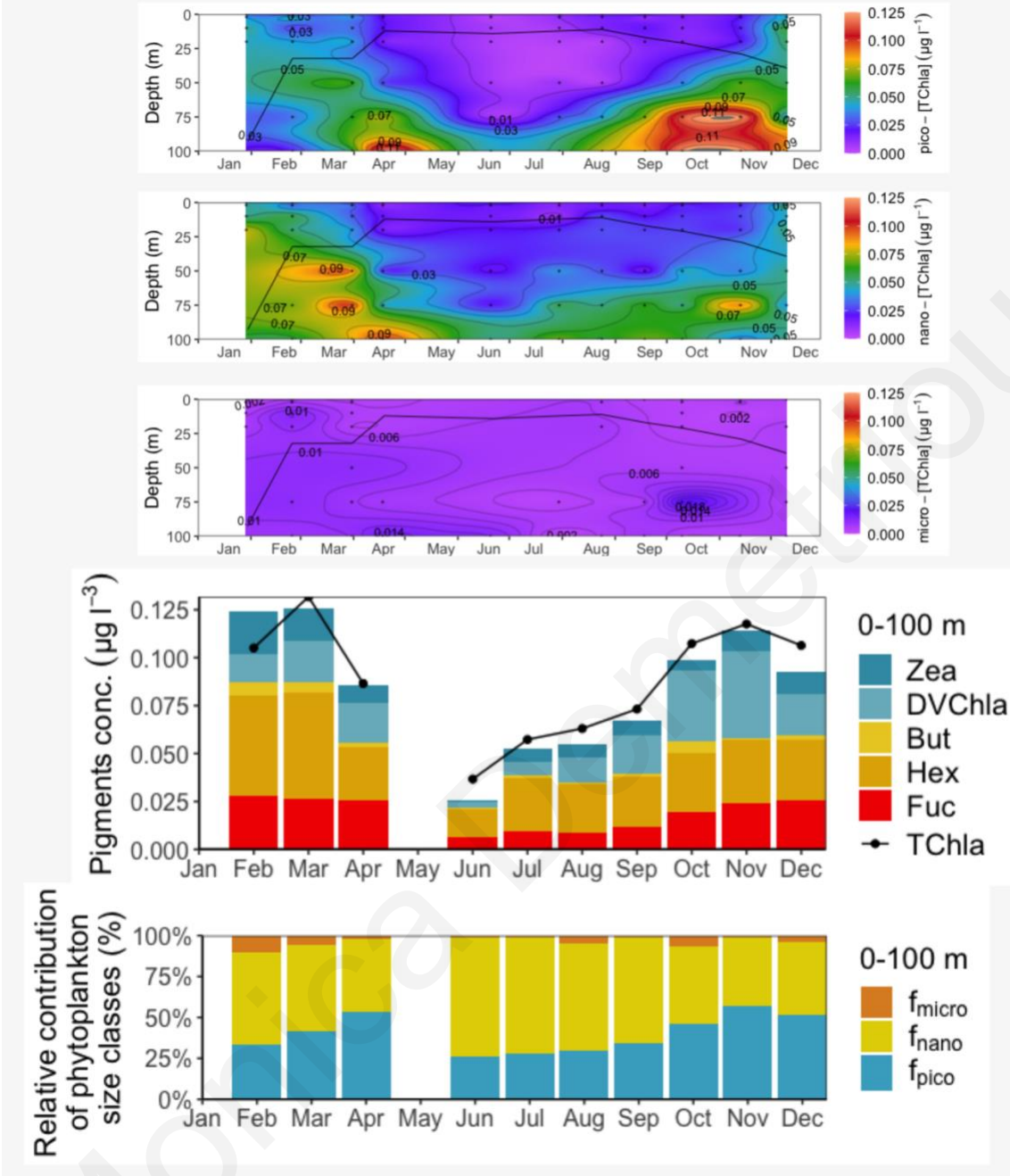

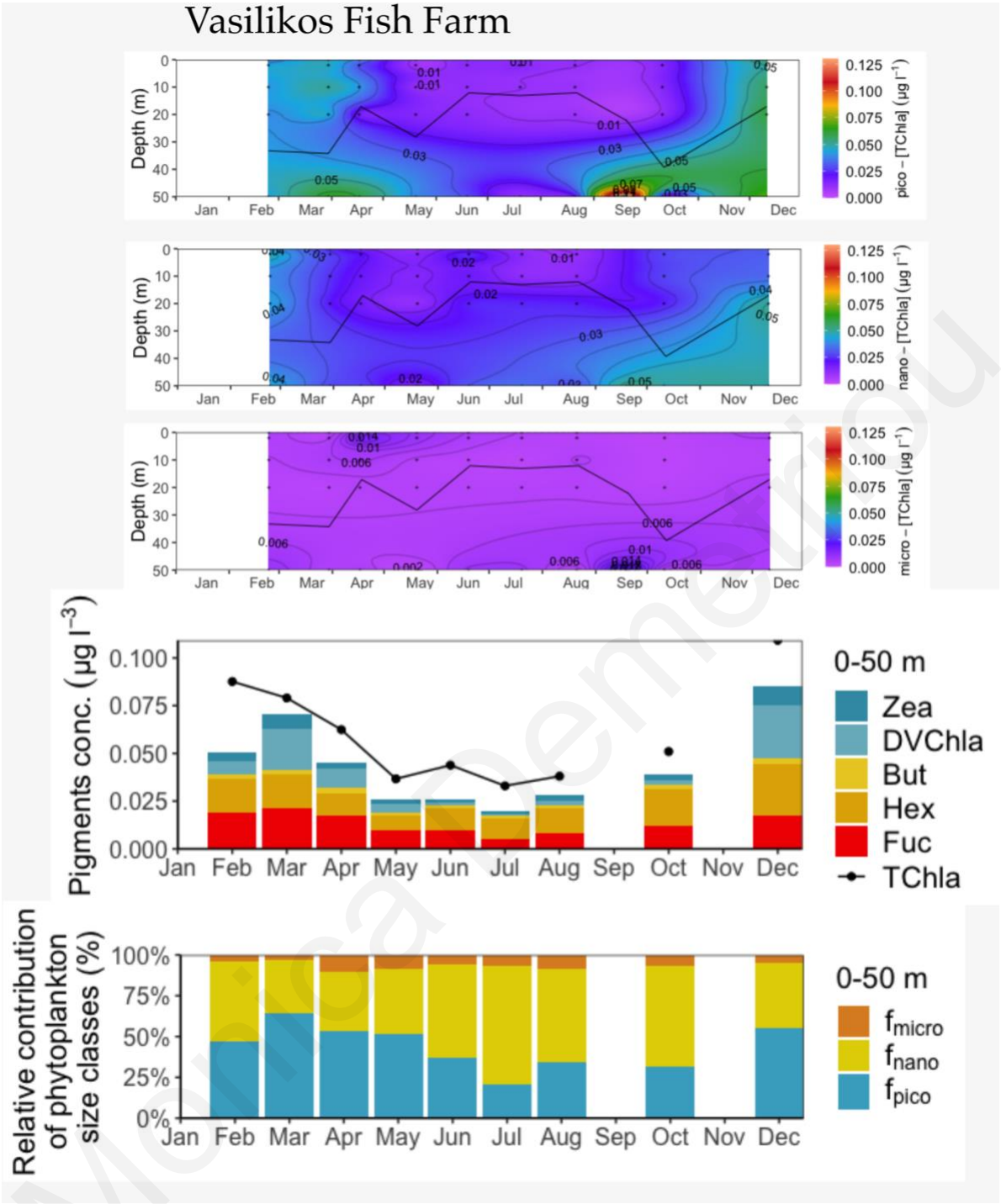

Figure S3: Total Chl-a concentrations associated to the pico-, nano- and microphytoplankton size classes, main diagnostic pigmets concentration and relative contribution of phytoplankton size classes, for stations PYR, AKR and VAS.

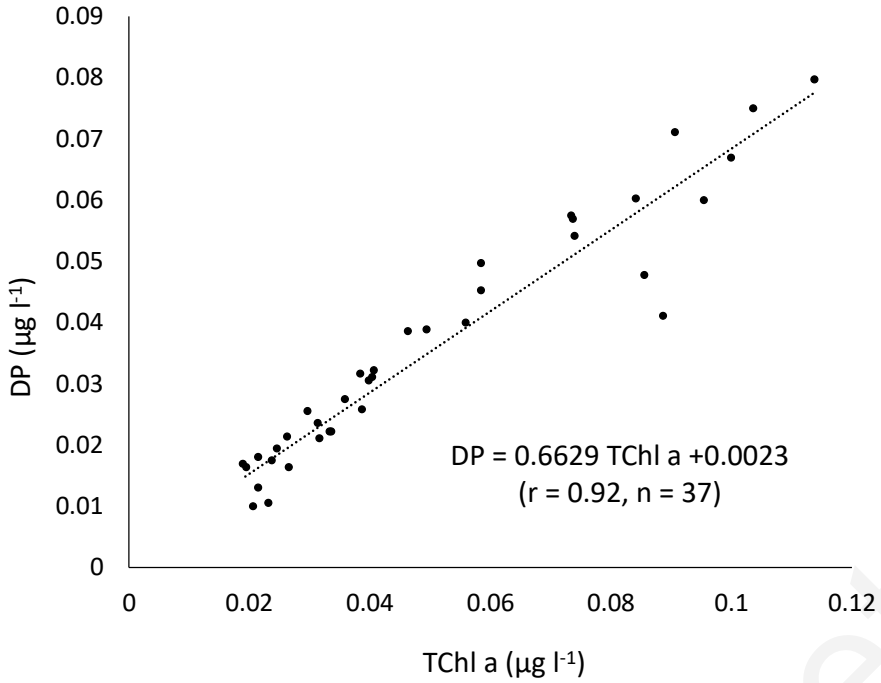

Figure S 4: Relationship between 0 – 20 m depth-integrated concentrations of DP and TChl a.

Appendix II